

# Relay-Selection Improves the Security-Reliability Trade-Off in Cognitive Radio Systems

Yulong Zou, *Senior Member, IEEE*, Benoit Champagne, *Senior Member, IEEE*,  
Wei-Ping Zhu, *Senior Member, IEEE*, and Lajos Hanzo, *Fellow, IEEE*

**Abstract**—We consider a cognitive radio (CR) network consisting of a secondary transmitter (ST), a secondary destination (SD) and multiple secondary relays (SRs) in the presence of an eavesdropper, where the ST transmits to the SD with the assistance of SRs, while the eavesdropper attempts to intercept the secondary transmission. We rely on careful relay selection for protecting the ST-SD transmission against the eavesdropper with the aid of both single-relay and multi-relay selection. To be specific, only the “best” SR is chosen in the single-relay selection for assisting the secondary transmission, whereas the multi-relay selection invokes multiple SRs for simultaneously forwarding the ST’s transmission to the SD. We analyze both the intercept probability and outage probability of the proposed single-relay and multi-relay selection schemes for the secondary transmission relying on realistic spectrum sensing. We also evaluate the performance of classic direct transmission and artificial noise based methods for the purpose of comparison with the proposed relay selection schemes. It is shown that as the intercept probability requirement is relaxed, the outage performance of the direct transmission, the artificial noise based and the relay selection schemes improves, and vice versa. This implies a trade-off between the security and reliability of the secondary transmission in the presence of eavesdropping attacks, which is referred to as the *security-reliability trade-off* (SRT). Furthermore, we demonstrate that the SRTs of the single-relay and multi-relay selection schemes are generally better than that of classic direct transmission, explicitly demonstrating the advantage of the proposed relay selection in terms of protecting the secondary transmissions against eavesdropping attacks. Moreover, as the number of SRs increases, the SRTs of the proposed single-relay and multi-relay

selection approaches significantly improve. Finally, our numerical results show that as expected, the multi-relay selection scheme achieves a better SRT performance than the single-relay selection.

**Index Terms**—Security-reliability trade-off, relay selection, intercept probability, outage probability, eavesdropping attack, cognitive radio.

## I. INTRODUCTION

THE security aspects of cognitive radio (CR) systems [1]–[3] have attracted increasing attention from the research community. Indeed, due to the highly dynamic nature of the CR network architecture, legitimate CR devices become exposed to both internal as well as to external attackers and hence they are extremely vulnerable to malicious behavior. For example, an illegitimate user may intentionally impose interference (i.e. jamming) for the sake of artificially contaminating the CR environment [4]. Hence, the CR users fail to accurately characterize their surrounding radio environment and may become misled or compromised, which leads to a malfunction. Alternatively, an illegitimate user may attempt to tap the communications of authorized CR users by eavesdropping, to intercept confidential information.

Clearly, CR networks face diverse security threats during both spectrum sensing [5], [6] as well as spectrum sharing [7], spectrum mobility [8] and spectrum management [9]. Extensive studies have been carried out for protecting CR networks both against primary user emulation (PUE) [10] and against denial-of-service (DoS) attacks [11]. In addition to PUE and DoS attacks, eavesdropping is another main concern in protecting the data confidentiality [12], although it has received less attention in the literature on CR network security. Traditionally, cryptographic techniques are employed for guaranteeing transmission confidentiality against an eavesdropping attack. However, this introduces a significant computational overhead [13] as well as imposing additional system complexity in terms of the secret key management [14]. Furthermore, the existing cryptographic approaches are not perfectly secure and can still be decrypted by an eavesdropper (E), provided that it has the capacity to carry out exhaustive key search with the aid of brute-force attack [15].

Physical-layer security [16], [17] is emerging as an efficient approach for defending authorized users against eavesdropping attacks by exploiting the physical characteristics of wireless channels. In [17], Leung-Yan-Cheong and Hellman demonstrated that perfectly secure and reliable transmission can be achieved, when the wiretap channel spanning from the source to the eavesdropper is a further degraded version of the main

Manuscript received May 7, 2014; revised August 21, 2014 and October 16, 2014; accepted November 27, 2014. This work was partially supported by the Priority Academic Program Development of Jiangsu Higher Education Institutions, the National Natural Science Foundation of China (Grant Nos. 61302104 and 61401223), the Scientific Research Foundation of Nanjing University of Posts and Telecommunications (Grant Nos. NY213014 and NY214001), the 1311 Talent Program of Nanjing University of Posts and Telecommunications, the Natural Science Foundation of Jiangsu Province (Grant No. BK20140887), and the Programme de bourses d’excellence pour étudiants étrangers (PBEEE) of the Government of Quebec. The associate editor coordinating the review of this paper and approving it for publication was H. Li.

Y. Zou is with the School of Telecommunications and Information Engineering, Nanjing University of Posts and Telecommunications, Nanjing 210003, China (e-mail: yulong.zou@njupt.edu.cn).

B. Champagne is with the Department of Electrical & Computer Engineering, McGill University, Montreal, QC H3A 1Y1, Canada (e-mail: benoit.champagne@mcgill.ca).

W.-P. Zhu is with the Department of Electrical & Computer Engineering, Concordia University, Montreal, QC H3G 1M8, Canada (e-mail: weiping@ece.concordia.ca).

L. Hanzo is with the Department of Electronics and Computer Science, University of Southampton, Southampton SO17 1BJ, U.K. (e-mail: lh@ecs.soton.ac.uk).

Color versions of one or more of the figures in this paper are available online at <http://ieeexplore.ieee.org>.

Digital Object Identifier 10.1109/TCOMM.2014.2377239

79 channel between the source and destination. They also showed  
 80 that the maximal secrecy rate achieved at the legitimate desti-  
 81 nation, which is termed the secrecy capacity, is the difference  
 82 between the capacity of the main channel and that of the  
 83 wiretap channel. In [18]–[20], the secrecy capacity limits of  
 84 wireless fading channels were further developed and character-  
 85 ized from an information-theoretic perspective, demonstrating  
 86 the detrimental impact of wireless fading on the physical-  
 87 layer security. To combat the fading effects, both multiple-input  
 88 multiple-output (MIMO) schemes [21], [22] as well as coop-  
 89 erative relaying [23]–[25] and beamforming techniques [26],  
 90 [27] were investigated for the sake of enhancing the achievable  
 91 wireless secrecy capacity. Although extensive research efforts  
 92 were devoted to improving the security of traditional wireless  
 93 networks [16]–[27], less attention has been dedicated to CR  
 94 networks. In [28] and [29], the achievable secrecy rate of  
 95 the secondary transmission was investigated under a specific  
 96 quality-of-service (QoS) constraint imposed on the primary  
 97 transmission. Additionally, an overview of the physical-layer  
 98 security aspects of CR networks was provided in [30], where  
 99 several security attacks as well as the related countermeasures  
 100 are discussed. In contrast to conventional non-cognitive wire-  
 101 less networks, the physical-layer security of CR networks has to  
 102 consider diverse additional challenges, including the protection  
 103 of the primary user’s QoS and the mitigation of the mutual  
 104 interference between the primary and secondary transmissions.  
 105 Motivated by the above considerations, we explore the  
 106 physical-layer security of a CR network comprised of a sec-  
 107 ondary transmitter (ST) communicating with a secondary des-  
 108 tination (SD) with the aid of multiple secondary relays (SRs)  
 109 in the presence of an unauthorized attacker. Our main focus  
 110 is on investigating the security-reliability trade-off (SRT) of  
 111 the cognitive relay transmission in the presence of realistic  
 112 spectrum sensing. The notion of the SRT in wireless physical-  
 113 layer security was introduced and examined in [31], where the  
 114 security and reliability was characterized in terms of the inter-  
 115 cept probability and outage probability, respectively. In contrast  
 116 to the conventional non-cognitive wireless networks studied in  
 117 [31], the SRT analysis of CR networks presented in this work  
 118 additionally takes into account the mutual interference between  
 119 the primary user (PU) and secondary user (SU).

120 The main contributions of this paper are summarized as  
 121 follows.

- 122 • We propose two relay selection schemes, namely both  
 123 single-relay and multi-relay selection, for protecting the  
 124 secondary transmissions against eavesdropping attacks.  
 125 More specifically, in the single-relay selection (SRS)  
 126 scheme, only a single relay is chosen from the set of mul-  
 127 tiple SRs for forwarding the secondary transmissions from  
 128 the ST to the SD. By contrast, the multi-relay selection  
 129 (MRS) scheme employs multiple SRs for simultaneously  
 130 assisting the ST-SD transmissions.
- 131 • We present the mathematical SRT analysis of the proposed  
 132 SRS and MRS schemes in the presence of realistic spec-  
 133 trum sensing. Closed-form expressions are derived for the  
 134 intercept probability (IP) and outage probability (OP) of  
 135 both schemes for transmission over Rayleigh fading chan-  
 136 nels. The numerical SRT results of conventional direct

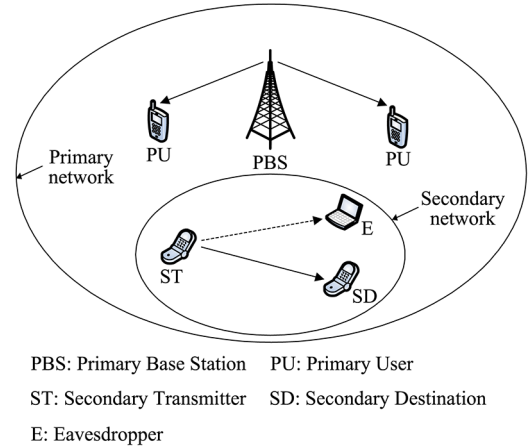


Fig. 1. A primary wireless network in coexistence with a secondary CR network.

transmission and artificial noise based schemes are also  
 provided for comparison purposes.

- It is shown that as the spectrum sensing reliability is increased and/or the false alarm probability is reduced, the SRTs of both the SRS and MRS schemes are improved. Numerical results demonstrate that the proposed SRS and MRS schemes generally outperform the conventional direct transmission and artificial noise based approaches in terms of their SRTs.

The remainder of this paper is organized as follows. Section II presents the system model of physical-layer security in CR networks in the context of both the direct transmission as well as the SRS and MRS schemes. In Section III, we analyze the SRTs of these schemes in the presence of realistic spectrum sensing over Rayleigh fading channels. Next, numerical SRT results of the direct transmission, SRS and MRS schemes are given in Section IV, where the SRT performance of the artificial noise based scheme is also numerically evaluated for comparison purposes. Finally, Section V provides our concluding remarks.

## II. RELAY SELECTION AIDED PROTECTION AGAINST EAVESDROPPING IN CR NETWORKS

We first introduce the overall system model of physical-layer security in CR networks. We then present the signal model of the conventional direct transmission approach, which will serve as our benchmark, as well as of the SRS and MRS schemes for improving the CR system’s security against eavesdropping attacks.

### A. System Model

As shown in Fig. 1, we consider a primary network in coexistence with a secondary network (also referred to as a *CR network*). The primary network includes a primary base station (PBS) and multiple primary users (PUs), which communicate with the PBS over the licensed spectrum. By contrast, the secondary network consisting of one or more STs and SDs exploits the licensed spectrum in an opportunistic way. To

173 be specific, a particular ST should first detect with the aid  
174 of spectrum sensing whether or not the licensed spectrum is  
175 occupied by the PBS. If so, the ST is not at liberty to transmit  
176 to avoid interfering with the PUs. If alternatively, the licensed  
177 spectrum is deemed to be unoccupied (i.e. a spectrum hole  
178 is detected), then the ST may transmit to the SD over the  
179 detected spectrum hole. Meanwhile, E attempts to intercept the  
180 secondary transmission from the ST to the SD. For notational  
181 convenience, let  $H_0$  and  $H_1$  represent the event that the licensed  
182 spectrum is unoccupied and occupied by the PBS during a  
183 particular time slot, respectively. Moreover, let  $\hat{H}$  denote the  
184 status of the licensed spectrum detected by spectrum sensing.  
185 Specifically,  $\hat{H} = H_0$  represents the case that the licensed  
186 spectrum is deemed to be unoccupied, while  $\hat{H} = H_1$  indicates  
187 that the licensed spectrum is deemed to be occupied.

188 The probability  $P_d$  of correct detection of the presence of  
189 PBS and the associated false alarm probability  $P_f$  are defined  
190 as  $P_d = \Pr(\hat{H} = H_1 | H_1)$  and  $P_f = \Pr(\hat{H} = H_1 | H_0)$ , respectively.  
191 Due to the background noise and fading effects, it is impossible  
192 to achieve perfectly reliable spectrum sensing without missing  
193 the detection of an active PU and without false alarm, which  
194 suggests that a spectral band is occupied by a PU, when it  
195 is actually unoccupied. Moreover, the missed detection of the  
196 presence of PBS will result in interference between the PU  
197 and SU. To guarantee that the interference imposed on the  
198 PUs is below a tolerable level, both the successful detection  
199 probability (SDP)  $P_d$  and false alarm probability (FAP)  $P_f$   
200 should be within a meaningful target range. For example, the  
201 IEEE 802.22 standard requires  $P_d > 0.9$  and  $P_f < 0.1$  [2]. For  
202 better protection of PUs, we consider  $P_d = 0.99$  and  $P_f = 0.01$ ,  
203 unless otherwise stated. Additionally, we consider a Rayleigh  
204 fading model for characterizing all the channels between any  
205 two nodes of Fig. 1. Finally, all the received signals are assumed  
206 to be corrupted by additive white Gaussian noise (AWGN)  
207 having a zero mean and a variance of  $N_0$ .

## 208 B. Direct Transmission

209 Let us first consider the conventional direct transmission  
210 as a benchmark scheme. Let  $x_p$  and  $x_s$  denote the random  
211 symbols transmitted by the PBS and the ST at a particular  
212 time instance. Without loss of generality, we assume  $E[|x_p|^2] =$   
213  $E[|x_s|^2] = 1$ , where  $E[\cdot]$  represents the expected value operator.  
214 The transmit powers of the PBS and ST are denoted by  $P_p$  and  
215  $P_s$ , respectively. Given that the licensed spectrum is deemed to  
216 be unoccupied by the PBS (i.e.  $\hat{H} = H_0$ ), ST transmits its signal  
217  $x_s$  at a power of  $P_s$ . Then, the signal received at the SD can be  
218 written as

$$y_d = h_{sd}\sqrt{P_s}x_s + h_{pd}\sqrt{\alpha P_p}x_p + n_d, \quad (1)$$

219 where  $h_{sd}$  and  $h_{pd}$  represent the fading coefficients of the  
220 channel spanning from ST to SD and that from PBS to SD,  
221 respectively. Furthermore,  $n_d$  represents the AWGN received at  
222 SD and the random variable (RV)  $\alpha$  is defined as

$$\alpha = \begin{cases} 0, & H_0 \\ 1, & H_1, \end{cases} \quad (2)$$

where  $H_0$  represents that the licensed spectrum is unoccupied  
223 by PBS and no primary signal is transmitted, leading to  $\alpha = 0$ .  
224 By contrast,  $H_1$  represents that PBS is transmitting its signal  $x_p$   
225 over the licensed spectrum, thus  $\alpha = 1$ . Meanwhile, due to the  
226 broadcast nature of the wireless medium, the ST's signal will  
227 be overheard by E and the overheard signal can be expressed as  
228

$$y_e = h_{se}\sqrt{P_s}x_s + h_{pe}\sqrt{\alpha P_p}x_p + n_e, \quad (3)$$

where  $h_{se}$  and  $h_{pe}$  represent the fading coefficients of the  
229 channel spanning from ST to E and that from PBS to E,  
230 respectively, while  $n_e$  represents the AWGN received at E.  
231 Upon combining Shannon's capacity formula [31] with (1), we  
232 obtain the capacity of the ST-SD channel as  
233

$$C_{sd} = \log_2 \left( 1 + \frac{|h_{sd}|^2 \gamma_s}{\alpha |h_{pd}|^2 \gamma_p + 1} \right), \quad (4)$$

where  $\gamma_s = P_s/N_0$  and  $\gamma_p = P_p/N_0$ . Similarly, the capacity of the  
234 ST-E channel is obtained from (3) as  
235

$$C_{se} = \log_2 \left( 1 + \frac{|h_{se}|^2 \gamma_s}{\alpha |h_{pe}|^2 \gamma_p + 1} \right). \quad (5)$$

## C. Single-Relay Selection

236 In this subsection, we consider the cognitive relay network  
237 of Fig. 2, where both SD and E are assumed to be beyond  
238 the coverage area of the ST [24], [25], and  $N$  secondary  
239 relays (SRs) are employed for assisting the cognitive ST-SD  
240 transmission. We assume that a common control channel (CCC)  
241 [6] is available for coordinating the actions of the different  
242 network nodes and the decode-and-forward (DF) relaying using  
243 two adjacent time slots is employed. More specifically, once  
244 the licensed spectrum is deemed to be unoccupied, the ST first  
245 broadcasts its signal  $x_s$  to the  $N$  SRs, which attempt to decode  
246  $x_s$  from their received signals. For notational convenience, let  
247  $\mathcal{D}$  represent the set of SRs that succeed in decoding  $x_s$ . Given  
248  $N$  SRs, there are  $2^N$  possible subsets  $\mathcal{D}$ , thus the sample space  
249 of  $\mathcal{D}$  is formulated as  
250

$$\Omega = \{\emptyset, \mathcal{D}_1, \mathcal{D}_2, \dots, \mathcal{D}_n, \dots, \mathcal{D}_{2^N-1}\}, \quad (6)$$

where  $\emptyset$  represents the empty set and  $\mathcal{D}_n$  represents the  $n$ -th  
251 non-empty subset of the  $N$  SRs. If the set  $\mathcal{D}$  is empty, implying  
252 that no SR decodes  $x_s$  successfully, then all the SRs remain  
253 silent and thus both SD and E are unable to decode  $x_s$  in this  
254 case. If the set  $\mathcal{D}$  is non-empty, a specific SR is chosen from  
255  $\mathcal{D}$  to forward its decoded signal  $x_s$  to SD. Therefore, given  
256  $\hat{H} = H_0$  (i.e. the licensed spectrum is deemed unoccupied), ST  
257 broadcasts its signal  $x_s$  to  $N$  SRs at a power of  $P_s$  and a rate of  
258  $R$ . Hence, the signal received at a specific SR <sub>$i$</sub>  is given by  
259

$$y_i = h_{si}\sqrt{P_s}x_s + h_{pi}\sqrt{\alpha P_p}x_p + n_i, \quad (7)$$

where  $h_{si}$  and  $h_{pi}$  represent the fading coefficients of the ST-SR <sub>$i$</sub>   
260 channel and that of the PBS-SR <sub>$i$</sub>  channel, respectively, with  
261

262  $n_i$  representing the AWGN at  $SR_i$ . From (7), we obtain the  
263 capacity of the ST- $SR_i$  channel as

$$C_{si} = \frac{1}{2} \log_2 \left( 1 + \frac{|h_{si}|^2 \gamma_s}{\alpha |h_{pi}|^2 \gamma_p + 1} \right), \quad (8)$$

264 where the factor  $\frac{1}{2}$  arises from the fact that two orthogonal time  
265 slots are required for completing the message transmission from  
266 ST to SD via  $SR_i$ . According to Shannon's coding theorem,  
267 if the data rate is higher than the channel capacity, the re-  
268 ceiver becomes unable to successfully decode the source signal,  
269 regardless of the decoding algorithm adopted. Otherwise, the  
270 receiver can succeed in decoding the source signal. Thus, using  
271 (8), we can describe the event of  $\mathcal{D} = \emptyset$  as

$$C_{si} < R, \quad i \in \{1, 2, \dots, N\}. \quad (9)$$

272 Meanwhile, the event of  $\mathcal{D} = \mathcal{D}_n$  is described as

$$\begin{aligned} C_{si} &> R, \quad i \in \mathcal{D}_n \\ C_{sj} &< R, \quad j \in \bar{\mathcal{D}}_n, \end{aligned} \quad (10)$$

273 where  $\bar{\mathcal{D}}_n$  represents the complementary set of  $\mathcal{D}_n$ . Without  
274 loss of generality, we assume that  $SR_i$  is chosen within  $\mathcal{D}_n$  to  
275 transmit its decoded result  $x_s$  at a power of  $P_s$ , thus the signal  
276 received at SD can be written as

$$y_d = h_{id} \sqrt{P_s} x_s + h_{pd} \sqrt{\alpha P_p} x_p + n_d, \quad (11)$$

277 where  $h_{id}$  represents the fading coefficient of the  $SR_i - SD$   
278 channel. From (11), the capacity of the  $SR_i - SD$  channel is  
279 given by

$$C_{id} = \frac{1}{2} \log_2 \left( 1 + \frac{|h_{id}|^2 \gamma_s}{\alpha |h_{pd}|^2 \gamma_p + 1} \right), \quad (12)$$

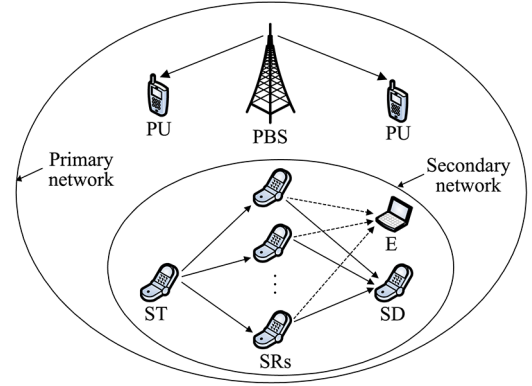
280 where  $i \in \mathcal{D}_n$ . In general, the specific  $SR_i$  having the highest  
281 instantaneous capacity to SD is chosen as the "best" SR for as-  
282 sisting the ST's transmission. Therefore, the best relay selection  
283 criterion is expressed from (12) as

$$\text{Best SR} = \arg \max_{i \in \mathcal{D}_n} C_{id} = \arg \max_{i \in \mathcal{D}_n} |h_{id}|^2, \quad (13)$$

284 which shows that only the channel state information (CSI)  $|h_{id}|^2$   
285 is required for performing the relay selection without the need  
286 for the eavesdropper's CSI knowledge. Upon combining (12)  
287 and (13), we obtain the capacity of the channel spanning from  
288 the "best" SR to SD as

$$C_{bd} = \frac{1}{2} \log_2 \left( 1 + \frac{\gamma_s}{\alpha |h_{pd}|^2 \gamma_p + 1} \max_{i \in \mathcal{D}_n} |h_{id}|^2 \right), \quad (14)$$

289 where the subscript 'b' in  $C_{bd}$  denotes the best SR. It is observed  
290 from (14) that the legitimate transmission capacity of the SRS  
291 scheme is determined by the maximum of independent random  
292 variables (RVs)  $|h_{id}|^2$  for different SRs. By contrast, one can  
293 see from (4) that the capacity of classic direct transmission is  
294 affected by the single RV  $|h_{sd}|^2$ . If all RVs  $|h_{id}|^2$  and  $|h_{sd}|^2$  are  
295 independent and identically distributed (i.i.d), it would be most  
296 likely that  $\max_{i \in \mathcal{D}_n} |h_{id}|^2$  is much higher than  $|h_{sd}|^2$  for a sufficiently



SRs: Secondary Relays

Fig. 2. A cognitive relay network consists of one ST, one SD and  $N$  SRs in the presence of an E.

large number of SRs, resulting in a performance improvement 297  
for the SRS scheme over the classic direct transmission. How- 298  
ever, if the RVs  $|h_{id}|^2$  and  $|h_{sd}|^2$  are non-identically distributed 299  
and the mean value of  $|h_{sd}|^2$  is much higher than that of  $|h_{id}|^2$ , 300  
then it may be more likely that  $\max_{i \in \mathcal{D}_n} |h_{id}|^2$  is smaller than  $|h_{sd}|^2$  301  
for a given number of SRs. In this extreme case, the classic 302  
direct transmission may perform better than the SRS scheme. 303  
It is worth mentioning that in practice, the average fading gain 304  
of the  $SR_i - SD$  channel,  $|h_{id}|^2$ , should not be less than that 305  
of the ST-SD channel  $|h_{sd}|^2$ , since SRs are typically placed 306  
in the middle between the ST and SD. Hence, a performance 307  
improvement for the SRS scheme over classic direct transmis- 308  
sion would be achieved in practical wireless systems. Note 309  
that although a factor 1/2 in (14) is imposed on the capacity 310  
of the main channel, it would not affect the performance of 311  
the SRS scheme from a SRT perspective, since the capacity 312  
of the wiretap channel is also multiplied by 1/2 as will be 313  
shown in (16). 314

Additionally, given that the selected SR transmits its 315  
decoded result  $x_s$  at a power of  $P_s$ , the signal received at E is 316  
expressed as 317

$$y_e = h_{be} \sqrt{P_s} x_s + h_{pe} \sqrt{\alpha P_p} x_p + n_e, \quad (15)$$

where  $h_{be}$  and  $h_{pe}$  represent the fading coefficients of the chan- 318  
nel from "best" SR to E and that from PBS to E, respectively. 319  
From (15), the capacity of the channel spanning from the "best" 320  
SR to E is given by 321

$$C_{be} = \frac{1}{2} \log_2 \left( 1 + \frac{|h_{be}|^2 \gamma_s}{\alpha |h_{pe}|^2 \gamma_p + 1} \right), \quad (16)$$

where  $b \in \mathcal{D}_n$  is determined by the relay selection criterion 322  
given in (13). As shown in (16), the eavesdropper's channel 323  
capacity is affected by the channel state information (CSI) 324  
 $|h_{be}|^2$  of the wiretap channel spanning from the "best" relay to 325  
the eavesdropper. However, one can see from (13) that the best 326  
relay is selected from the decoding set  $\mathcal{D}_n$  solely based on the 327  
main channel's CSI  $|h_{id}|^2$  i.e. without taking into account the 328  
eavesdropper's CSI knowledge of  $|h_{ie}|^2$ . This means that the 329  
selection of the best relay aiming for maximizing the legitimate 330  
transmission capacity of (14) would not lead to significantly 331

332 beneficial or adverse impact on the eavesdropper's channel  
333 capacity, since the main channel and the wiretap channel are  
334 independent of each other.

335 For example, if the random variables (RVs)  $|h_{ie}|^2$  related to  
336 the different relays are i.i.d, we can readily infer by the law  
337 of total probability that  $|h_{pe}|^2$  has the same probability den-  
338 sity function (PDF) as  $|h_{ie}|^2$ , implying that the eavesdropper's  
339 channel capacity of (16) is not affected by the selection of the  
340 best relay given by (13). Therefore, the SRS scheme has no  
341 obvious advantage over the classic direct transmission in terms  
342 of minimizing the capacity of the wiretap channel. To elaborate  
343 a little further, according to the SRT trade-off, a reduction of  
344 the outage probability (OP) due to the capacity enhancement  
345 of the main channel achieved by using the selection of the  
346 best relay would be converted into an intercept probability  
347 (IP) improvement, which will be numerically illustrated in  
348 Section IV.

#### 349 D. Multi-Relay Selection

350 This subsection presents a MRS scheme, where multiple SRs  
351 are employed for simultaneously forwarding the source signal  
352  $x_s$  to SD. To be specific, ST first transmits  $x_s$  to  $N$  SRs over a  
353 detected spectrum hole. As mentioned in Subsection II-C, we  
354 denote by  $\mathcal{D}$  the set of SRs that successfully decode  $x_s$ . If  $\mathcal{D}$   
355 is empty, all SRs fail to decode  $x_s$  and will not forward the  
356 source signal, thus both SD and E are unable to decode  $x_s$ . If  
357  $\mathcal{D}$  is non-empty (i.e.  $\mathcal{D} = \mathcal{D}_n$ ), all SRs within  $\mathcal{D}_n$  are utilized  
358 for simultaneously transmitting  $x_s$  to SD. This differs from the  
359 SRS scheme, where only a single SR is chosen from  $\mathcal{D}_n$  for  
360 forwarding  $x_s$  to SD. To make effective use of multiple SRs, a  
361 weight vector denoted by  $w = [w_1, w_2, \dots, w_{|\mathcal{D}_n|}]^T$  is employed  
362 at the SRs for transmitting  $x_s$ , where  $|\mathcal{D}_n|$  is the cardinality of  
363 the set  $\mathcal{D}_n$ . For the sake of a fair comparison with the SRS  
364 scheme in terms of power consumption, the total transmit power  
365 across all SRs within  $\mathcal{D}_n$  shall be constrained to  $P_s$  and thus the  
366 weight vector  $w$  should be normalized according to  $\|w\| = 1$ .  
367 Thus, given  $\mathcal{D} = \mathcal{D}_n$  and considering that all SRs within  $\mathcal{D}_n$  are  
368 selected for simultaneously transmitting  $x_s$  with a weight vector  
369  $w$ , the signal received at SD is expressed as

$$y_d^{\text{multi}} = \sqrt{P_s} w^T H_d x_s + \sqrt{\alpha P_p} h_{pd} x_p + n_d, \quad (17)$$

370 where  $H_d = [h_{1d}, h_{2d}, \dots, h_{|\mathcal{D}_n|d}]^T$ . Similarly, the signal received  
371 at E can be written as

$$y_e^{\text{multi}} = \sqrt{P_s} w^T H_e x_s + \sqrt{\alpha P_p} h_{pe} x_p + n_e, \quad (18)$$

372 where  $H_e = [h_{1e}, h_{2e}, \dots, h_{|\mathcal{D}_n|e}]^T$ . From (17) and (18), the  
373 signal-to-interference-plus-noise ratios (SINRs) at SD and E  
374 are, respectively, given by

$$\text{SINR}_d^{\text{multi}} = \frac{\gamma_s}{\alpha |h_{pd}|^2 \gamma_p + 1} |w^T H_d|^2, \quad (19)$$

375 and

$$\text{SINR}_e^{\text{multi}} = \frac{\gamma_s}{\alpha |h_{pe}|^2 \gamma_p + 1} |w^T H_e|^2. \quad (20)$$

In this work, the weight vector  $w$  is optimized by maximizing  
the SINR at SD, yielding

$$\max_w \text{SINR}_d^{\text{multi}}, \quad \text{s.t. } \|w\| = 1, \quad (21)$$

where the constraint is used for normalization purposes. Using  
the Cauchy-Schwarz inequality [32], we can readily obtain the  
optimal weight vector  $w_{\text{opt}}$  from (21) as

$$w_{\text{opt}} = \frac{H_d^*}{|H_d|}, \quad (22)$$

which indicates that the optimal vector design only requires the  
SR-SD CSI  $H_d$ , whilst dispensing with the eavesdropper's CSI  
 $H_e$ . Substituting the optimal vector  $w_{\text{opt}}$  from (22) into (19) and  
using Shannon's capacity formula, we can obtain the  
channel capacities achieved at both SD and E as

$$C_d^{\text{multi}} = \frac{1}{2} \log_2 \left( 1 + \frac{\gamma_s}{\alpha \gamma_p |h_{pd}|^2 + 1} \sum_{i \in \mathcal{D}_n} |h_{id}|^2 \right), \quad (23)$$

and

$$C_e^{\text{multi}} = \frac{1}{2} \log_2 \left( 1 + \frac{\gamma_s}{\alpha \gamma_p |h_{pe}|^2 + 1} \frac{|H_d^H H_e|^2}{|H_d|^2} \right), \quad (24)$$

for  $\mathcal{D} = \mathcal{D}_n$ , where  $H$  represents the Hermitian transpose. One  
can observe from (14) and (23) that the difference between the  
capacity expressions  $C_{bd}$  and  $C_d^{\text{multi}}$  only lies in the fact that  
the maximum of RVs  $|h_{id}|^2$  for different SRs (i.e.,  $\max_{i \in \mathcal{D}_n} |h_{id}|^2$ )  
is used for the SRS scheme, while the sum of RVs  $|h_{id}|^2$   
(i.e.,  $\sum_{i \in \mathcal{D}_n} |h_{id}|^2$ ) is employed for the MRS scheme. Clearly,  
we have  $\sum_{i \in \mathcal{D}_n} |h_{id}|^2 > \max_{i \in \mathcal{D}_n} |h_{id}|^2$ , resulting in a performance  
gain for MRS over SRS in terms of maximizing the legitimate  
transmission capacity. Moreover, since the main channel  $H_d$   
and the wiretap channel  $H_e$  are independent of each other, the  
optimal weights assigned for the multiple relays based on  $H_d$   
will only slightly affect the eavesdropper's channel capacity.  
This means that the MRS and SRS schemes achieve more or  
less the same performance in terms of the capacity of the wire-  
tap channel. Nevertheless, given a fixed outage requirement,  
the MRS scheme can achieve a better intercept performance  
than the SRS scheme, because according to the SRT, an outage  
reduction achieved by the capacity enhancement of the legiti-  
mate transmission relying on the MRS would be converted into  
an intercept improvement. To be specific, given an enhanced  
capacity of the legitimate transmission, we may increase the  
data rate  $R$  based on the OP definition of (25) for maintaining  
a fixed OP, which, in turn leads to a reduction of the IP, since  
a higher data rate would result in a lower IP, according to the IP  
definition of (26).

It needs to be pointed out that in the MRS scheme, a  
high-complexity symbol-level synchronization is required for  
multiple distributed SRs, when simultaneously transmitting to  
SD, whereas the SRS does not require such a complex synchro-  
nization process. Thus, the performance improvement of MRS  
over SRS is achieved at the cost of a higher implementation

418 complexity. Additionally, the synchronization imperfections of  
419 the MRS scheme will impose a performance degradation, which  
420 may even lead to a performance for the MRS scheme becoming  
421 worse than that of the SRS scheme.

422 Throughout this paper, the Rayleigh model is used for char-  
423 acterizing the fading amplitudes (e.g.,  $|h_{sd}|$ ,  $|h_{si}|$ ,  $|h_{id}|$ , etc.) of  
424 wireless channels, which, in turn, implies that the fading square  
425 magnitudes  $|h_{sd}|^2$ ,  $|h_{si}|^2$  and  $|h_{id}|^2$  are exponentially distributed  
426 random variables (RVs). So far, we have completed the presen-  
427 tation of the signal model of the direct transmission, of the SRS,  
428 and of the MRS schemes for CR networks applications in the  
429 presence of eavesdropping attacks.

### 430 III. SRT ANALYSIS OVER RAYLEIGH FADING CHANNELS

431 This section presents the SRT analysis of the direct transmis-  
432 sion, SRS and MRS schemes over Rayleigh fading channels.  
433 As discussed in [31], the security and reliability are quantified  
434 in terms of the IP and OP experienced by the eavesdropper and  
435 destination, respectively. It is pointed out that in CR networks,  
436 ST starts to transmit its signal only when an available spectrum  
437 hole is detected. Similarly to [34], the OP and IP are thus  
438 calculated under the condition that the licensed spectrum is  
439 detected to be unoccupied by the PBS. The following gives the  
440 definition of OP and IP.

441 *Definition 1:* Let  $C_d$  and  $C_e$  represent the channel capacities  
442 achieved at the destination and eavesdropper, respectively. The  
443 OP and IP are, respectively, defined as

$$P_{\text{out}} = \Pr(C_d < R | \hat{H} = H_0), \quad (25)$$

444 and

$$P_{\text{int}} = \Pr(C_e > R | \hat{H} = H_0), \quad (26)$$

445 where  $R$  is the data rate.

#### 446 A. Direct Transmission

447 Let us first analyze the SRT performance of the conventional  
448 direct transmission. Given that a spectrum hole has been de-  
449 tected, the OP of direct transmission is obtained from (25) as

$$P_{\text{out}}^{\text{direct}} = \Pr(C_{sd} < R | \hat{H} = H_0), \quad (27)$$

450 where  $C_{sd}$  is given by (4). Using the law of total probability, we  
451 can rewrite (27) as

$$P_{\text{out}}^{\text{direct}} = \Pr(C_{sd} < R, H_0 | \hat{H} = H_0) + \Pr(C_{sd} < R, H_1 | \hat{H} = H_0), \quad (28)$$

452 which can be further expressed as

$$P_{\text{out}}^{\text{direct}} = \Pr(C_{sd} < R | H_0, \hat{H} = H_0) \Pr(H_0 | \hat{H} = H_0) \\ + \Pr(C_{sd} < R | H_1, \hat{H} = H_0) \Pr(H_1 | \hat{H} = H_0). \quad (29)$$

453 It is shown from (2) that given  $H_0$  and  $H_1$ , the parameter  $\alpha$  is  
454 obtained as  $\alpha = 0$  and  $\alpha = 1$ , respectively. Thus, combining (2)

and (4), we have  $C_{sd} = \log_2(1 + |h_{sd}|^2 \gamma_s)$  given  $H_0$  and  $C_{sd} = 455$   
 $\log_2\left(1 + \frac{|h_{sd}|^2 \gamma_s}{|h_{pd}|^2 \gamma_p + 1}\right)$  given  $H_1$ . Substituting this result into (29) 456  
yields 457

$$P_{\text{out}}^{\text{direct}} = \Pr(|h_{sd}|^2 \gamma_s < 2^R - 1) \Pr(H_0 | \hat{H} = H_0) \\ + \Pr\left(\frac{|h_{sd}|^2 \gamma_s}{|h_{pd}|^2 \gamma_p + 1} < 2^R - 1\right) \Pr(H_1 | \hat{H} = H_0). \quad (30)$$

Moreover, the terms  $\Pr(H_0 | \hat{H} = H_0)$  and  $\Pr(H_1 | \hat{H} = H_0)$  can be 458  
obtained by using Bayes' theorem as 459

$$\Pr(H_0 | \hat{H} = H_0) = \frac{\Pr(\hat{H} = H_0 | H_0) \Pr(H_0)}{\sum_{i \in \{0,1\}} \Pr(\hat{H} = H_0 | H_i) \Pr(H_i)} \\ = \frac{P_0(1 - P_f)}{P_0(1 - P_f) + (1 - P_0)(1 - P_d)} \triangleq \pi_0, \quad (31)$$

and 460

$$\Pr(H_1 | \hat{H} = H_0) = \frac{(1 - P_0)(1 - P_d)}{P_0(1 - P_f) + (1 - P_0)(1 - P_d)} \triangleq \pi_1, \quad (32)$$

where  $P_0 = \Pr(H_0)$  is the probability that the licensed spec- 461  
trum band is unoccupied by PBS, while  $P_d = \Pr(\hat{H} = H_1 | H_1)$  462  
and  $P_f = \Pr(\hat{H} = H_1 | H_0)$  are the SDP and FAP, respectively. 463  
For notational convenience, we introduce the shorthand  $\pi_0 = 464$   
 $\Pr(H_0 | \hat{H} = H_0)$ ,  $\pi_1 = \Pr(H_1 | \hat{H} = H_0)$  and  $\Delta = \frac{2^R - 1}{\gamma_s}$ . Then, 465  
using (31) and (32), we rewrite (30) as 466

$$P_{\text{out}}^{\text{direct}} = \pi_0 \Pr(|h_{sd}|^2 < \Delta) + \pi_1 \Pr(|h_{sd}|^2 - |h_{pd}|^2 \gamma_p \Delta < \Delta). \quad (33)$$

Noting that  $|h_{sd}|^2$  and  $|h_{pd}|^2$  are independently and exponen- 467  
tially distributed RVs with respective means of  $\sigma_{sd}^2$  and  $\sigma_{pd}^2$ , 468  
we obtain 469

$$\Pr(|h_{sd}|^2 < \Delta) = 1 - \exp\left(-\frac{\Delta}{\sigma_{sd}^2}\right), \quad (34)$$

and 470

$$\Pr(|h_{sd}|^2 - |h_{pd}|^2 \gamma_p \Delta < \Delta) = 1 - \frac{\sigma_{sd}^2}{\sigma_{pd}^2 \gamma_p \Delta + \sigma_{sd}^2} \exp\left(-\frac{\Delta}{\sigma_{sd}^2}\right). \quad (35)$$

Additionally, we observe from (26) that an intercept event 471  
occurs, when the capacity of the ST-E channel becomes higher 472  
than the data rate. Thus, given that a spectrum hole has been de- 473  
tected (i.e.  $\hat{H} = H_0$ ), ST starts transmitting its signal to SD and 474  
E may overhear the ST-SD transmission. The corresponding IP 475  
is given by 476

$$P_{\text{int}}^{\text{direct}} = \Pr(C_{se} > R | \hat{H} = H_0), \quad (36)$$

which can be further expressed as 477

$$P_{\text{int}}^{\text{direct}} = \Pr(C_{se} > R | \hat{H} = H_0, H_0) \Pr(H_0 | \hat{H} = H_0) \\ + \Pr(C_{se} > R | \hat{H} = H_0, H_1) \Pr(H_1 | \hat{H} = H_0) \\ = \pi_0 \Pr(|h_{se}|^2 > \Delta) + \pi_1 \Pr(|h_{se}|^2 - |h_{pe}|^2 \gamma_p \Delta > \Delta), \quad (37)$$

478 where the second equality is obtained by using  $C_{se}$  from (5).  
 479 Noting that RVs  $|h_{se}|^2$  and  $|h_{pe}|^2$  are exponentially distributed  
 480 and independent of each other, we can express the terms  
 481  $\Pr(|h_{se}|^2 > \Delta)$  and  $\Pr(|h_{se}|^2 - |h_{pe}|^2 \gamma_p \Delta > \Delta)$  as

$$\Pr(|h_{se}|^2 > \Delta) = \exp\left(-\frac{\Delta}{\sigma_{se}^2}\right), \quad (38)$$

482 and

$$\Pr(|h_{se}|^2 - |h_{pe}|^2 \gamma_p \Delta > \Delta) = \frac{\sigma_{se}^2}{\sigma_{pe}^2 \gamma_p \Delta + \sigma_{se}^2} \exp\left(-\frac{\Delta}{\sigma_{se}^2}\right), \quad (39)$$

483 where  $\sigma_{se}^2$  and  $\sigma_{pe}^2$  are the expected values of RVs  $|h_{se}|^2$  and  
 484  $|h_{pe}|^2$ , respectively.

### 485 B. Single-Relay Selection

486 In this subsection, we present the SRT analysis of the pro-  
 487 posed SRS scheme. Given  $\hat{H} = H_0$ , the OP of the cognitive  
 488 transmission relying on SRS is given by

$$P_{\text{out}}^{\text{single}} = \Pr(C_{bd} < R, \mathcal{D} = \emptyset | \hat{H} = H_0) + \sum_{n=1}^{2^N-1} \Pr(C_{bd} < R, \mathcal{D} = \mathcal{D}_n | \hat{H} = H_0), \quad (40)$$

489 where  $C_{bd}$  represents the capacity of the channel from the  
 490 ‘‘best’’ SR to SD. In the case of  $\mathcal{D} = \emptyset$ , no SR is chosen to  
 491 forward the source signal, which leads to  $C_{bd} = 0$  for  $\mathcal{D} = \emptyset$ .  
 492 Substituting this result into (40) gives

$$P_{\text{out}}^{\text{single}} = \Pr(\mathcal{D} = \emptyset | \hat{H} = H_0) + \sum_{n=1}^{2^N-1} \Pr(C_{bd} < R, \mathcal{D} = \mathcal{D}_n | \hat{H} = H_0), \quad (41)$$

493 Using (2), (9), (10), and (14), we can rewrite (41) as (42),  
 494 shown at the bottom of the page, where  $\Lambda = \frac{2^{2R}-1}{\gamma_s}$ . Noting  
 495 that  $|h_{si}|^2$  and  $|h_{pi}|^2$  are independent exponentially distributed

random variables with respective means of  $\sigma_{si}^2$  and  $\sigma_{pi}^2$ , we have 496

$$\Pr(|h_{si}|^2 < \Lambda) = 1 - \exp\left(-\frac{\Lambda}{\sigma_{si}^2}\right), \quad (43)$$

and 497

$$\Pr(|h_{si}|^2 < \Lambda | h_{pi}|^2 \gamma_p + \Lambda) = 1 - \frac{\sigma_{si}^2}{\sigma_{pi}^2 \gamma_p \Lambda + \sigma_{si}^2} \exp\left(-\frac{\Lambda}{\sigma_{si}^2}\right), \quad (44)$$

where the terms  $\Pr(|h_{si}|^2 > \Lambda)$ ,  $\Pr(|h_{sj}|^2 < \Lambda)$ , and  $\Pr(|h_{si}|^2 > 498$   
 $\Lambda | h_{pi}|^2 \gamma_p + \Lambda)$  can be similarly determined in closed-form. 499  
 Moreover, based on Appendix A, we obtain  $\Pr(\max_{i \in \mathcal{D}_n} |h_{id}|^2 < \Lambda)$  500

and  $\Pr(\max_{i \in \mathcal{D}_n} |h_{id}|^2 < \Lambda | h_{pd}|^2 \gamma_p + \Lambda)$  as 501

$$\Pr\left(\max_{i \in \mathcal{D}_n} |h_{id}|^2 < \Lambda\right) = \prod_{i \in \mathcal{D}_n} \left[1 - \exp\left(-\frac{\Lambda}{\sigma_{id}^2}\right)\right], \quad (45)$$

and 502

$$\begin{aligned} & \Pr\left(\max_{i \in \mathcal{D}_n} |h_{id}|^2 < \Lambda | h_{pd}|^2 \gamma_p + \Lambda\right) \\ &= 1 + \sum_{m=1}^{2^{|\mathcal{D}_n|}-1} (-1)^{|\tilde{\mathcal{D}}_n(m)|} \exp\left(-\sum_{i \in \tilde{\mathcal{D}}_n(m)} \frac{\Lambda}{\sigma_{id}^2}\right) \\ & \quad \times \left(1 + \sum_{i \in \mathcal{D}_n(m)} \frac{\Lambda \gamma_p \sigma_{pd}^2}{\sigma_{id}^2}\right)^{-1}, \end{aligned} \quad (46)$$

where  $\tilde{\mathcal{D}}_n(m)$  represents the  $m$ -th non-empty subset of  $\mathcal{D}_n$ . 503  
 Additionally, the IP of the SRS scheme can be expressed as 504

$$P_{\text{int}}^{\text{single}} = \Pr(C_{be} > R, \mathcal{D} = \emptyset | \hat{H} = H_0) + \sum_{n=1}^{2^N-1} \Pr(C_{be} > R, \mathcal{D} = \mathcal{D}_n | \hat{H} = H_0), \quad (47)$$

where  $C_{be}$  represents the capacity of the channel spanning from 505  
 the ‘‘best’’ SR to E. Given  $\mathcal{D} = \emptyset$ , we have  $C_{be} = 0$ , since 506  
 no relay is chosen for forwarding the source signal. Thus, 507

---


$$\begin{aligned} P_{\text{out}}^{\text{single}} &= \pi_0 \prod_{i=1}^N \Pr(|h_{si}|^2 < \Lambda) + \pi_1 \prod_{i=1}^N \Pr(|h_{si}|^2 < \Lambda | h_{pi}|^2 \gamma_p + \Lambda) \\ &+ \pi_0 \sum_{n=1}^{2^N-1} \prod_{i \in \mathcal{D}_n} \Pr(|h_{si}|^2 > \Lambda) \prod_{j \in \tilde{\mathcal{D}}_n} \Pr(|h_{sj}|^2 < \Lambda) \Pr\left(\max_{i \in \mathcal{D}_n} |h_{id}|^2 < \Lambda\right) \\ &+ \pi_1 \sum_{n=1}^{2^N-1} \prod_{i \in \mathcal{D}_n} \Pr(|h_{si}|^2 > \Lambda | h_{pi}|^2 \gamma_p + \Lambda) \prod_{j \in \tilde{\mathcal{D}}_n} \Pr(|h_{sj}|^2 < \Lambda | h_{pj}|^2 \gamma_p + \Lambda) \\ & \quad \times \Pr\left(\max_{i \in \mathcal{D}_n} |h_{id}|^2 < \Lambda | h_{pd}|^2 \gamma_p + \Lambda\right) \end{aligned} \quad (42)$$

508 substituting this result into (47) and using (2), (9), (10), and  
509 (16), we arrive at

$$\begin{aligned}
P_{\text{int}}^{\text{single}} &= \pi_0 \sum_{n=1}^{2^N-1} \prod_{i \in \mathcal{D}_n} \Pr(|h_{si}|^2 > \Lambda) \prod_{j \in \overline{\mathcal{D}}_n} \Pr(|h_{sj}|^2 < \Lambda) \\
&\quad \times \Pr(|h_{be}|^2 > \Lambda) \\
&+ \pi_1 \sum_{n=1}^{2^N-1} \prod_{i \in \mathcal{D}_n} \Pr(|h_{si}|^2 > \Lambda |h_{pi}|^2 \gamma_p + \Lambda) \\
&\quad \times \prod_{j \in \overline{\mathcal{D}}_n} \Pr(|h_{sj}|^2 < \Lambda |h_{pj}|^2 \gamma_p + \Lambda) \\
&\quad \times \Pr(|h_{be}|^2 > \Lambda |h_{pe}|^2 \gamma_p + \Lambda), \quad (48)
\end{aligned}$$

510 where the closed-form expressions of  $\Pr(|h_{si}|^2 > \Lambda)$  and  
511  $\Pr(|h_{si}|^2 > \Lambda |h_{pi}|^2 \gamma_p + \Lambda)$  can be readily obtained by using  
512 (43) and (44). Using the results in Appendix B, we can express  
513  $\Pr(|h_{be}|^2 > \Lambda)$  and  $\Pr(|h_{be}|^2 > \Lambda |h_{pe}|^2 \gamma_p + \Lambda)$  as

$$\begin{aligned}
\Pr(|h_{be}|^2 > \Lambda) &= \sum_{i \in \mathcal{D}_n} \exp\left(-\frac{\Lambda}{\sigma_{ie}^2}\right) \\
&\times \left[ 1 + \sum_{m=1}^{2^{|\mathcal{D}_n|-1}-1} (-1)^{|C_n(m)|} \left( 1 + \sum_{j \in C_n(m)} \frac{\sigma_{id}^2}{\sigma_{jd}^2} \right)^{-1} \right], \quad (49)
\end{aligned}$$

514 and

$$\begin{aligned}
\Pr(|h_{be}|^2 > \Lambda |h_{pe}|^2 \gamma_p + \Lambda) &= \sum_{i \in \mathcal{D}_n} \frac{\sigma_{ie}^2}{\sigma_{pe}^2 \gamma_p \Lambda + \sigma_{ie}^2} \exp\left(-\frac{\Lambda}{\sigma_{ie}^2}\right) \\
&\times \left[ 1 + \sum_{m=1}^{2^{|\mathcal{D}_n|-1}-1} (-1)^{|C_n(m)|} \left( 1 + \sum_{j \in C_n(m)} \frac{\sigma_{id}^2}{\sigma_{jd}^2} \right)^{-1} \right], \quad (50)
\end{aligned}$$

515 where  $C_n(m)$  represents the  $m$ -th non-empty subset of  $\mathcal{D}_n - \{i\}$   
516 and ‘-’ represents the set difference.

### 517 C. Multi-Relay Selection

518 This subsection analyzes the SRT of our MRS scheme for  
519 transmission over Rayleigh fading channels. Similarly to (41),

the OP in this case is given by

520

$$\begin{aligned}
P_{\text{out}}^{\text{multi}} &= \Pr(\mathcal{D} = \emptyset | \hat{H} = H_0) \\
&+ \sum_{n=1}^{2^N-1} \Pr\left(C_d^{\text{multi}} < R, \mathcal{D} = \mathcal{D}_n | \hat{H} = H_0\right). \quad (51)
\end{aligned}$$

Using (2), (9), (10) and (23), we can rewrite (51) as (52), shown  
521 at the bottom of the page, where the closed-form expressions  
522 of  $\Pr(|h_{si}|^2 < \Lambda)$ ,  $\Pr(|h_{si}|^2 < \Lambda |h_{pi}|^2 \gamma_p + \Lambda)$ ,  $\Pr(|h_{si}|^2 > \Lambda)$ ,  
523  $\Pr(|h_{sj}|^2 < \Lambda)$  and  $\Pr(|h_{si}|^2 > \Lambda |h_{pi}|^2 \gamma_p + \Lambda)$  can be readily  
524 derived, as shown in (43) and (44). However, it is challenging  
525 to obtain the closed-form expressions of  $\Pr(\sum_{i \in \mathcal{D}_n} |h_{id}|^2 < \Lambda)$  and  
526  $\Pr(\sum_{i \in \mathcal{D}_n} |h_{id}|^2 < \gamma_p \Lambda |h_{pd}|^2 + \Lambda)$ . For simplicity, we assume that

527 the fading coefficients of all SRs-SD channels, i.e.  $|h_{id}|^2$  for  
528  $i \in \{1, 2, \dots, N\}$ , are i.i.d. RVs having the same mean (average  
529 channel gain) denoted by  $\sigma_d^2 = E(|h_{id}|^2)$ . This assumption is  
530 widely used in the cooperative relaying literature and it is  
531 valid in a statistical sense, provided that all SRs are uniformly  
532 distributed over a certain geographical area. Assuming that  
533 RVs of  $|h_{id}|^2$  for  $i \in \mathcal{D}_n$  are i.i.d., based on Appendix C,  
534 we arrive at

$$\Pr\left(\sum_{i \in \mathcal{D}_n} |h_{id}|^2 < \Lambda\right) = \Gamma\left(\frac{\Lambda}{\sigma_d^2}, |\mathcal{D}_n|\right), \quad (53)$$

and

536

$$\begin{aligned}
\Pr\left(\sum_{i \in \mathcal{D}_n} |h_{id}|^2 < \gamma_p \Lambda |h_{pd}|^2 + \Lambda\right) &= \Gamma\left(\frac{\Lambda}{\sigma_d^2}, |\mathcal{D}_n|\right) \\
&+ \frac{\left[1 - \Gamma\left(\Lambda \sigma_d^{-2} + \sigma_{pd}^{-2} \gamma_p^{-1}, |\mathcal{D}_n|\right)\right]}{\left(1 + \sigma_d^2 \sigma_{pd}^{-2} \gamma_p^{-1} \Lambda^{-1}\right)^{|\mathcal{D}_n|}} e^{1/(\sigma_{pd}^2 \gamma_p)}, \quad (54)
\end{aligned}$$

537 where  $\Gamma(x, k) = \int_0^x \frac{t^{k-1}}{\Gamma(k)} e^{-t} dt$  is known as the incomplete  
538 Gamma function [32]. Substituting (53) and (54) into (52)  
539 yields a closed-form OP expression for the proposed MRS  
540 scheme.

$$\begin{aligned}
P_{\text{out}}^{\text{multi}} &= \pi_0 \prod_{i=1}^N \Pr(|h_{si}|^2 < \Lambda) + \pi_1 \prod_{i=1}^N \Pr(|h_{si}|^2 < \Lambda |h_{pi}|^2 \gamma_p + \Lambda) \\
&+ \pi_0 \sum_{n=1}^{2^N-1} \prod_{i \in \mathcal{D}_n} \Pr(|h_{si}|^2 > \Lambda) \prod_{j \in \overline{\mathcal{D}}_n} \Pr(|h_{sj}|^2 < \Lambda) \Pr\left(\sum_{i \in \mathcal{D}_n} |h_{id}|^2 < \Lambda\right) \\
&+ \pi_1 \sum_{n=1}^{2^N-1} \prod_{i \in \mathcal{D}_n} \Pr(|h_{si}|^2 > \Lambda |h_{pi}|^2 \gamma_p + \Lambda) \prod_{j \in \overline{\mathcal{D}}_n} \Pr(|h_{sj}|^2 < \Lambda |h_{pj}|^2 \gamma_p + \Lambda) \\
&\quad \times \Pr\left(\sum_{i \in \mathcal{D}_n} |h_{id}|^2 < \gamma_p \Lambda |h_{pd}|^2 + \Lambda\right) \quad (52)
\end{aligned}$$

541 Next, we present the IP analysis of the MRS scheme. Simi-  
 542 larly to (48), the IP of the MRS can be obtained from (24) as

$$\begin{aligned}
 P_{\text{int}}^{\text{multi}} = & \pi_0 \sum_{n=1}^{2^N-1} \prod_{i \in \mathcal{D}_n} \Pr(|h_{si}|^2 > \Lambda) \prod_{j \in \mathcal{D}_n} \Pr(|h_{sj}|^2 < \Lambda) \\
 & \times \Pr\left(\frac{|H_d^H H_e|^2}{|H_d|^2} > \Lambda\right) \\
 & + \pi_1 \sum_{n=1}^{2^N-1} \prod_{i \in \mathcal{D}_n} \Pr(|h_{si}|^2 > \Lambda |h_{pi}|^2 \gamma_p + \Lambda) \\
 & \times \prod_{j \in \mathcal{D}_n} \Pr(|h_{sj}|^2 < \Lambda |h_{pj}|^2 \gamma_p + \Lambda) \\
 & \times \Pr\left(\frac{|H_d^H H_e|^2}{|H_d|^2} > \gamma_p \Lambda |h_{pe}|^2 + \Lambda\right), \quad (55)
 \end{aligned}$$

543 where the closed-form expressions of  $\Pr(|h_{si}|^2 > \Lambda)$ ,  
 544  $\Pr(|h_{sj}|^2 < \Lambda)$ ,  $\Pr(|h_{si}|^2 > \Lambda |h_{pi}|^2 \gamma_p + \Lambda)$  and  $\Pr(|h_{sj}|^2 < \Lambda$   
 545  $\Lambda |h_{pj}|^2 \gamma_p + \Lambda)$  may be readily derived by using (43) and (44).  
 546 However, it is challenging to obtain the closed-form solutions  
 547 for  $\Pr\left(\frac{|H_d^H H_e|^2}{|H_d|^2} > \Lambda\right)$  and  $\Pr\left(\frac{|H_d^H H_e|^2}{|H_d|^2} > \gamma_p \Lambda |h_{pe}|^2 + \Lambda\right)$ .  
 548 Although finding a general closed-form IP expression for the  
 549 MRS scheme is challenging, we can obtain the numerical IP  
 550 results with the aid of computer simulations.

#### 551 IV. NUMERICAL RESULTS AND DISCUSSIONS

552 In this section, we present our performance comparisons  
 553 among the direct transmission, the SRS and MRS schemes  
 554 in terms of their SRT. To be specific, the analytic IP versus  
 555 OP of the three schemes are obtained by plotting (33), (37),  
 556 (42), (48), (52), and (55). The simulated IP and OP results of  
 557 the three schemes are also given to verify the correctness of  
 558 the theoretical SRT analysis. In our computer simulations, the  
 559 fading amplitudes (e.g.,  $|h_{sd}|$ ,  $|h_{si}|$ ,  $|h_{id}|$ , etc.) are first generated  
 560 based on the Rayleigh distribution having different variances  
 561 for different channels. Then, the randomly generated fading  
 562 amplitudes are substituted into the definition of an outage (or  
 563 intercept) event, which would determine whether an outage (or  
 564 intercept) event occurs or not. By repeatedly achieving this pro-  
 565 cess, we can calculate the relative frequency of occurrence for  
 566 an outage (intercept) event, which is the simulated OP (or IP).  
 567 Additionally, the SDP  $P_d$  and FAP  $P_f$  are set to  $P_d = 0.99$   
 568 and  $P_f = 0.01$ , unless otherwise stated. The primary signal-  
 569 to-noise ratio (SNR) of  $\gamma_p = 10$  dB and the data rate of  
 570  $R = 1$  bit/s/Hz are used in our numerical evaluations.

571 The artificial noise based method [35], [36] is also consid-  
 572 ered for the purpose of numerical comparison with the relay  
 573 selection schemes. To be specific, in the artificial noise based  
 574 scheme, ST directly transmits its signal  $x_s$  to SD, while  $N$  SRs  
 575 attempt to confuse the eavesdropper by sending an interfering  
 576 signal (referred to as artificial noise) that is approximately  
 577 designed to lie in the null-space of the legitimate main channel.  
 578 In this way, the artificial noise will impose interference on the  
 579 eavesdropper without affecting the SD. For a fair comparison,  
 580 the total transmit power of the desired signal  $x_s$  and the artificial  
 581 noise are constrained to  $P_s$ . Moreover, the equal power alloca-  
 582 tion method [35] is used in the numerical evaluation.

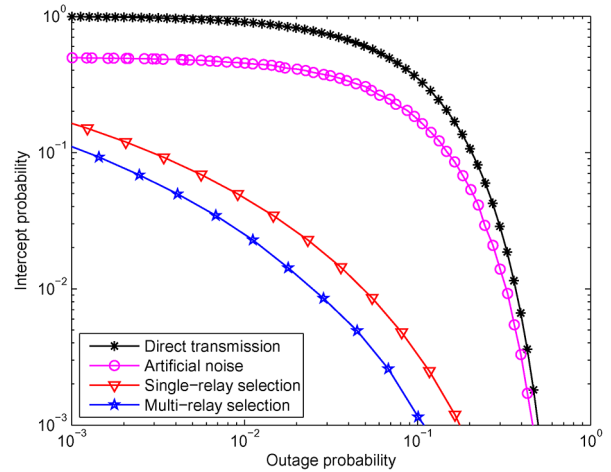


Fig. 3. IP versus OP of the direct transmission, the SRS and the MRS schemes for different  $P_0$  with  $P_0 = 0.8$ ,  $\gamma_s \in [0, 35]$  dB,  $N = 6$ ,  $\sigma_{sd}^2 = \sigma_{si}^2 = \sigma_{id}^2 = 1$ ,  $\sigma_{se}^2 = \sigma_{ie}^2 = 0.1$ , and  $\sigma_{pd}^2 = \sigma_{pe}^2 = \sigma_{pi}^2 = 0.2$ .

Fig. 3 shows the IP versus OP of the direct transmission,  
 583 as well as the SRS and MRS schemes for  $P_0 = 0.8$ , where  
 584 the solid lines and discrete marker symbols represent the an-  
 585 alytic and simulated results, respectively. It can be seen from  
 586 Fig. 3 that the IP of the direct transmission, the artificial noise  
 587 based as well as of the proposed SRS and MRS schemes all  
 588 improve upon tolerating a higher OP, implying that a trade-off  
 589 exists between the IP (security) and the OP (reliability) of CR  
 590 transmissions. Fig. 3 also shows that both the proposed SRS  
 591 and MRS schemes outperform the direct transmission and the  
 592 artificial noise based approaches in terms of their SRT, showing  
 593 the advantage of exploiting relay selection against the eaves-  
 594 dropping attack. Moreover, the SRT performance of the MRS is  
 595 better than that of the SRS. Although the MRS achieves a better  
 596 SRT performance than its SRS-aided counterpart, this result  
 597 is obtained at the cost of a higher implementation complexity,  
 598 since multiple SRs require high-complexity symbol-level syn-  
 599 chronization for simultaneously transmitting to the SD, whereas  
 600 the SRS does not require such elaborate synchronization. 601

Fig. 4 illustrates our numerical SRT comparison between the  
 602 SRS and MRS schemes for  $P_0 = 0.2$  and  $P_0 = 0.8$ . Observe  
 603 from Fig. 4 that the MRS scheme performs better than the SRS  
 604 in terms of its SRT performance for both  $P_0 = 0.2$  and  $P_0 = 0.8$ .  
 605 It is also seen from Fig. 4 that as  $P_0$  increases from 0.2 to  
 606 0.8, the SRT of both the SRS and MRS schemes improves.  
 607 This is because upon increasing  $P_0$ , the licensed band becomes  
 608 unoccupied by the PUs with a higher probability and hence the  
 609 secondary users (SUs) have more opportunities for accessing  
 610 the licensed band for their data transmissions, which leads  
 611 to a reduction of the OP for CR transmissions. Meanwhile,  
 612 increasing  $P_0$  may simultaneously result in an increase of the IP,  
 613 since the eavesdropper also has more opportunities for tapping  
 614 the cognitive transmissions. However, in both the SRS and  
 615 MRS schemes, the relay selection is performed for the sake  
 616 of maximizing the legitimate transmission capacity without  
 617 affecting the eavesdropper's channel capacity. Hence, upon  
 618 increasing  $P_0$ , it becomes more likely that the reduction of OP  
 619 is more significant than the increase of IP, hence leading to an  
 620 overall SRT improvement for the SRS and MRS schemes. 621

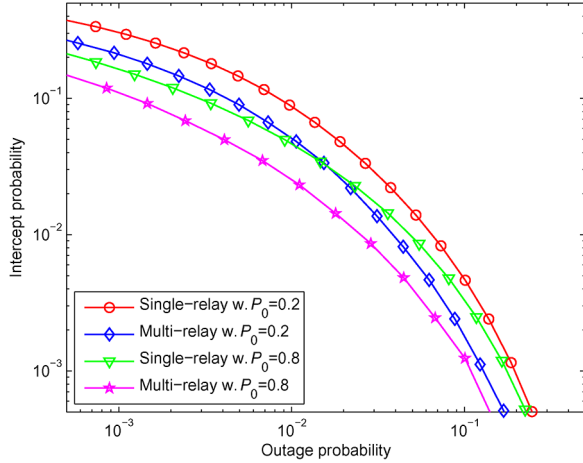


Fig. 4. IP versus OP of the SRS and MRS schemes for different  $P_0$  with  $\gamma_s \in [0, 30]$  dB,  $N = 6$ ,  $\sigma_{sd}^2 = \sigma_{si}^2 = \sigma_{id}^2 = 1$ ,  $\sigma_{se}^2 = \sigma_{ie}^2 = 0.1$ , and  $\sigma_{pd}^2 = \sigma_{pe}^2 = \sigma_{pi}^2 = 0.2$ .

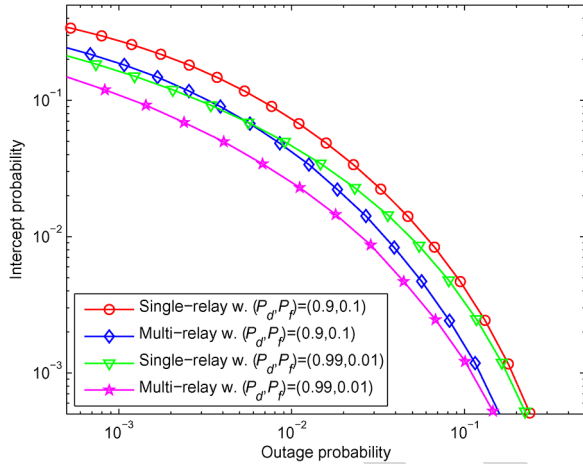


Fig. 5. IP versus OP of the SRS and the MRS schemes for different  $(P_d, P_f)$  with  $P_0 = 0.8$ ,  $\gamma_s \in [0, 30]$  dB,  $N = 6$ ,  $\sigma_{sd}^2 = \sigma_{si}^2 = \sigma_{id}^2 = 1$ ,  $\sigma_{se}^2 = \sigma_{ie}^2 = 0.1$ , and  $\sigma_{pd}^2 = \sigma_{pe}^2 = \sigma_{pi}^2 = 0.2$ .

In Fig. 5, we depict the IP versus OP of the SRS and MRS schemes for different spectrum sensing reliabilities, where  $(P_d, P_f) = (0.9, 0.1)$  and  $(P_d, P_f) = (0.99, 0.01)$  are considered. It is observed that as the spectrum sensing reliability is improved from  $(P_d, P_f) = (0.9, 0.1)$  to  $(P_d, P_f) = (0.99, 0.01)$ , the SRTs of the SRS and MRS schemes improve accordingly. This is due to the fact that for an improved sensing reliability, an unoccupied licensed band would be detected more accurately and hence less mutual interference occurs between the PUs and SUs, which results in a better SRT for the secondary transmissions. Fig. 5 also shows that for  $(P_d, P_f) = (0.9, 0.1)$  and  $(P_d, P_f) = (0.99, 0.01)$ , the MRS approach outperforms the SRS scheme in terms of the SRT, which further confirms the advantage of the MRS for protecting the secondary transmissions against eavesdropping attacks.

Fig. 6 shows the IP versus OP of the conventional direct transmission as well as of the proposed SRS and MRS schemes for  $N = 2, N = 4$ , and  $N = 8$ . It is seen from Fig. 6 that the SRTs

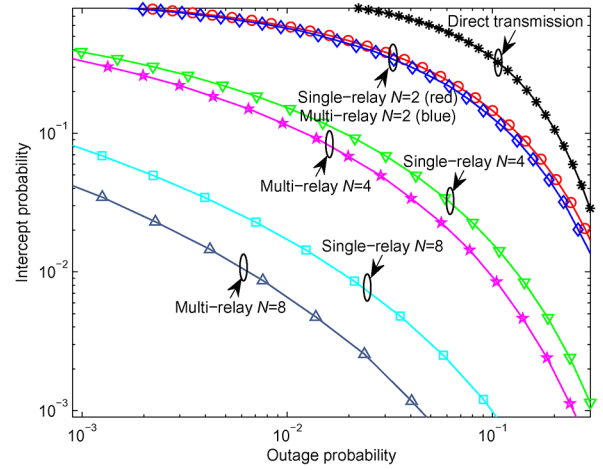


Fig. 6. IP versus OP of the direct transmission, the SRS and the MRS schemes for different  $N$  with  $P_0 = 0.8$ ,  $\gamma_s \in [0, 30]$  dB,  $\sigma_{sd}^2 = \sigma_{si}^2 = \sigma_{id}^2 = 1$ ,  $\sigma_{se}^2 = \sigma_{ie}^2 = 0.1$ , and  $\sigma_{pd}^2 = \sigma_{pe}^2 = \sigma_{pi}^2 = 0.2$ .

of the proposed SRS and MRS schemes are generally better than that of the conventional direct transmission for  $N = 2, 4$  and  $N = 8$ . Moreover, as the number of SRs increases from  $N = 2$  to  $8$ , the SRT of the SRS and MRS schemes significantly improves, explicitly demonstrating the security and reliability benefits of exploiting multiple SRs for assisting the secondary transmissions. In other words, the security and reliability of the secondary transmissions can be concurrently improved by increasing the number of SRs. Additionally, as shown in Fig. 6, upon increasing the number of SRs from  $N = 2$  to  $8$ , the SRT improvement of MRS over SRS becomes more notable. Again, the SRT advantage of the MRS over the SRS comes at the expense of requiring elaborate symbol-level synchronization among the multiple SRs for simultaneously transmitting to the SD.

## V. CONCLUSION

In this paper, we proposed relay selection schemes for a CR network consisting of a ST, a SD and multiple SRs communicating in the presence of an eavesdropper. We examined the SRT performance of the SRS and MRS assisted secondary transmissions in the presence of realistic spectrum sensing, where both the security and reliability of secondary transmissions are characterized in terms of their IP and OP respectively. We also analyzed the SRT of the conventional direct transmission as a benchmark. It was illustrated that as the spectrum sensing reliability increases, the SRTs of both the SRS and MRS schemes improve. We also showed that the proposed SRS and MRS schemes generally outperform the conventional direct transmission and artificial noise based approaches in terms of their SRT. Moreover, the SRT performance of MRS is better than that of SRS. Additionally, as the number of SRs increases, the SRTs of both the SRS and of the MRS schemes improve significantly, demonstrating their benefits in terms of enhancing both the security and reliability of secondary transmissions.

675 APPENDIX A  
676 DERIVATION OF (45) AND (46)

677 Letting  $|h_{id}|^2 = x_i$  and  $|h_{pd}|^2 = y$ , the left hand side of (45)  
678 and (46) can be rewritten as  $\Pr(\max_{i \in \mathcal{D}_n} x_i < \Lambda)$  and  $\Pr(\max_{i \in \mathcal{D}_n} x_i <$   
679  $\Lambda \gamma_p y + \Lambda)$ , respectively. Noting that random variables  $|h_{id}|^2$  and  
680  $|h_{pd}|^2$  are exponentially distributed with respective means  $\sigma_{id}^2$   
681 and  $\sigma_{pd}^2$ , and independent of each other, we obtain

$$\begin{aligned} \Pr\left(\max_{i \in \mathcal{D}_n} x_i < \Lambda\right) &= \prod_{i \in \mathcal{D}_n} \Pr(|h_{id}|^2 < \Lambda) \\ &= \prod_{i \in \mathcal{D}_n} \left[1 - \exp\left(-\frac{\Lambda}{\sigma_{id}^2}\right)\right], \end{aligned} \quad (\text{A.1})$$

682 which is (45). Similarly, the term  $\Pr(\max_{i \in \mathcal{D}_n} x_i < \Lambda \gamma_p y + \Lambda)$  can be  
683 computed as

$$\begin{aligned} \Pr\left(\max_{i \in \mathcal{D}_n} x_i < \Lambda \gamma_p y + \Lambda\right) \\ &= \int_0^\infty \frac{1}{\sigma_{pd}^2} \exp\left(-\frac{y}{\sigma_{pd}^2}\right) \prod_{i \in \mathcal{D}_n} \left(1 - \exp\left(-\frac{\Lambda \gamma_p y + \Lambda}{\sigma_{id}^2}\right)\right) dy, \end{aligned} \quad (\text{A.2})$$

684 wherein  $\prod_{i \in \mathcal{D}_n} \left(1 - \exp\left(-\frac{\Lambda \gamma_p y + \Lambda}{\sigma_{id}^2}\right)\right)$  can be further expanded  
685 as

$$\begin{aligned} \prod_{i \in \mathcal{D}_n} \left(1 - \exp\left(-\frac{\Lambda \gamma_p y + \Lambda}{\sigma_{id}^2}\right)\right) &= 1 \\ &+ \sum_{m=1}^{2^{|\mathcal{D}_n|-1}} (-1)^{|\tilde{\mathcal{D}}_n(m)|} \exp\left(-\sum_{i \in \tilde{\mathcal{D}}_n(m)} \frac{\Lambda \gamma_p y + \Lambda}{\sigma_{id}^2}\right), \end{aligned} \quad (\text{A.3})$$

686 where  $|\mathcal{D}_n|$  is the cardinality of set  $\mathcal{D}_n$ ,  $\tilde{\mathcal{D}}_n(m)$  represents the  
687  $m$ -th non-empty subset of  $\mathcal{D}_n$ , and  $|\tilde{\mathcal{D}}_n(m)|$  is the cardinality  
688 of set  $\tilde{\mathcal{D}}_n(m)$ . Substituting  $\prod_{i \in \mathcal{D}_n} \left(1 - \exp\left(-\frac{\Lambda \gamma_p y + \Lambda}{\sigma_{id}^2}\right)\right)$  from  
689 (A.3) into (A.2) yields

$$\begin{aligned} \Pr\left(\max_{i \in \mathcal{D}_n} x_i < \Lambda \gamma_p y + \Lambda\right) &= \int_0^\infty \frac{1}{\sigma_{pd}^2} \exp\left(-\frac{y}{\sigma_{pd}^2}\right) dy \\ &+ \sum_{m=1}^{2^{|\mathcal{D}_n|-1}} (-1)^{|\tilde{\mathcal{D}}_n(m)|} \frac{1}{\sigma_{pd}^2} \\ &\times \int_0^\infty \exp\left(-\frac{y}{\sigma_{pd}^2} - \sum_{i \in \tilde{\mathcal{D}}_n(m)} \frac{\Lambda \gamma_p y + \Lambda}{\sigma_{id}^2}\right) dy. \end{aligned} \quad (\text{A.4})$$

Finally, performing the integration of (A.4) yields

$$\begin{aligned} \Pr\left(\max_{i \in \mathcal{D}_n} x_i < \Lambda \gamma_p y + \Lambda\right) &= 1 \\ &+ \sum_{m=1}^{2^{|\mathcal{D}_n|-1}} (-1)^{|\tilde{\mathcal{D}}_n(m)|} \exp\left(-\sum_{i \in \tilde{\mathcal{D}}_n(m)} \frac{\Lambda}{\sigma_{id}^2}\right) \\ &\times \left(1 + \sum_{i \in \tilde{\mathcal{D}}_n(m)} \frac{\Lambda \gamma_p \sigma_{pd}^2}{\sigma_{id}^2}\right)^{-1}. \end{aligned} \quad (\text{A.5})$$

This completes the proof of (45) and (46).

692 APPENDIX B  
693 PROOF OF (49) AND (50)

Given  $\mathcal{D} = \mathcal{D}_n$ , any SR within  $\mathcal{D}_n$  can be selected as the  
“best” relay for forwarding the source signal. Thus, using the  
law of total probability, we have

$$\begin{aligned} \Pr(|h_{be}|^2 > \Lambda) &= \sum_{i \in \mathcal{D}_n} \Pr(|h_{ie}|^2 > \Lambda, b = i) \\ &= \sum_{i \in \mathcal{D}_n} \Pr\left(|h_{ie}|^2 > \Lambda, |h_{id}|^2 > \max_{j \in \mathcal{D}_n - \{i\}} |h_{jd}|^2\right) \\ &= \sum_{i \in \mathcal{D}_n} \Pr(|h_{ie}|^2 > \Lambda) \Pr\left(\max_{j \in \mathcal{D}_n - \{i\}} |h_{jd}|^2 < |h_{id}|^2\right), \end{aligned} \quad (\text{B.1})$$

where in the first line, variable ‘ $b$ ’ stands for the best SR and  
the second equality is obtained from (13) and ‘ $-$ ’ represents the  
set difference. Noting that  $|h_{ie}|^2$  is an exponentially distributed  
random variable with a mean of  $\sigma_{ie}^2$ , we obtain

$$\Pr(|h_{ie}|^2 > \Lambda) = \exp\left(-\frac{\Lambda}{\sigma_{ie}^2}\right). \quad (\text{B.2})$$

Letting  $|h_{jd}|^2 = x_j$  and  $|h_{id}|^2 = y$ , we have

$$\begin{aligned} \Pr\left(\max_{j \in \mathcal{D}_n - \{i\}} |h_{jd}|^2 < |h_{id}|^2\right) \\ &= \int_0^\infty \frac{1}{\sigma_{id}^2} \exp\left(-\frac{y}{\sigma_{id}^2}\right) \prod_{j \in \mathcal{D}_n - \{i\}} \left(1 - \exp\left(-\frac{y}{\sigma_{jd}^2}\right)\right) dy, \end{aligned} \quad (\text{B.3})$$

wherein  $\prod_{j \in \mathcal{D}_n - \{i\}} \left(1 - \exp\left(-\frac{y}{\sigma_{jd}^2}\right)\right)$  is expanded by

$$\begin{aligned} \prod_{j \in \mathcal{D}_n - \{i\}} \left(1 - \exp\left(-\frac{y}{\sigma_{jd}^2}\right)\right) &= 1 \\ &+ \sum_{m=1}^{2^{|\mathcal{D}_n|-1}-1} (-1)^{|C_n(m)|} \exp\left(-\sum_{j \in C_n(m)} \frac{y}{\sigma_{jd}^2}\right), \end{aligned} \quad (\text{B.4})$$

where  $|\mathcal{D}_n|$  denotes the cardinality of the set  $\mathcal{D}_n$  and  $C_n(m)$   
represents the  $m$ -th non-empty subset of “ $\mathcal{D}_n - \{i\}$ ”. Combining  
(B.3) and (B.4), we obtain

$$\begin{aligned} \Pr\left(\max_{j \in \mathcal{D}_n - \{i\}} |h_{jd}|^2 < |h_{id}|^2\right) &= 1 \\ &+ \sum_{m=1}^{2^{|\mathcal{D}_n|-1}-1} (-1)^{|C_n(m)|} \left(1 + \sum_{j \in C_n(m)} \frac{\sigma_{id}^2}{\sigma_{jd}^2}\right)^{-1}. \end{aligned} \quad (\text{B.5})$$

706 Substituting (B.2) and (B.5) into (B.1) gives (B.6), shown at  
707 the bottom of the page, which is (49). Similarly to (B.1), we  
708 can rewrite  $\Pr(|h_{be}|^2 > \Lambda|h_{pe}|^2\gamma_p + \Lambda)$  as

$$\begin{aligned} & \Pr(|h_{be}|^2 > \Lambda|h_{pe}|^2\gamma_p + \Lambda) \\ &= \sum_{i \in \mathcal{D}_n} \Pr(|h_{ie}|^2 > \Lambda|h_{pe}|^2\gamma_p + \Lambda) \\ & \quad \times \Pr\left(\max_{j \in \{\mathcal{D}_n - i\}} |h_{jd}|^2 < |h_{id}|^2\right). \end{aligned} \quad (\text{B.7})$$

709 Since the random variables  $|h_{ie}|^2$  and  $|h_{pe}|^2$  are independently  
710 and exponentially distributed with respective means of  $\sigma_{ie}^2$  and  
711  $\sigma_{pe}^2$ , we readily arrive at

$$\Pr(|h_{ie}|^2 > \Lambda|h_{pe}|^2\gamma_p + \Lambda) = \frac{\sigma_{ie}^2}{\sigma_{pe}^2\gamma_p\Lambda + \sigma_{ie}^2} \exp\left(-\frac{\Lambda}{\sigma_{ie}^2}\right). \quad (\text{B.8})$$

712 Substituting (B.5) and (B.8) into (B.7) gives (B.9), shown at the  
713 bottom of the page, which is (50).

#### APPENDIX C

#### PROOF OF (53) AND (54)

714 Upon introducing the notation of  $X = \sum_{i \in \mathcal{D}_n} |h_{id}|^2$  and  $Y =$   
715  $|h_{pd}|^2$ , we can rewrite the terms  $\Pr(\sum_{i \in \mathcal{D}_n} |h_{id}|^2 < \Lambda)$  and  
716  $\Pr(\sum_{i \in \mathcal{D}_n} |h_{id}|^2 < \gamma_p\Lambda|h_{pd}|^2 + \Lambda)$  as  $\Pr(X < \Lambda)$  and  $\Pr(X <$   
717  $\gamma_p\Lambda Y + \Lambda)$ , respectively. Noting that the fading coefficients of  
718 all SR-SD channels, i.e.  $|h_{id}|^2$  for  $i \in \{1, 2, \dots, N\}$ , are assumed  
719 to be i.i.d., we obtain the probability density function (PDF) of  
720  $X = \sum_{i \in \mathcal{D}_n} |h_{id}|^2$  as

$$f_X(x) = \frac{1}{\Gamma(|\mathcal{D}_n|)\sigma_d^{2|\mathcal{D}_n|}} x^{|\mathcal{D}_n|-1} \exp\left(-\frac{x}{\sigma_d^2}\right), \quad (\text{C.1})$$

723 where  $\sigma_d^2 = E(|h_{id}|^2)$ . Meanwhile, the random variable  $Y =$   
724  $|h_{pd}|^2$  is exponentially distributed and its PDF is given by

$$f_Y(y) = \frac{1}{\sigma_{pd}^2} \exp\left(-\frac{y}{\sigma_{pd}^2}\right), \quad (\text{C.2})$$

where  $\sigma_{pd}^2 = E(|h_{pd}|^2)$ . Using (C.1), we arrive at

$$\begin{aligned} \Pr(X < \Lambda) &= \int_0^\Lambda \frac{1}{\Gamma(|\mathcal{D}_n|)\sigma_d^{2|\mathcal{D}_n|}} x^{|\mathcal{D}_n|-1} \exp\left(-\frac{x}{\sigma_d^2}\right) dx \\ &= \int_0^{\frac{\Lambda}{\sigma_d^2}} \frac{t^{|\mathcal{D}_n|-1}}{\Gamma(|\mathcal{D}_n|)} \exp(-t) dt \\ &= \Gamma\left(\frac{\Lambda}{\sigma_d^2}, |\mathcal{D}_n|\right), \end{aligned} \quad (\text{C.3})$$

725 where the second equality is obtained by substituting  $\frac{x}{\sigma_d^2} = t$  and

726  $\Gamma(a, k) = \int_0^k \frac{t^{a-1}}{\Gamma(a)} \exp(-t) dt$  is known as the incomplete Gamma  
727 function. Additionally, considering that the random variables  $X$   
728 and  $Y$  are independent of each other, we obtain  $\Pr(X < \gamma_p\Lambda Y +$   
729  $\Lambda)$  as

$$\begin{aligned} \Pr(X < \gamma_p\Lambda Y + \Lambda) &= \int_0^\Lambda f_X(x) dx \\ & \quad + \int_\Lambda^\infty \int_{-\frac{x}{\gamma_p\Lambda} - \frac{1}{\gamma_p}}^\infty f_X(x) f_Y(y) dx dy. \end{aligned} \quad (\text{C.4})$$

730 Substituting  $f_X(x)$  and  $f_Y(y)$  from (C.1) and (C.2) into (C.4)  
731 yields

$$\begin{aligned} & \Pr(X < \gamma_p\Lambda Y + \Lambda) \\ &= \Gamma\left(\frac{\Lambda}{\sigma_d^2}, |\mathcal{D}_n|\right) \\ & \quad + \int_\Lambda^\infty \frac{e^{1/(\sigma_{pd}^2\gamma_p)} x^{|\mathcal{D}_n|-1}}{\Gamma(|\mathcal{D}_n|)\sigma_d^{2|\mathcal{D}_n|}} \exp\left(-\frac{x}{\sigma_d^2} - \frac{x}{\sigma_{pd}^2\gamma_p\Lambda}\right) dx \\ &= \Gamma\left(\frac{\Lambda}{\sigma_d^2}, |\mathcal{D}_n|\right) + \frac{\left[1 - \Gamma\left(\Lambda\sigma_d^{-2} + \sigma_{pd}^{-2}\gamma_p^{-1}, |\mathcal{D}_n|\right)\right]}{\left(1 + \sigma_d^2\sigma_{pd}^{-2}\gamma_p^{-1}\Lambda^{-1}\right)^{|\mathcal{D}_n|}} e^{1/(\sigma_{pd}^2\gamma_p)}, \end{aligned} \quad (\text{C.5})$$

732 where the second equality is obtained by using  $\frac{x}{\sigma_d^2} + \frac{x}{\sigma_{pd}^2\gamma_p\Lambda} = t$ .

733 Hence, we have completed the proof of (53) and (54) as (C.3)  
734 and (C.5), respectively. 735

$$\Pr(|h_{be}|^2 > \Lambda) = \sum_{i \in \mathcal{D}_n} \exp\left(-\frac{\Lambda}{\sigma_{ie}^2}\right) \left[1 + \sum_{m=1}^{2^{|\mathcal{D}_n|-1}-1} (-1)^{|C_n(m)|} \left(1 + \sum_{j \in C_n(m)} \frac{\sigma_{id}^2}{\sigma_{jd}^2}\right)^{-1}\right] \quad (\text{B.6})$$

$$\Pr(|h_{be}|^2 > \Lambda|h_{pe}|^2\gamma_p + \Lambda) = \sum_{i \in \mathcal{D}_n} \frac{\sigma_{ie}^2}{\sigma_{pe}^2\gamma_p\Lambda + \sigma_{ie}^2} \exp\left(-\frac{\Lambda}{\sigma_{ie}^2}\right) \left[1 + \sum_{m=1}^{2^{|\mathcal{D}_n|-1}-1} (-1)^{|C_n(m)|} \left(1 + \sum_{j \in C_n(m)} \frac{\sigma_{id}^2}{\sigma_{jd}^2}\right)^{-1}\right] \quad (\text{B.9})$$

## REFERENCES

- 736
- 737 [1] J. Mitola and G. Q. Maguire, "Cognitive radio: Making software radios  
738 more personal," *IEEE Pers. Commun.*, vol. 6, no. 4, pp. 13–18, Aug. 1999.
- 739 [2] IEEE 802.22 Working Group, IEEE P802.22/D1.0 draft standard for  
740 wireless regional area networks part 22: Cognitive wireless RAN medium  
741 access control (MAC) and physical layer (PHY) specifications: Policies  
742 and procedures for operation in the TV bands, Apr. 2008.
- 743 [3] G. Baldini, T. Sturman, A. R. Biswas, and R. Leschhorn, "Security aspects  
744 in software defined radio and cognitive radio networks: A survey and a  
745 way ahead," *IEEE Commun. Surveys Tuts.*, vol. 14, no. 2, pp. 355–379,  
746 May 2012.
- 747 [4] D. Cabric, S. M. Mishra, and R. W. Brodersen, "Implementation issues in  
748 spectrum sensing for cognitive radios," in *Proc. 38th Asil. Conf. Signal,  
749 Syst. Comput.*, Pacific Grove, CA, USA, Nov. 2004, pp. 772–776.
- 750 [5] H. Li, "Cooperative spectrum sensing via belief propagation in spectrum-  
751 heterogeneous cognitive radio systems," in *Proc. IEEE WCNC*, Sydney,  
752 N.S.W., Australia, Apr. 2010, pp. 1–6.
- 753 [6] J. Ma, G. Zhao, and Y. Li, "Soft combination and detection for cooperative  
754 spectrum sensing in cognitive radio networks," *IEEE Trans. Wireless  
755 Commun.*, vol. 7, no. 11, pp. 4502–4507, Nov. 2008.
- 756 [7] A. Ghasemi and E. S. Sousa, "Fundamental limits of spectrum-sharing  
757 in fading environments," *IEEE Trans. Wireless Commun.*, vol. 6, no. 2,  
758 pp. 649–658, Feb. 2007.
- 759 [8] R. Southwell, J. Huang, and X. Liu, "Spectrum mobility games," in *Proc.  
760 31st INFOCOM*, Orlando, FL, USA, Mar. 2012, pp. 37–45.
- 761 [9] I. F. Akyildiz, W.-Y. Lee, M. C. Vuran, and S. Mohanty, "A survey on  
762 spectrum management in cognitive radio networks," *IEEE Commun.  
763 Mag.*, vol. 46, no. 4, pp. 40–48, Apr. 2008.
- 764 [10] H. Li and Z. Han, "Dogfight in spectrum: Combating primary user em-  
765 ulation attacks in cognitive radio systems part I: Known channel statis-  
766 tics," *IEEE Trans. Wireless Commun.*, vol. 9, no. 11, pp. 3566–3577,  
767 Nov. 2010.
- 768 [11] T. Brown and A. Sethi, "Potential cognitive radio denial-of-service vulner-  
769 abilities and protection countermeasures: A multi-dimensional analysis  
770 and assessment," in *Proc. 2nd Int. Conf. CROWCOM*, Orlando, FL,  
771 USA, Aug. 2007, pp. 456–464.
- 772 [12] S. Lakshmanan, C. Tsao, R. Sivakumar, and K. Sundaresan, "Securing  
773 wireless data networks against eavesdropping using smart antennas," in  
774 *Proc. 28th ICDCS*, Beijing, China, Jun. 2008, pp. 19–27.
- 775 [13] A. Olteanu and Y. Xiao, "Security overhead and performance for aggrega-  
776 tion with fragment retransmission (AFR) in very high-speed wireless  
777 802.11 LANs," *IEEE Trans. Wireless Commun.*, vol. 9, no. 1, pp. 218–  
778 226, Jan. 2010.
- 779 [14] Y. Xiao, V. K. Rayi, X. Du, F. Hu, and M. Galloway, "A survey of key  
780 management schemes in wireless sensor networks," *Comput. Commun.*,  
781 vol. 30, no. 11–12, pp. 2314–2341, Sep. 2007.
- 782 [15] A. Mukherjee, S. A. Fakoorian, J. Huang, and A. L. Swindlehurst,  
783 "Principles of physical layer security in multiuser wireless networks: A  
784 survey," *IEEE Commun. Surveys Tuts.*, vol. 16, no. 3, pp. 1550–1573,  
785 Aug. 2014.
- 786 [16] A. D. Wyner, "The wire-tap channel," *Bell Syst. Tech. J.*, vol. 54, no. 8,  
787 pp. 1355–1387, 1975.
- 788 [17] S. K. Leung-Yan-Cheong and M. E. Hellman, "The Gaussian wire-  
789 tap channel," *IEEE Trans. Inf. Theory*, vol. 24, no. 4, pp. 451–456,  
790 Jul. 1978.
- 791 [18] P. Parada and R. Blahut, "Secrecy capacity of SIMO and slow fading  
792 channels," in *Proc. IEEE ISIT*, Adelaide, SA, Australia, Sep. 2005,  
793 pp. 2152–2155.
- 794 [19] M. Bloch, J. O. Barros, M. R. D. Rodrigues, and S. W. McLaughlin,  
795 "Wireless information-theoretic security," *IEEE Trans. Inf. Theory*, vol. 54,  
796 no. 6, pp. 2515–2534, Jun. 2008.
- 797 [20] P. K. Gopala, L. Lai, and H. Gamal, "On the secrecy capacity of fading  
798 channels," *IEEE Trans. Inf. Theory*, vol. 54, no. 10, pp. 4687–4698,  
799 Oct. 2008.
- 800 [21] Z. Li, W. Trappe, and R. Yates, "Secret communication via multi-antenna  
801 transmission," in *Proc. 41st Conf. Inf. Sci. Syst.*, Baltimore, MD, USA,  
802 Mar. 2007, pp. 905–910.
- 803 [22] F. Oggier and B. Hassibi, "The secrecy capacity of the MIMO wire-  
804 tap channel," *IEEE Trans. Inf. Theory*, vol. 57, no. 8, pp. 4961–4972,  
805 Aug. 2007.
- 806 [23] M. Yuksel and E. Erkip, "Secure communication with a relay helping the  
807 wiretapper," in *Proc. IEEE Inf. Theory Workshop*, Lake Tahoe, CA, USA,  
808 Sep. 2007, pp. 595–600.
- 809 [24] L. Dong, Z. Han, A. P. Petropulu, and H. V. Poor, "Improving wire-  
810 less physical layer security via cooperating relays," *IEEE Trans. Signal  
811 Process.*, vol. 58, no. 3, pp. 1875–1888, Mar. 2010.
- [25] Y. Zou, X. Wang, and W. Shen, "Optimal relay selection for physical-layer  
812 security in cooperative wireless networks," *IEEE J. Sel. Areas Commun.*, 813  
vol. 31, no. 10, pp. 2099–2111, Oct. 2013. 814
- [26] A. Mukherjee and A. Swindlehurst, "Robust beamforming for security  
815 in MIMO wiretap channels with imperfect CSI," *IEEE Trans. Signal  
816 Process.*, vol. 59, no. 1, pp. 351–361, Jan. 2011. 817
- [27] C. Jeong, I. Kim, and K. Dong, "Joint secure beamforming design at  
818 the source and the relay for an amplify-and-forward MIMO untrusted  
819 relay system," *IEEE Trans. Signal Process.*, vol. 60, no. 1, pp. 310–325, 820  
Jan. 2012. 821
- [28] Y. Pei, Y.-C. Liang, K. C. Teh, and K. Li, "Secure communication in  
822 multiantenna cognitive radio networks with imperfect channel state in-  
823 formation," *IEEE Trans. Signal Process.*, vol. 59, no. 4, pp. 1683–1693, 824  
Apr. 2011. 825
- [29] Y. Zou, X. Wang, and W. Shen, "Physical-layer security with multiuser  
826 scheduling in cognitive radio networks," *IEEE Trans. Commun.*, vol. 61,  
827 no. 12, pp. 5103–5113, Dec. 2013. 828
- [30] Z. Shu, Y. Qian, and S. Ci, "On physical layer security for cognitive radio  
829 networks," *IEEE Netw. Mag.*, vol. 27, no. 3, pp. 28–33, Jun. 2013. 830
- [31] Y. Zou, X. Wang, W. Shen, and L. Hanzo, "Security versus reliability  
831 analysis of opportunistic relaying," *IEEE Trans. Veh. Tech.*, vol. 63, no. 6,  
832 pp. 2653–2661, Jun. 2014. 833
- [32] L. Di Stefano and S. Mattoccia, "A sufficient condition based on the  
834 Cauchy-Schwarz inequality for efficient template matching," in *Proc. Int.  
835 Conf. Image Process.*, Catalonia, Spain, Sep. 2003, pp. 269–272. 836
- [33] M. Abramowitz and I. A. Stegun, *Handbook of Mathematical Functions  
837 with Formulas, Graphs, Mathematical Tables*, 9th ed. New York, NY, 838  
USA: Dover, 1970. 839
- [34] Y. Zou, Y.-D. Yao, and B. Zheng, "Diversity-multiplexing tradeoff in  
840 selective cooperation for cognitive radio," *IEEE Trans. Commun.*, vol. 60,  
841 no. 9, pp. 2467–2481, Sep. 2012. 842
- [35] S. Goel and R. Negi, "Guaranteeing secrecy using artificial noise," *IEEE  
843 Trans. Wireless Commun.*, vol. 7, no. 6, pp. 2180–2189, Jun. 2008. 844
- [36] W. Li, M. Ghogho, B. Chen, and C. Xiong, "Artificial noise by the  
845 receiver: Outage secrecy capacity/region analysis," *IEEE Commun. Lett.*,  
846 vol. 16, no. 10, pp. 1628–1631, Oct. 2012. 847



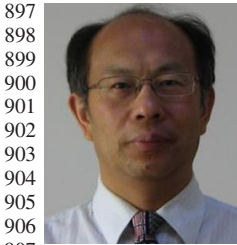
**Yulong Zou** (S'07–M'12–SM'13) received the 848  
B.Eng. degree in information engineering from 849  
NUPT, Nanjing, China, in July 2006, the first Ph.D. 850  
degree in electrical engineering from the Stevens In- 851  
stitute of Technology, New Jersey, the United States, 852  
in May 2012, and the second Ph.D. degree in signal 853  
and information processing from NUPT, Nanjing, 854  
China, in July 2012. He is a Full Professor at the 855  
Nanjing University of Posts and Telecommunica- 856  
tions (NUPT), Nanjing, China. His research interests 857  
span a wide range of topics in wireless commu- 858  
nications and signal processing, including the cooperative 859  
cognitive radio, wireless security, and energy-efficient 860  
communications.

He is currently serving as an editor for the IEEE Communications Surveys 861  
& Tutorials, IEEE COMMUNICATIONS LETTERS, EURASIP Journal on Ad- 862  
vances in Signal Processing, and KSII Transactions on Internet and Information 863  
Systems. He served as the lead guest editor for a special issue on "Security 864  
Challenges and Issues in Cognitive Radio Networks" in the EURASIP Journal 865  
on Advances in Signal Processing. He is also serving as the lead guest 866  
editor for a special issue on "Security and Reliability Challenges in Industrial 867  
Wireless Sensor Networks" in the IEEE TRANSACTIONS ON INDUSTRIAL 868  
INFORMATICS. In addition, he has acted as symposium chairs, session chairs, 869  
and TPC members for a number of IEEE sponsored conferences, including the 870  
IEEE WIRELESS COMMUNICATIONS and Networking Conference (WCNC), 871  
IEEE Global Communications Conference (GLOBECOM), IEEE International 872  
Conference on Communications (ICC), IEEE Vehicular Technology Confer- 873  
ence (VTC), International Conference on Communications in China (ICCC), 874  
and so on. 875



**Benoit Champagne** (S'87–M'89–SM'03) was born in Joliette (PQ), Canada, in 1961. He received the B.Eng. degree in engineering physics and the M.Sc. degree in physics from the University of Montreal in 1983 and 1985, respectively, and the Ph.D. degree in electrical engineering from the University of Toronto in 1990. From 1990 to 1999, he was with INRS, University of Quebec, where he held the positions of Assistant and then Associate Professor. In 1999, he joined McGill University, Montreal, as an Associate Professor with the Department of Electrical and

Computer Engineering. He served as Associate Chairman of Graduate Studies in the Department from 2004 to 2007 and is now a Full Professor. His research interests focus on the investigation of new computational algorithms for the digital processing of information bearing signals and overlap many sub-areas of statistical signal processing, including: detection and estimation, sensor array processing, adaptive filtering, multirate systems, and applications thereof to broadband voice and data communications. Over the years, he has supervised many graduate students in these areas and co-authored several papers, including key works on subspace tracking, speech enhancement, time delay estimation and spread sources localization.



**Wei-Ping Zhu** (SM'97) received the B.E. and M.E. degrees from Nanjing University of Posts and Telecommunications, and the Ph.D. degree from Southeast University, Nanjing, China, in 1982, 1985, and 1991, respectively, all in electrical engineering. He was a Postdoctoral Fellow from 1991 to 1992 and a Research Associate from 1996 to 1998 with the Department of Electrical and Computer Engineering, Concordia University, Montreal, Canada. During 1993–1996, he was an Associate Professor with the Department of Information Engineering,

Nanjing University of Posts and Telecommunications. From 1998 to 2001, he worked with hi-tech companies in Ottawa, Canada, including Nortel Networks and SR Telecom Inc. Since July 2001, he has been with Concordia's Electrical and Computer Engineering Department as a full-time faculty member, where he is presently a Full Professor. His research interests include digital signal processing fundamentals, speech and audio processing, and signal processing for wireless communication with a particular focus on MIMO systems and cooperative relay networks.

Dr. Zhu was an Associate Editor of the IEEE TRANSACTIONS ON CIRCUITS AND SYSTEMS PART I: Fundamental Theory and Applications from 2001 to 2003, and an Associate Editor of Circuits, Systems and Signal Processing from 2006 to 2009. He was also a Guest Editor for the IEEE JOURNAL ON SELECTED AREAS IN COMMUNICATIONS for the special issues of: Broadband Wireless Communications for High Speed Vehicles, and Virtual MIMO during 2011–2013. Since 2011, he has served as an Associate Editor for the IEEE TRANSACTIONS ON CIRCUITS AND SYSTEMS PART II: Express Briefs. Dr. Zhu was the Secretary of Digital Signal Processing Technical Committee (DSPTC) of the IEEE Circuits and System Society during 2012–2014, where he is presently the Chair of the DSPTC.



**Lajos Hanzo** received the degree in electronics in 1976 and the doctorate in 1983. In 2009 he was awarded "Doctor Honoris Causa" by the Technical University of Budapest. During his 37-year career in telecommunications he has held various research and academic posts in Hungary, Germany, and the UK. Since 1986 he has been with the School of Electronics and Computer Science, University of Southampton, UK, where he holds the chair in telecommunications. He has successfully supervised 80+ Ph.D. students, co-authored 20 John Wiley/IEEE Press books

on mobile radio communications totalling in excess of 10 000 pages, published 1400+ research entries at IEEE Xplore, acted both as TPC and General Chair of IEEE conferences, presented keynote lectures and has been awarded a number of distinctions. Currently he is directing a 100-strong academic research team working on a range of research projects in the field of wireless multimedia communications sponsored by industry, the Engineering and Physical Sciences Research Council (EPSRC) UK, the European Research Council's Advanced Fellow Grant and the Royal Society's Wolfson Research Merit Award. He is an enthusiastic supporter of industrial and academic liaison and he offers a range of industrial courses. He is also a Governor of the IEEE VTS. During 2008–2012 he was the Editor-in-Chief of the IEEE Press and a Chaired Professor also at Tsinghua University, Beijing. His research is funded by the European Research Council's Senior Research Fellow Grant. For further information on research in progress and associated publications please refer to <http://www-mobile.ecs.soton.ac.uk> Lajos has 20 000+ citations.

952

AUTHOR QUERY

NO QUERY.

IEEE  
Proof

# Relay-Selection Improves the Security-Reliability Trade-Off in Cognitive Radio Systems

Yulong Zou, *Senior Member, IEEE*, Benoit Champagne, *Senior Member, IEEE*,  
Wei-Ping Zhu, *Senior Member, IEEE*, and Lajos Hanzo, *Fellow, IEEE*

**Abstract**—We consider a cognitive radio (CR) network consisting of a secondary transmitter (ST), a secondary destination (SD) and multiple secondary relays (SRs) in the presence of an eavesdropper, where the ST transmits to the SD with the assistance of SRs, while the eavesdropper attempts to intercept the secondary transmission. We rely on careful relay selection for protecting the ST-SD transmission against the eavesdropper with the aid of both single-relay and multi-relay selection. To be specific, only the “best” SR is chosen in the single-relay selection for assisting the secondary transmission, whereas the multi-relay selection invokes multiple SRs for simultaneously forwarding the ST’s transmission to the SD. We analyze both the intercept probability and outage probability of the proposed single-relay and multi-relay selection schemes for the secondary transmission relying on realistic spectrum sensing. We also evaluate the performance of classic direct transmission and artificial noise based methods for the purpose of comparison with the proposed relay selection schemes. It is shown that as the intercept probability requirement is relaxed, the outage performance of the direct transmission, the artificial noise based and the relay selection schemes improves, and vice versa. This implies a trade-off between the security and reliability of the secondary transmission in the presence of eavesdropping attacks, which is referred to as the *security-reliability trade-off* (SRT). Furthermore, we demonstrate that the SRTs of the single-relay and multi-relay selection schemes are generally better than that of classic direct transmission, explicitly demonstrating the advantage of the proposed relay selection in terms of protecting the secondary transmissions against eavesdropping attacks. Moreover, as the number of SRs increases, the SRTs of the proposed single-relay and multi-relay

selection approaches significantly improve. Finally, our numerical results show that as expected, the multi-relay selection scheme achieves a better SRT performance than the single-relay selection.

**Index Terms**—Security-reliability trade-off, relay selection, intercept probability, outage probability, eavesdropping attack, cognitive radio.

## I. INTRODUCTION

THE security aspects of cognitive radio (CR) systems [1]–[3] have attracted increasing attention from the research community. Indeed, due to the highly dynamic nature of the CR network architecture, legitimate CR devices become exposed to both internal as well as to external attackers and hence they are extremely vulnerable to malicious behavior. For example, an illegitimate user may intentionally impose interference (i.e. jamming) for the sake of artificially contaminating the CR environment [4]. Hence, the CR users fail to accurately characterize their surrounding radio environment and may become misled or compromised, which leads to a malfunction. Alternatively, an illegitimate user may attempt to tap the communications of authorized CR users by eavesdropping, to intercept confidential information.

Clearly, CR networks face diverse security threats during both spectrum sensing [5], [6] as well as spectrum sharing [7], spectrum mobility [8] and spectrum management [9]. Extensive studies have been carried out for protecting CR networks both against primary user emulation (PUE) [10] and against denial-of-service (DoS) attacks [11]. In addition to PUE and DoS attacks, eavesdropping is another main concern in protecting the data confidentiality [12], although it has received less attention in the literature on CR network security. Traditionally, cryptographic techniques are employed for guaranteeing transmission confidentiality against an eavesdropping attack. However, this introduces a significant computational overhead [13] as well as imposing additional system complexity in terms of the secret key management [14]. Furthermore, the existing cryptographic approaches are not perfectly secure and can still be decrypted by an eavesdropper (E), provided that it has the capacity to carry out exhaustive key search with the aid of brute-force attack [15].

Physical-layer security [16], [17] is emerging as an efficient approach for defending authorized users against eavesdropping attacks by exploiting the physical characteristics of wireless channels. In [17], Leung-Yan-Cheong and Hellman demonstrated that perfectly secure and reliable transmission can be achieved, when the wiretap channel spanning from the source to the eavesdropper is a further degraded version of the main

Manuscript received May 7, 2014; revised August 21, 2014 and October 16, 2014; accepted November 27, 2014. This work was partially supported by the Priority Academic Program Development of Jiangsu Higher Education Institutions, the National Natural Science Foundation of China (Grant Nos. 61302104 and 61401223), the Scientific Research Foundation of Nanjing University of Posts and Telecommunications (Grant Nos. NY213014 and NY214001), the 1311 Talent Program of Nanjing University of Posts and Telecommunications, the Natural Science Foundation of Jiangsu Province (Grant No. BK20140887), and the Programme de bourses d’excellence pour étudiants étrangers (PBEEE) of the Government of Quebec. The associate editor coordinating the review of this paper and approving it for publication was H. Li.

Y. Zou is with the School of Telecommunications and Information Engineering, Nanjing University of Posts and Telecommunications, Nanjing 210003, China (e-mail: yulong.zou@njupt.edu.cn).

B. Champagne is with the Department of Electrical & Computer Engineering, McGill University, Montreal, QC H3A 1Y1, Canada (e-mail: benoit.champagne@mcgill.ca).

W.-P. Zhu is with the Department of Electrical & Computer Engineering, Concordia University, Montreal, QC H3G 1M8, Canada (e-mail: weiping@ece.concordia.ca).

L. Hanzo is with the Department of Electronics and Computer Science, University of Southampton, Southampton SO17 1BJ, U.K. (e-mail: lh@ecs.soton.ac.uk).

Color versions of one or more of the figures in this paper are available online at <http://ieeexplore.ieee.org>.

Digital Object Identifier 10.1109/TCOMM.2014.2377239

79 channel between the source and destination. They also showed  
 80 that the maximal secrecy rate achieved at the legitimate desti-  
 81 nation, which is termed the secrecy capacity, is the difference  
 82 between the capacity of the main channel and that of the  
 83 wiretap channel. In [18]–[20], the secrecy capacity limits of  
 84 wireless fading channels were further developed and character-  
 85 ized from an information-theoretic perspective, demonstrating  
 86 the detrimental impact of wireless fading on the physical-  
 87 layer security. To combat the fading effects, both multiple-input  
 88 multiple-output (MIMO) schemes [21], [22] as well as coop-  
 89 erative relaying [23]–[25] and beamforming techniques [26],  
 90 [27] were investigated for the sake of enhancing the achievable  
 91 wireless secrecy capacity. Although extensive research efforts  
 92 were devoted to improving the security of traditional wireless  
 93 networks [16]–[27], less attention has been dedicated to CR  
 94 networks. In [28] and [29], the achievable secrecy rate of  
 95 the secondary transmission was investigated under a specific  
 96 quality-of-service (QoS) constraint imposed on the primary  
 97 transmission. Additionally, an overview of the physical-layer  
 98 security aspects of CR networks was provided in [30], where  
 99 several security attacks as well as the related countermeasures  
 100 are discussed. In contrast to conventional non-cognitive wire-  
 101 less networks, the physical-layer security of CR networks has to  
 102 consider diverse additional challenges, including the protection  
 103 of the primary user’s QoS and the mitigation of the mutual  
 104 interference between the primary and secondary transmissions.  
 105 Motivated by the above considerations, we explore the  
 106 physical-layer security of a CR network comprised of a sec-  
 107 ondary transmitter (ST) communicating with a secondary des-  
 108 tination (SD) with the aid of multiple secondary relays (SRs)  
 109 in the presence of an unauthorized attacker. Our main focus  
 110 is on investigating the security-reliability trade-off (SRT) of  
 111 the cognitive relay transmission in the presence of realistic  
 112 spectrum sensing. The notion of the SRT in wireless physical-  
 113 layer security was introduced and examined in [31], where the  
 114 security and reliability was characterized in terms of the inter-  
 115 cept probability and outage probability, respectively. In contrast  
 116 to the conventional non-cognitive wireless networks studied in  
 117 [31], the SRT analysis of CR networks presented in this work  
 118 additionally takes into account the mutual interference between  
 119 the primary user (PU) and secondary user (SU).

120 The main contributions of this paper are summarized as  
 121 follows.

- 122 • We propose two relay selection schemes, namely both  
 123 single-relay and multi-relay selection, for protecting the  
 124 secondary transmissions against eavesdropping attacks.  
 125 More specifically, in the single-relay selection (SRS)  
 126 scheme, only a single relay is chosen from the set of mul-  
 127 tiple SRs for forwarding the secondary transmissions from  
 128 the ST to the SD. By contrast, the multi-relay selection  
 129 (MRS) scheme employs multiple SRs for simultaneously  
 130 assisting the ST-SD transmissions.
- 131 • We present the mathematical SRT analysis of the proposed  
 132 SRS and MRS schemes in the presence of realistic spec-  
 133 trum sensing. Closed-form expressions are derived for the  
 134 intercept probability (IP) and outage probability (OP) of  
 135 both schemes for transmission over Rayleigh fading chan-  
 136 nels. The numerical SRT results of conventional direct

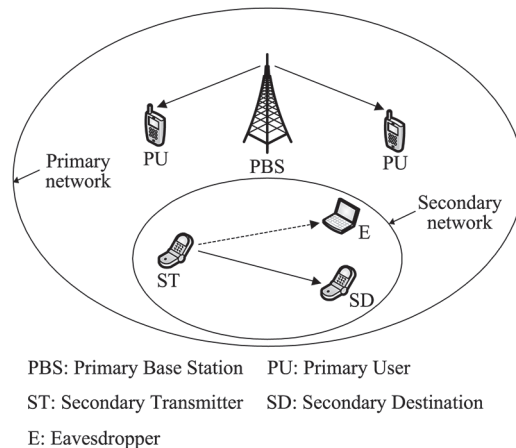


Fig. 1. A primary wireless network in coexistence with a secondary CR network.

transmission and artificial noise based schemes are also  
 provided for comparison purposes.

- It is shown that as the spectrum sensing reliability is increased and/or the false alarm probability is reduced, the SRTs of both the SRS and MRS schemes are improved. Numerical results demonstrate that the proposed SRS and MRS schemes generally outperform the conventional direct transmission and artificial noise based approaches in terms of their SRTs.

The remainder of this paper is organized as follows. Section II presents the system model of physical-layer security in CR networks in the context of both the direct transmission as well as the SRS and MRS schemes. In Section III, we analyze the SRTs of these schemes in the presence of realistic spectrum sensing over Rayleigh fading channels. Next, numerical SRT results of the direct transmission, SRS and MRS schemes are given in Section IV, where the SRT performance of the artificial noise based scheme is also numerically evaluated for comparison purposes. Finally, Section V provides our concluding remarks.

## II. RELAY SELECTION AIDED PROTECTION AGAINST EAVESDROPPING IN CR NETWORKS

We first introduce the overall system model of physical-layer security in CR networks. We then present the signal model of the conventional direct transmission approach, which will serve as our benchmark, as well as of the SRS and MRS schemes for improving the CR system’s security against eavesdropping attacks.

### A. System Model

As shown in Fig. 1, we consider a primary network in coexistence with a secondary network (also referred to as a *CR network*). The primary network includes a primary base station (PBS) and multiple primary users (PUs), which communicate with the PBS over the licensed spectrum. By contrast, the secondary network consisting of one or more STs and SDs exploits the licensed spectrum in an opportunistic way. To

173 be specific, a particular ST should first detect with the aid  
174 of spectrum sensing whether or not the licensed spectrum is  
175 occupied by the PBS. If so, the ST is not at liberty to transmit  
176 to avoid interfering with the PUs. If alternatively, the licensed  
177 spectrum is deemed to be unoccupied (i.e. a spectrum hole  
178 is detected), then the ST may transmit to the SD over the  
179 detected spectrum hole. Meanwhile, E attempts to intercept the  
180 secondary transmission from the ST to the SD. For notational  
181 convenience, let  $H_0$  and  $H_1$  represent the event that the licensed  
182 spectrum is unoccupied and occupied by the PBS during a  
183 particular time slot, respectively. Moreover, let  $\hat{H}$  denote the  
184 status of the licensed spectrum detected by spectrum sensing.  
185 Specifically,  $\hat{H} = H_0$  represents the case that the licensed  
186 spectrum is deemed to be unoccupied, while  $\hat{H} = H_1$  indicates  
187 that the licensed spectrum is deemed to be occupied.

188 The probability  $P_d$  of correct detection of the presence of  
189 PBS and the associated false alarm probability  $P_f$  are defined  
190 as  $P_d = \Pr(\hat{H} = H_1 | H_1)$  and  $P_f = \Pr(\hat{H} = H_1 | H_0)$ , respectively.  
191 Due to the background noise and fading effects, it is impossible  
192 to achieve perfectly reliable spectrum sensing without missing  
193 the detection of an active PU and without false alarm, which  
194 suggests that a spectral band is occupied by a PU, when it  
195 is actually unoccupied. Moreover, the missed detection of the  
196 presence of PBS will result in interference between the PU  
197 and SU. To guarantee that the interference imposed on the  
198 PUs is below a tolerable level, both the successful detection  
199 probability (SDP)  $P_d$  and false alarm probability (FAP)  $P_f$   
200 should be within a meaningful target range. For example, the  
201 IEEE 802.22 standard requires  $P_d > 0.9$  and  $P_f < 0.1$  [2]. For  
202 better protection of PUs, we consider  $P_d = 0.99$  and  $P_f = 0.01$ ,  
203 unless otherwise stated. Additionally, we consider a Rayleigh  
204 fading model for characterizing all the channels between any  
205 two nodes of Fig. 1. Finally, all the received signals are assumed  
206 to be corrupted by additive white Gaussian noise (AWGN)  
207 having a zero mean and a variance of  $N_0$ .

## 208 B. Direct Transmission

209 Let us first consider the conventional direct transmission  
210 as a benchmark scheme. Let  $x_p$  and  $x_s$  denote the random  
211 symbols transmitted by the PBS and the ST at a particular  
212 time instance. Without loss of generality, we assume  $E[|x_p|^2] =$   
213  $E[|x_s|^2] = 1$ , where  $E[\cdot]$  represents the expected value operator.  
214 The transmit powers of the PBS and ST are denoted by  $P_p$  and  
215  $P_s$ , respectively. Given that the licensed spectrum is deemed to  
216 be unoccupied by the PBS (i.e.  $\hat{H} = H_0$ ), ST transmits its signal  
217  $x_s$  at a power of  $P_s$ . Then, the signal received at the SD can be  
218 written as

$$y_d = h_{sd}\sqrt{P_s}x_s + h_{pd}\sqrt{\alpha P_p}x_p + n_d, \quad (1)$$

219 where  $h_{sd}$  and  $h_{pd}$  represent the fading coefficients of the  
220 channel spanning from ST to SD and that from PBS to SD,  
221 respectively. Furthermore,  $n_d$  represents the AWGN received at  
222 SD and the random variable (RV)  $\alpha$  is defined as

$$\alpha = \begin{cases} 0, & H_0 \\ 1, & H_1, \end{cases} \quad (2)$$

where  $H_0$  represents that the licensed spectrum is unoccupied  
223 by PBS and no primary signal is transmitted, leading to  $\alpha = 0$ .  
224 By contrast,  $H_1$  represents that PBS is transmitting its signal  $x_p$   
225 over the licensed spectrum, thus  $\alpha = 1$ . Meanwhile, due to the  
226 broadcast nature of the wireless medium, the ST's signal will  
227 be overheard by E and the overheard signal can be expressed as  
228

$$y_e = h_{se}\sqrt{P_s}x_s + h_{pe}\sqrt{\alpha P_p}x_p + n_e, \quad (3)$$

where  $h_{se}$  and  $h_{pe}$  represent the fading coefficients of the  
229 channel spanning from ST to E and that from PBS to E,  
230 respectively, while  $n_e$  represents the AWGN received at E.  
231 Upon combining Shannon's capacity formula [31] with (1), we  
232 obtain the capacity of the ST-SD channel as  
233

$$C_{sd} = \log_2 \left( 1 + \frac{|h_{sd}|^2 \gamma_s}{\alpha |h_{pd}|^2 \gamma_p + 1} \right), \quad (4)$$

where  $\gamma_s = P_s/N_0$  and  $\gamma_p = P_p/N_0$ . Similarly, the capacity of the  
234 ST-E channel is obtained from (3) as  
235

$$C_{se} = \log_2 \left( 1 + \frac{|h_{se}|^2 \gamma_s}{\alpha |h_{pe}|^2 \gamma_p + 1} \right). \quad (5)$$

## C. Single-Relay Selection

236 In this subsection, we consider the cognitive relay network  
237 of Fig. 2, where both SD and E are assumed to be beyond  
238 the coverage area of the ST [24], [25], and  $N$  secondary  
239 relays (SRs) are employed for assisting the cognitive ST-SD  
240 transmission. We assume that a common control channel (CCC)  
241 [6] is available for coordinating the actions of the different  
242 network nodes and the decode-and-forward (DF) relaying using  
243 two adjacent time slots is employed. More specifically, once  
244 the licensed spectrum is deemed to be unoccupied, the ST first  
245 broadcasts its signal  $x_s$  to the  $N$  SRs, which attempt to decode  
246  $x_s$  from their received signals. For notational convenience, let  
247  $\mathcal{D}$  represent the set of SRs that succeed in decoding  $x_s$ . Given  
248  $N$  SRs, there are  $2^N$  possible subsets  $\mathcal{D}$ , thus the sample space  
249 of  $\mathcal{D}$  is formulated as  
250

$$\Omega = \{\emptyset, \mathcal{D}_1, \mathcal{D}_2, \dots, \mathcal{D}_n, \dots, \mathcal{D}_{2^N-1}\}, \quad (6)$$

where  $\emptyset$  represents the empty set and  $\mathcal{D}_n$  represents the  $n$ -th  
251 non-empty subset of the  $N$  SRs. If the set  $\mathcal{D}$  is empty, implying  
252 that no SR decodes  $x_s$  successfully, then all the SRs remain  
253 silent and thus both SD and E are unable to decode  $x_s$  in this  
254 case. If the set  $\mathcal{D}$  is non-empty, a specific SR is chosen from  
255  $\mathcal{D}$  to forward its decoded signal  $x_s$  to SD. Therefore, given  
256  $\hat{H} = H_0$  (i.e. the licensed spectrum is deemed unoccupied), ST  
257 broadcasts its signal  $x_s$  to  $N$  SRs at a power of  $P_s$  and a rate of  
258  $R$ . Hence, the signal received at a specific SR <sub>$i$</sub>  is given by  
259

$$y_i = h_{si}\sqrt{P_s}x_s + h_{pi}\sqrt{\alpha P_p}x_p + n_i, \quad (7)$$

where  $h_{si}$  and  $h_{pi}$  represent the fading coefficients of the ST-SR <sub>$i$</sub>   
260 channel and that of the PBS-SR <sub>$i$</sub>  channel, respectively, with  
261

262  $n_i$  representing the AWGN at  $SR_i$ . From (7), we obtain the  
263 capacity of the ST- $SR_i$  channel as

$$C_{si} = \frac{1}{2} \log_2 \left( 1 + \frac{|h_{si}|^2 \gamma_s}{\alpha |h_{pi}|^2 \gamma_p + 1} \right), \quad (8)$$

264 where the factor  $\frac{1}{2}$  arises from the fact that two orthogonal time  
265 slots are required for completing the message transmission from  
266 ST to SD via  $SR_i$ . According to Shannon's coding theorem,  
267 if the data rate is higher than the channel capacity, the re-  
268 ceiver becomes unable to successfully decode the source signal,  
269 regardless of the decoding algorithm adopted. Otherwise, the  
270 receiver can succeed in decoding the source signal. Thus, using  
271 (8), we can describe the event of  $\mathcal{D} = \emptyset$  as

$$C_{si} < R, \quad i \in \{1, 2, \dots, N\}. \quad (9)$$

272 Meanwhile, the event of  $\mathcal{D} = \mathcal{D}_n$  is described as

$$\begin{aligned} C_{si} &> R, \quad i \in \mathcal{D}_n \\ C_{sj} &< R, \quad j \in \bar{\mathcal{D}}_n, \end{aligned} \quad (10)$$

273 where  $\bar{\mathcal{D}}_n$  represents the complementary set of  $\mathcal{D}_n$ . Without  
274 loss of generality, we assume that  $SR_i$  is chosen within  $\mathcal{D}_n$  to  
275 transmit its decoded result  $x_s$  at a power of  $P_s$ , thus the signal  
276 received at SD can be written as

$$y_d = h_{id} \sqrt{P_s} x_s + h_{pd} \sqrt{\alpha P_p} x_p + n_d, \quad (11)$$

277 where  $h_{id}$  represents the fading coefficient of the  $SR_i - SD$   
278 channel. From (11), the capacity of the  $SR_i - SD$  channel is  
279 given by

$$C_{id} = \frac{1}{2} \log_2 \left( 1 + \frac{|h_{id}|^2 \gamma_s}{\alpha |h_{pd}|^2 \gamma_p + 1} \right), \quad (12)$$

280 where  $i \in \mathcal{D}_n$ . In general, the specific  $SR_i$  having the highest  
281 instantaneous capacity to SD is chosen as the "best" SR for as-  
282 sisting the ST's transmission. Therefore, the best relay selection  
283 criterion is expressed from (12) as

$$\text{Best SR} = \arg \max_{i \in \mathcal{D}_n} C_{id} = \arg \max_{i \in \mathcal{D}_n} |h_{id}|^2, \quad (13)$$

284 which shows that only the channel state information (CSI)  $|h_{id}|^2$   
285 is required for performing the relay selection without the need  
286 for the eavesdropper's CSI knowledge. Upon combining (12)  
287 and (13), we obtain the capacity of the channel spanning from  
288 the "best" SR to SD as

$$C_{bd} = \frac{1}{2} \log_2 \left( 1 + \frac{\gamma_s}{\alpha |h_{pd}|^2 \gamma_p + 1} \max_{i \in \mathcal{D}_n} |h_{id}|^2 \right), \quad (14)$$

289 where the subscript 'b' in  $C_{bd}$  denotes the best SR. It is observed  
290 from (14) that the legitimate transmission capacity of the SRS  
291 scheme is determined by the maximum of independent random  
292 variables (RVs)  $|h_{id}|^2$  for different SRs. By contrast, one can  
293 see from (4) that the capacity of classic direct transmission is  
294 affected by the single RV  $|h_{sd}|^2$ . If all RVs  $|h_{id}|^2$  and  $|h_{sd}|^2$  are  
295 independent and identically distributed (i.i.d), it would be most  
296 likely that  $\max_{i \in \mathcal{D}_n} |h_{id}|^2$  is much higher than  $|h_{sd}|^2$  for a sufficiently

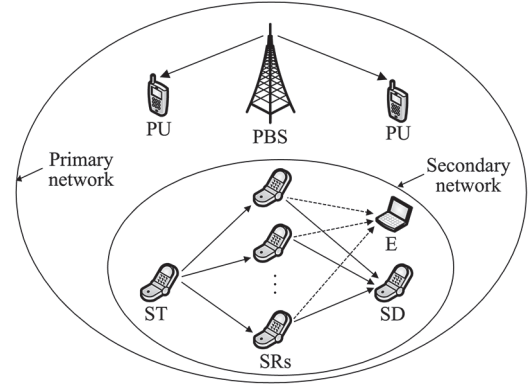


Fig. 2. A cognitive relay network consists of one ST, one SD and  $N$  SRs in the presence of an E.

large number of SRs, resulting in a performance improvement 297  
for the SRS scheme over the classic direct transmission. How- 298  
ever, if the RVs  $|h_{id}|^2$  and  $|h_{sd}|^2$  are non-identically distributed 299  
and the mean value of  $|h_{sd}|^2$  is much higher than that of  $|h_{id}|^2$ , 300  
then it may be more likely that  $\max_{i \in \mathcal{D}_n} |h_{id}|^2$  is smaller than  $|h_{sd}|^2$  301  
for a given number of SRs. In this extreme case, the classic 302  
direct transmission may perform better than the SRS scheme. 303  
It is worth mentioning that in practice, the average fading gain 304  
of the  $SR_i - SD$  channel,  $|h_{id}|^2$ , should not be less than that 305  
of the ST-SD channel  $|h_{sd}|^2$ , since SRs are typically placed 306  
in the middle between the ST and SD. Hence, a performance 307  
improvement for the SRS scheme over classic direct transmis- 308  
sion would be achieved in practical wireless systems. Note 309  
that although a factor 1/2 in (14) is imposed on the capacity 310  
of the main channel, it would not affect the performance of 311  
the SRS scheme from a SRT perspective, since the capacity 312  
of the wiretap channel is also multiplied by 1/2 as will be 313  
shown in (16). 314

Additionally, given that the selected SR transmits its 315  
decoded result  $x_s$  at a power of  $P_s$ , the signal received at E is 316  
expressed as 317

$$y_e = h_{be} \sqrt{P_s} x_s + h_{pe} \sqrt{\alpha P_p} x_p + n_e, \quad (15)$$

where  $h_{be}$  and  $h_{pe}$  represent the fading coefficients of the chan- 318  
nel from "best" SR to E and that from PBS to E, respectively. 319  
From (15), the capacity of the channel spanning from the "best" 320  
SR to E is given by 321

$$C_{be} = \frac{1}{2} \log_2 \left( 1 + \frac{|h_{be}|^2 \gamma_s}{\alpha |h_{pe}|^2 \gamma_p + 1} \right), \quad (16)$$

where  $b \in \mathcal{D}_n$  is determined by the relay selection criterion 322  
given in (13). As shown in (16), the eavesdropper's channel 323  
capacity is affected by the channel state information (CSI) 324  
 $|h_{be}|^2$  of the wiretap channel spanning from the "best" relay to 325  
the eavesdropper. However, one can see from (13) that the best 326  
relay is selected from the decoding set  $\mathcal{D}_n$  solely based on the 327  
main channel's CSI  $|h_{id}|^2$  i.e. without taking into account the 328  
eavesdropper's CSI knowledge of  $|h_{ie}|^2$ . This means that the 329  
selection of the best relay aiming for maximizing the legitimate 330  
transmission capacity of (14) would not lead to significantly 331

332 beneficial or adverse impact on the eavesdropper's channel  
333 capacity, since the main channel and the wiretap channel are  
334 independent of each other.

335 For example, if the random variables (RVs)  $|h_{ie}|^2$  related to  
336 the different relays are i.i.d, we can readily infer by the law  
337 of total probability that  $|h_{pe}|^2$  has the same probability den-  
338 sity function (PDF) as  $|h_{ie}|^2$ , implying that the eavesdropper's  
339 channel capacity of (16) is not affected by the selection of the  
340 best relay given by (13). Therefore, the SRS scheme has no  
341 obvious advantage over the classic direct transmission in terms  
342 of minimizing the capacity of the wiretap channel. To elaborate  
343 a little further, according to the SRT trade-off, a reduction of  
344 the outage probability (OP) due to the capacity enhancement  
345 of the main channel achieved by using the selection of the  
346 best relay would be converted into an intercept probability  
347 (IP) improvement, which will be numerically illustrated in  
348 Section IV.

#### 349 D. Multi-Relay Selection

350 This subsection presents a MRS scheme, where multiple SRs  
351 are employed for simultaneously forwarding the source signal  
352  $x_s$  to SD. To be specific, ST first transmits  $x_s$  to  $N$  SRs over a  
353 detected spectrum hole. As mentioned in Subsection II-C, we  
354 denote by  $\mathcal{D}$  the set of SRs that successfully decode  $x_s$ . If  $\mathcal{D}$   
355 is empty, all SRs fail to decode  $x_s$  and will not forward the  
356 source signal, thus both SD and E are unable to decode  $x_s$ . If  
357  $\mathcal{D}$  is non-empty (i.e.  $\mathcal{D} = \mathcal{D}_n$ ), all SRs within  $\mathcal{D}_n$  are utilized  
358 for simultaneously transmitting  $x_s$  to SD. This differs from the  
359 SRS scheme, where only a single SR is chosen from  $\mathcal{D}_n$  for  
360 forwarding  $x_s$  to SD. To make effective use of multiple SRs, a  
361 weight vector denoted by  $w = [w_1, w_2, \dots, w_{|\mathcal{D}_n|}]^T$  is employed  
362 at the SRs for transmitting  $x_s$ , where  $|\mathcal{D}_n|$  is the cardinality of  
363 the set  $\mathcal{D}_n$ . For the sake of a fair comparison with the SRS  
364 scheme in terms of power consumption, the total transmit power  
365 across all SRs within  $\mathcal{D}_n$  shall be constrained to  $P_s$  and thus the  
366 weight vector  $w$  should be normalized according to  $\|w\| = 1$ .  
367 Thus, given  $\mathcal{D} = \mathcal{D}_n$  and considering that all SRs within  $\mathcal{D}_n$  are  
368 selected for simultaneously transmitting  $x_s$  with a weight vector  
369  $w$ , the signal received at SD is expressed as

$$y_d^{\text{multi}} = \sqrt{P_s} w^T H_d x_s + \sqrt{\alpha P_p} h_{pd} x_p + n_d, \quad (17)$$

370 where  $H_d = [h_{1d}, h_{2d}, \dots, h_{|\mathcal{D}_n|d}]^T$ . Similarly, the signal received  
371 at E can be written as

$$y_e^{\text{multi}} = \sqrt{P_s} w^T H_e x_s + \sqrt{\alpha P_p} h_{pe} x_p + n_e, \quad (18)$$

372 where  $H_e = [h_{1e}, h_{2e}, \dots, h_{|\mathcal{D}_n|e}]^T$ . From (17) and (18), the  
373 signal-to-interference-plus-noise ratios (SINRs) at SD and E  
374 are, respectively, given by

$$\text{SINR}_d^{\text{multi}} = \frac{\gamma_s}{\alpha |h_{pd}|^2 \gamma_p + 1} |w^T H_d|^2, \quad (19)$$

375 and

$$\text{SINR}_e^{\text{multi}} = \frac{\gamma_s}{\alpha |h_{pe}|^2 \gamma_p + 1} |w^T H_e|^2. \quad (20)$$

In this work, the weight vector  $w$  is optimized by maximizing  
the SINR at SD, yielding

$$\max_w \text{SINR}_d^{\text{multi}}, \quad \text{s.t. } \|w\| = 1, \quad (21)$$

where the constraint is used for normalization purposes. Using  
the Cauchy-Schwarz inequality [32], we can readily obtain the  
optimal weight vector  $w_{\text{opt}}$  from (21) as

$$w_{\text{opt}} = \frac{H_d^*}{|H_d|}, \quad (22)$$

which indicates that the optimal vector design only requires the  
SR-SD CSI  $H_d$ , whilst dispensing with the eavesdropper's CSI  
 $H_e$ . Substituting the optimal vector  $w_{\text{opt}}$  from (22) into (19) and  
(20) and using Shannon's capacity formula, we can obtain the  
channel capacities achieved at both SD and E as

$$C_d^{\text{multi}} = \frac{1}{2} \log_2 \left( 1 + \frac{\gamma_s}{\alpha \gamma_p |h_{pd}|^2 + 1} \sum_{i \in \mathcal{D}_n} |h_{id}|^2 \right), \quad (23)$$

and

$$C_e^{\text{multi}} = \frac{1}{2} \log_2 \left( 1 + \frac{\gamma_s}{\alpha \gamma_p |h_{pe}|^2 + 1} \frac{|H_d^H H_e|^2}{|H_d|^2} \right), \quad (24)$$

for  $\mathcal{D} = \mathcal{D}_n$ , where  $H$  represents the Hermitian transpose. One  
can observe from (14) and (23) that the difference between the  
capacity expressions  $C_{bd}$  and  $C_d^{\text{multi}}$  only lies in the fact that  
the maximum of RVs  $|h_{id}|^2$  for different SRs (i.e.,  $\max_{i \in \mathcal{D}_n} |h_{id}|^2$ )  
is used for the SRS scheme, while the sum of RVs  $|h_{id}|^2$   
(i.e.,  $\sum_{i \in \mathcal{D}_n} |h_{id}|^2$ ) is employed for the MRS scheme. Clearly,  
we have  $\sum_{i \in \mathcal{D}_n} |h_{id}|^2 > \max_{i \in \mathcal{D}_n} |h_{id}|^2$ , resulting in a performance  
gain for MRS over SRS in terms of maximizing the legitimate  
transmission capacity. Moreover, since the main channel  $H_d$   
and the wiretap channel  $H_e$  are independent of each other, the  
optimal weights assigned for the multiple relays based on  $H_d$   
will only slightly affect the eavesdropper's channel capacity.  
This means that the MRS and SRS schemes achieve more or  
less the same performance in terms of the capacity of the wire-  
tap channel. Nevertheless, given a fixed outage requirement,  
the MRS scheme can achieve a better intercept performance  
than the SRS scheme, because according to the SRT, an outage  
reduction achieved by the capacity enhancement of the legiti-  
mate transmission relying on the MRS would be converted into  
an intercept improvement. To be specific, given an enhanced  
capacity of the legitimate transmission, we may increase the  
data rate  $R$  based on the OP definition of (25) for maintaining  
a fixed OP, which, in turn leads to a reduction of the IP, since  
a higher data rate would result in a lower IP, according to the IP  
definition of (26).

It needs to be pointed out that in the MRS scheme, a  
high-complexity symbol-level synchronization is required for  
multiple distributed SRs, when simultaneously transmitting to  
SD, whereas the SRS does not require such a complex synchro-  
nization process. Thus, the performance improvement of MRS  
over SRS is achieved at the cost of a higher implementation

418 complexity. Additionally, the synchronization imperfections of  
419 the MRS scheme will impose a performance degradation, which  
420 may even lead to a performance for the MRS scheme becoming  
421 worse than that of the SRS scheme.

422 Throughout this paper, the Rayleigh model is used for char-  
423 acterizing the fading amplitudes (e.g.,  $|h_{sd}|$ ,  $|h_{si}|$ ,  $|h_{id}|$ , etc.) of  
424 wireless channels, which, in turn, implies that the fading square  
425 magnitudes  $|h_{sd}|^2$ ,  $|h_{si}|^2$  and  $|h_{id}|^2$  are exponentially distributed  
426 random variables (RVs). So far, we have completed the presen-  
427 tation of the signal model of the direct transmission, of the SRS,  
428 and of the MRS schemes for CR networks applications in the  
429 presence of eavesdropping attacks.

### 430 III. SRT ANALYSIS OVER RAYLEIGH FADING CHANNELS

431 This section presents the SRT analysis of the direct transmis-  
432 sion, SRS and MRS schemes over Rayleigh fading channels.  
433 As discussed in [31], the security and reliability are quantified  
434 in terms of the IP and OP experienced by the eavesdropper and  
435 destination, respectively. It is pointed out that in CR networks,  
436 ST starts to transmit its signal only when an available spectrum  
437 hole is detected. Similarly to [34], the OP and IP are thus  
438 calculated under the condition that the licensed spectrum is  
439 detected to be unoccupied by the PBS. The following gives the  
440 definition of OP and IP.

441 *Definition 1:* Let  $C_d$  and  $C_e$  represent the channel capacities  
442 achieved at the destination and eavesdropper, respectively. The  
443 OP and IP are, respectively, defined as

$$P_{\text{out}} = \Pr(C_d < R | \hat{H} = H_0), \quad (25)$$

444 and

$$P_{\text{int}} = \Pr(C_e > R | \hat{H} = H_0), \quad (26)$$

445 where  $R$  is the data rate.

#### 446 A. Direct Transmission

447 Let us first analyze the SRT performance of the conventional  
448 direct transmission. Given that a spectrum hole has been de-  
449 tected, the OP of direct transmission is obtained from (25) as

$$P_{\text{out}}^{\text{direct}} = \Pr(C_{sd} < R | \hat{H} = H_0), \quad (27)$$

450 where  $C_{sd}$  is given by (4). Using the law of total probability, we  
451 can rewrite (27) as

$$P_{\text{out}}^{\text{direct}} = \Pr(C_{sd} < R, H_0 | \hat{H} = H_0) + \Pr(C_{sd} < R, H_1 | \hat{H} = H_0), \quad (28)$$

452 which can be further expressed as

$$\begin{aligned} P_{\text{out}}^{\text{direct}} &= \Pr(C_{sd} < R | H_0, \hat{H} = H_0) \Pr(H_0 | \hat{H} = H_0) \\ &+ \Pr(C_{sd} < R | H_1, \hat{H} = H_0) \Pr(H_1 | \hat{H} = H_0). \end{aligned} \quad (29)$$

453 It is shown from (2) that given  $H_0$  and  $H_1$ , the parameter  $\alpha$  is  
454 obtained as  $\alpha = 0$  and  $\alpha = 1$ , respectively. Thus, combining (2)

and (4), we have  $C_{sd} = \log_2(1 + |h_{sd}|^2 \gamma_s)$  given  $H_0$  and  $C_{sd} = 455$   
 $\log_2\left(1 + \frac{|h_{sd}|^2 \gamma_s}{|h_{pd}|^2 \gamma_p + 1}\right)$  given  $H_1$ . Substituting this result into (29) 456  
yields 457

$$\begin{aligned} P_{\text{out}}^{\text{direct}} &= \Pr(|h_{sd}|^2 \gamma_s < 2^R - 1) \Pr(H_0 | \hat{H} = H_0) \\ &+ \Pr\left(\frac{|h_{sd}|^2 \gamma_s}{|h_{pd}|^2 \gamma_p + 1} < 2^R - 1\right) \Pr(H_1 | \hat{H} = H_0). \end{aligned} \quad (30)$$

Moreover, the terms  $\Pr(H_0 | \hat{H} = H_0)$  and  $\Pr(H_1 | \hat{H} = H_0)$  can be 458  
obtained by using Bayes' theorem as 459

$$\begin{aligned} \Pr(H_0 | \hat{H} = H_0) &= \frac{\Pr(\hat{H} = H_0 | H_0) \Pr(H_0)}{\sum_{i \in \{0,1\}} \Pr(\hat{H} = H_0 | H_i) \Pr(H_i)} \\ &= \frac{P_0(1 - P_f)}{P_0(1 - P_f) + (1 - P_0)(1 - P_d)} \triangleq \pi_0, \end{aligned} \quad (31)$$

and 460

$$\Pr(H_1 | \hat{H} = H_0) = \frac{(1 - P_0)(1 - P_d)}{P_0(1 - P_f) + (1 - P_0)(1 - P_d)} \triangleq \pi_1, \quad (32)$$

where  $P_0 = \Pr(H_0)$  is the probability that the licensed spec- 461  
trum band is unoccupied by PBS, while  $P_d = \Pr(\hat{H} = H_1 | H_1)$  462  
and  $P_f = \Pr(\hat{H} = H_1 | H_0)$  are the SDP and FAP, respectively. 463  
For notational convenience, we introduce the shorthand  $\pi_0 = 464$   
 $\Pr(H_0 | \hat{H} = H_0)$ ,  $\pi_1 = \Pr(H_1 | \hat{H} = H_0)$  and  $\Delta = \frac{2^R - 1}{\gamma_s}$ . Then, 465  
using (31) and (32), we rewrite (30) as 466

$$P_{\text{out}}^{\text{direct}} = \pi_0 \Pr(|h_{sd}|^2 < \Delta) + \pi_1 \Pr(|h_{sd}|^2 - |h_{pd}|^2 \gamma_p \Delta < \Delta). \quad (33)$$

Noting that  $|h_{sd}|^2$  and  $|h_{pd}|^2$  are independently and exponen- 467  
tially distributed RVs with respective means of  $\sigma_{sd}^2$  and  $\sigma_{pd}^2$ , 468  
we obtain 469

$$\Pr(|h_{sd}|^2 < \Delta) = 1 - \exp\left(-\frac{\Delta}{\sigma_{sd}^2}\right), \quad (34)$$

and 470

$$\Pr(|h_{sd}|^2 - |h_{pd}|^2 \gamma_p \Delta < \Delta) = 1 - \frac{\sigma_{sd}^2}{\sigma_{pd}^2 \gamma_p \Delta + \sigma_{sd}^2} \exp\left(-\frac{\Delta}{\sigma_{sd}^2}\right). \quad (35)$$

Additionally, we observe from (26) that an intercept event 471  
occurs, when the capacity of the ST-E channel becomes higher 472  
than the data rate. Thus, given that a spectrum hole has been de- 473  
tected (i.e.  $\hat{H} = H_0$ ), ST starts transmitting its signal to SD and 474  
E may overhear the ST-SD transmission. The corresponding IP 475  
is given by 476

$$P_{\text{int}}^{\text{direct}} = \Pr(C_{se} > R | \hat{H} = H_0), \quad (36)$$

which can be further expressed as 477

$$\begin{aligned} P_{\text{int}}^{\text{direct}} &= \Pr(C_{se} > R | \hat{H} = H_0, H_0) \Pr(H_0 | \hat{H} = H_0) \\ &+ \Pr(C_{se} > R | \hat{H} = H_0, H_1) \Pr(H_1 | \hat{H} = H_0) \\ &= \pi_0 \Pr(|h_{se}|^2 > \Delta) + \pi_1 \Pr(|h_{se}|^2 - |h_{pe}|^2 \gamma_p \Delta > \Delta), \end{aligned} \quad (37)$$

478 where the second equality is obtained by using  $C_{se}$  from (5).  
 479 Noting that RVs  $|h_{se}|^2$  and  $|h_{pe}|^2$  are exponentially distributed  
 480 and independent of each other, we can express the terms  
 481  $\Pr(|h_{se}|^2 > \Delta)$  and  $\Pr(|h_{se}|^2 - |h_{pe}|^2 \gamma_p \Delta > \Delta)$  as

$$\Pr(|h_{se}|^2 > \Delta) = \exp\left(-\frac{\Delta}{\sigma_{se}^2}\right), \quad (38)$$

482 and

$$\Pr(|h_{se}|^2 - |h_{pe}|^2 \gamma_p \Delta > \Delta) = \frac{\sigma_{se}^2}{\sigma_{pe}^2 \gamma_p \Delta + \sigma_{se}^2} \exp\left(-\frac{\Delta}{\sigma_{se}^2}\right), \quad (39)$$

483 where  $\sigma_{se}^2$  and  $\sigma_{pe}^2$  are the expected values of RVs  $|h_{se}|^2$  and  
 484  $|h_{pe}|^2$ , respectively.

### 485 B. Single-Relay Selection

486 In this subsection, we present the SRT analysis of the pro-  
 487 posed SRS scheme. Given  $\hat{H} = H_0$ , the OP of the cognitive  
 488 transmission relying on SRS is given by

$$P_{\text{out}}^{\text{single}} = \Pr(C_{bd} < R, \mathcal{D} = \emptyset | \hat{H} = H_0) + \sum_{n=1}^{2^N-1} \Pr(C_{bd} < R, \mathcal{D} = \mathcal{D}_n | \hat{H} = H_0), \quad (40)$$

489 where  $C_{bd}$  represents the capacity of the channel from the  
 490 ‘‘best’’ SR to SD. In the case of  $\mathcal{D} = \emptyset$ , no SR is chosen to  
 491 forward the source signal, which leads to  $C_{bd} = 0$  for  $\mathcal{D} = \emptyset$ .  
 492 Substituting this result into (40) gives

$$P_{\text{out}}^{\text{single}} = \Pr(\mathcal{D} = \emptyset | \hat{H} = H_0) + \sum_{n=1}^{2^N-1} \Pr(C_{bd} < R, \mathcal{D} = \mathcal{D}_n | \hat{H} = H_0), \quad (41)$$

493 Using (2), (9), (10), and (14), we can rewrite (41) as (42),  
 494 shown at the bottom of the page, where  $\Lambda = \frac{2^{2R}-1}{\gamma_s}$ . Noting  
 495 that  $|h_{si}|^2$  and  $|h_{pi}|^2$  are independent exponentially distributed

random variables with respective means of  $\sigma_{si}^2$  and  $\sigma_{pi}^2$ , we have 496

$$\Pr(|h_{si}|^2 < \Lambda) = 1 - \exp\left(-\frac{\Lambda}{\sigma_{si}^2}\right), \quad (43)$$

and

497

$$\Pr(|h_{si}|^2 < \Lambda | h_{pi}|^2 \gamma_p + \Lambda) = 1 - \frac{\sigma_{si}^2}{\sigma_{pi}^2 \gamma_p \Lambda + \sigma_{si}^2} \exp\left(-\frac{\Lambda}{\sigma_{si}^2}\right), \quad (44)$$

where the terms  $\Pr(|h_{si}|^2 > \Lambda)$ ,  $\Pr(|h_{sj}|^2 < \Lambda)$ , and  $\Pr(|h_{si}|^2 > 498$   
 $\Lambda | h_{pi}|^2 \gamma_p + \Lambda)$  can be similarly determined in closed-form. 499  
 Moreover, based on Appendix A, we obtain  $\Pr(\max_{i \in \mathcal{D}_n} |h_{id}|^2 < \Lambda)$  500

and  $\Pr(\max_{i \in \mathcal{D}_n} |h_{id}|^2 < \Lambda | h_{pd}|^2 \gamma_p + \Lambda)$  as 501

$$\Pr\left(\max_{i \in \mathcal{D}_n} |h_{id}|^2 < \Lambda\right) = \prod_{i \in \mathcal{D}_n} \left[1 - \exp\left(-\frac{\Lambda}{\sigma_{id}^2}\right)\right], \quad (45)$$

and

502

$$\begin{aligned} & \Pr\left(\max_{i \in \mathcal{D}_n} |h_{id}|^2 < \Lambda | h_{pd}|^2 \gamma_p + \Lambda\right) \\ &= 1 + \sum_{m=1}^{2^{|\mathcal{D}_n|}-1} (-1)^{|\tilde{\mathcal{D}}_n(m)|} \exp\left(-\sum_{i \in \tilde{\mathcal{D}}_n(m)} \frac{\Lambda}{\sigma_{id}^2}\right) \\ & \quad \times \left(1 + \sum_{i \in \mathcal{D}_n(m)} \frac{\Lambda \gamma_p \sigma_{pd}^2}{\sigma_{id}^2}\right)^{-1}, \end{aligned} \quad (46)$$

where  $\tilde{\mathcal{D}}_n(m)$  represents the  $m$ -th non-empty subset of  $\mathcal{D}_n$ . 503  
 Additionally, the IP of the SRS scheme can be expressed as 504

$$P_{\text{int}}^{\text{single}} = \Pr(C_{be} > R, \mathcal{D} = \emptyset | \hat{H} = H_0) + \sum_{n=1}^{2^N-1} \Pr(C_{be} > R, \mathcal{D} = \mathcal{D}_n | \hat{H} = H_0), \quad (47)$$

where  $C_{be}$  represents the capacity of the channel spanning from 505  
 the ‘‘best’’ SR to E. Given  $\mathcal{D} = \emptyset$ , we have  $C_{be} = 0$ , since 506  
 no relay is chosen for forwarding the source signal. Thus, 507

---


$$\begin{aligned} P_{\text{out}}^{\text{single}} &= \pi_0 \prod_{i=1}^N \Pr(|h_{si}|^2 < \Lambda) + \pi_1 \prod_{i=1}^N \Pr(|h_{si}|^2 < \Lambda | h_{pi}|^2 \gamma_p + \Lambda) \\ &+ \pi_0 \sum_{n=1}^{2^N-1} \prod_{i \in \mathcal{D}_n} \Pr(|h_{si}|^2 > \Lambda) \prod_{j \in \tilde{\mathcal{D}}_n} \Pr(|h_{sj}|^2 < \Lambda) \Pr\left(\max_{i \in \mathcal{D}_n} |h_{id}|^2 < \Lambda\right) \\ &+ \pi_1 \sum_{n=1}^{2^N-1} \prod_{i \in \mathcal{D}_n} \Pr(|h_{si}|^2 > \Lambda | h_{pi}|^2 \gamma_p + \Lambda) \prod_{j \in \tilde{\mathcal{D}}_n} \Pr(|h_{sj}|^2 < \Lambda | h_{pj}|^2 \gamma_p + \Lambda) \\ & \quad \times \Pr\left(\max_{i \in \mathcal{D}_n} |h_{id}|^2 < \Lambda | h_{pd}|^2 \gamma_p + \Lambda\right) \end{aligned} \quad (42)$$

508 substituting this result into (47) and using (2), (9), (10), and  
509 (16), we arrive at

$$\begin{aligned}
P_{\text{int}}^{\text{single}} &= \pi_0 \sum_{n=1}^{2^N-1} \prod_{i \in \mathcal{D}_n} \Pr(|h_{si}|^2 > \Lambda) \prod_{j \in \overline{\mathcal{D}}_n} \Pr(|h_{sj}|^2 < \Lambda) \\
&\quad \times \Pr(|h_{be}|^2 > \Lambda) \\
&+ \pi_1 \sum_{n=1}^{2^N-1} \prod_{i \in \mathcal{D}_n} \Pr(|h_{si}|^2 > \Lambda |h_{pi}|^2 \gamma_p + \Lambda) \\
&\quad \times \prod_{j \in \overline{\mathcal{D}}_n} \Pr(|h_{sj}|^2 < \Lambda |h_{pj}|^2 \gamma_p + \Lambda) \\
&\quad \times \Pr(|h_{be}|^2 > \Lambda |h_{pe}|^2 \gamma_p + \Lambda), \quad (48)
\end{aligned}$$

510 where the closed-form expressions of  $\Pr(|h_{si}|^2 > \Lambda)$  and  
511  $\Pr(|h_{si}|^2 > \Lambda |h_{pi}|^2 \gamma_p + \Lambda)$  can be readily obtained by using  
512 (43) and (44). Using the results in Appendix B, we can express  
513  $\Pr(|h_{be}|^2 > \Lambda)$  and  $\Pr(|h_{be}|^2 > \Lambda |h_{pe}|^2 \gamma_p + \Lambda)$  as

$$\begin{aligned}
\Pr(|h_{be}|^2 > \Lambda) &= \sum_{i \in \mathcal{D}_n} \exp\left(-\frac{\Lambda}{\sigma_{ie}^2}\right) \\
&\times \left[ 1 + \sum_{m=1}^{2^{|\mathcal{D}_n|-1}-1} (-1)^{|C_n(m)|} \left( 1 + \sum_{j \in C_n(m)} \frac{\sigma_{id}^2}{\sigma_{jd}^2} \right)^{-1} \right], \quad (49)
\end{aligned}$$

514 and

$$\begin{aligned}
\Pr(|h_{be}|^2 > \Lambda |h_{pe}|^2 \gamma_p + \Lambda) &= \sum_{i \in \mathcal{D}_n} \frac{\sigma_{ie}^2}{\sigma_{pe}^2 \gamma_p \Lambda + \sigma_{ie}^2} \exp\left(-\frac{\Lambda}{\sigma_{ie}^2}\right) \\
&\times \left[ 1 + \sum_{m=1}^{2^{|\mathcal{D}_n|-1}-1} (-1)^{|C_n(m)|} \left( 1 + \sum_{j \in C_n(m)} \frac{\sigma_{id}^2}{\sigma_{jd}^2} \right)^{-1} \right], \quad (50)
\end{aligned}$$

515 where  $C_n(m)$  represents the  $m$ -th non-empty subset of  $\mathcal{D}_n - \{i\}$   
516 and ‘ $-$ ’ represents the set difference.

### 517 C. Multi-Relay Selection

518 This subsection analyzes the SRT of our MRS scheme for  
519 transmission over Rayleigh fading channels. Similarly to (41),

the OP in this case is given by

520

$$\begin{aligned}
P_{\text{out}}^{\text{multi}} &= \Pr(\mathcal{D} = \emptyset | \hat{H} = H_0) \\
&+ \sum_{n=1}^{2^N-1} \Pr\left(C_d^{\text{multi}} < R, \mathcal{D} = \mathcal{D}_n | \hat{H} = H_0\right). \quad (51)
\end{aligned}$$

Using (2), (9), (10) and (23), we can rewrite (51) as (52), shown  
521 at the bottom of the page, where the closed-form expressions  
522 of  $\Pr(|h_{si}|^2 < \Lambda)$ ,  $\Pr(|h_{si}|^2 < \Lambda |h_{pi}|^2 \gamma_p + \Lambda)$ ,  $\Pr(|h_{si}|^2 > \Lambda)$ ,  
523  $\Pr(|h_{sj}|^2 < \Lambda)$  and  $\Pr(|h_{si}|^2 > \Lambda |h_{pi}|^2 \gamma_p + \Lambda)$  can be readily  
524 derived, as shown in (43) and (44). However, it is challenging  
525 to obtain the closed-form expressions of  $\Pr(\sum_{i \in \mathcal{D}_n} |h_{id}|^2 < \Lambda)$  and  
526  $\Pr(\sum_{i \in \mathcal{D}_n} |h_{id}|^2 < \gamma_p \Lambda |h_{pd}|^2 + \Lambda)$ . For simplicity, we assume that

527 the fading coefficients of all SRs-SD channels, i.e.  $|h_{id}|^2$  for  
528  $i \in \{1, 2, \dots, N\}$ , are i.i.d. RVs having the same mean (average  
529 channel gain) denoted by  $\sigma_d^2 = E(|h_{id}|^2)$ . This assumption is  
530 widely used in the cooperative relaying literature and it is  
531 valid in a statistical sense, provided that all SRs are uniformly  
532 distributed over a certain geographical area. Assuming that  
533 RVs of  $|h_{id}|^2$  for  $i \in \mathcal{D}_n$  are i.i.d., based on Appendix C,  
534 we arrive at

$$\Pr\left(\sum_{i \in \mathcal{D}_n} |h_{id}|^2 < \Lambda\right) = \Gamma\left(\frac{\Lambda}{\sigma_d^2}, |\mathcal{D}_n|\right), \quad (53)$$

and

536

$$\begin{aligned}
\Pr\left(\sum_{i \in \mathcal{D}_n} |h_{id}|^2 < \gamma_p \Lambda |h_{pd}|^2 + \Lambda\right) &= \Gamma\left(\frac{\Lambda}{\sigma_d^2}, |\mathcal{D}_n|\right) \\
&+ \frac{\left[1 - \Gamma\left(\Lambda \sigma_d^{-2} + \sigma_{pd}^{-2} \gamma_p^{-1}, |\mathcal{D}_n|\right)\right]}{\left(1 + \sigma_d^2 \sigma_{pd}^{-2} \gamma_p^{-1} \Lambda^{-1}\right)^{|\mathcal{D}_n|}} e^{1/(\sigma_{pd}^2 \gamma_p)}, \quad (54)
\end{aligned}$$

537 where  $\Gamma(x, k) = \int_0^x \frac{t^{k-1}}{\Gamma(k)} e^{-t} dt$  is known as the incomplete  
538 Gamma function [32]. Substituting (53) and (54) into (52)  
539 yields a closed-form OP expression for the proposed MRS  
540 scheme.

$$\begin{aligned}
P_{\text{out}}^{\text{multi}} &= \pi_0 \prod_{i=1}^N \Pr(|h_{si}|^2 < \Lambda) + \pi_1 \prod_{i=1}^N \Pr(|h_{si}|^2 < \Lambda |h_{pi}|^2 \gamma_p + \Lambda) \\
&+ \pi_0 \sum_{n=1}^{2^N-1} \prod_{i \in \mathcal{D}_n} \Pr(|h_{si}|^2 > \Lambda) \prod_{j \in \overline{\mathcal{D}}_n} \Pr(|h_{sj}|^2 < \Lambda) \Pr\left(\sum_{i \in \mathcal{D}_n} |h_{id}|^2 < \Lambda\right) \\
&+ \pi_1 \sum_{n=1}^{2^N-1} \prod_{i \in \mathcal{D}_n} \Pr(|h_{si}|^2 > \Lambda |h_{pi}|^2 \gamma_p + \Lambda) \prod_{j \in \overline{\mathcal{D}}_n} \Pr(|h_{sj}|^2 < \Lambda |h_{pj}|^2 \gamma_p + \Lambda) \\
&\quad \times \Pr\left(\sum_{i \in \mathcal{D}_n} |h_{id}|^2 < \gamma_p \Lambda |h_{pd}|^2 + \Lambda\right) \quad (52)
\end{aligned}$$

541 Next, we present the IP analysis of the MRS scheme. Simi-  
542 larly to (48), the IP of the MRS can be obtained from (24) as

$$\begin{aligned}
 P_{\text{int}}^{\text{multi}} = & \pi_0 \sum_{n=1}^{2^N-1} \prod_{i \in \mathcal{D}_n} \Pr(|h_{si}|^2 > \Lambda) \prod_{j \in \mathcal{D}_n} \Pr(|h_{sj}|^2 < \Lambda) \\
 & \times \Pr\left(\frac{|H_d^H H_e|^2}{|H_d|^2} > \Lambda\right) \\
 & + \pi_1 \sum_{n=1}^{2^N-1} \prod_{i \in \mathcal{D}_n} \Pr(|h_{si}|^2 > \Lambda |h_{pi}|^2 \gamma_p + \Lambda) \\
 & \times \prod_{j \in \mathcal{D}_n} \Pr(|h_{sj}|^2 < \Lambda |h_{pj}|^2 \gamma_p + \Lambda) \\
 & \times \Pr\left(\frac{|H_d^H H_e|^2}{|H_d|^2} > \gamma_p \Lambda |h_{pe}|^2 + \Lambda\right), \quad (55)
 \end{aligned}$$

543 where the closed-form expressions of  $\Pr(|h_{si}|^2 > \Lambda)$ ,  
544  $\Pr(|h_{sj}|^2 < \Lambda)$ ,  $\Pr(|h_{si}|^2 > \Lambda |h_{pi}|^2 \gamma_p + \Lambda)$  and  $\Pr(|h_{sj}|^2 < \Lambda$   
545  $\Lambda |h_{pj}|^2 \gamma_p + \Lambda)$  may be readily derived by using (43) and (44).  
546 However, it is challenging to obtain the closed-form solutions  
547 for  $\Pr\left(\frac{|H_d^H H_e|^2}{|H_d|^2} > \Lambda\right)$  and  $\Pr\left(\frac{|H_d^H H_e|^2}{|H_d|^2} > \gamma_p \Lambda |h_{pe}|^2 + \Lambda\right)$ .  
548 Although finding a general closed-form IP expression for the  
549 MRS scheme is challenging, we can obtain the numerical IP  
550 results with the aid of computer simulations.

#### 551 IV. NUMERICAL RESULTS AND DISCUSSIONS

552 In this section, we present our performance comparisons  
553 among the direct transmission, the SRS and MRS schemes  
554 in terms of their SRT. To be specific, the analytic IP versus  
555 OP of the three schemes are obtained by plotting (33), (37),  
556 (42), (48), (52), and (55). The simulated IP and OP results of  
557 the three schemes are also given to verify the correctness of  
558 the theoretical SRT analysis. In our computer simulations, the  
559 fading amplitudes (e.g.,  $|h_{sd}|$ ,  $|h_{si}|$ ,  $|h_{id}|$ , etc.) are first generated  
560 based on the Rayleigh distribution having different variances  
561 for different channels. Then, the randomly generated fading  
562 amplitudes are substituted into the definition of an outage (or  
563 intercept) event, which would determine whether an outage (or  
564 intercept) event occurs or not. By repeatedly achieving this pro-  
565 cess, we can calculate the relative frequency of occurrence for  
566 an outage (intercept) event, which is the simulated OP (or IP).  
567 Additionally, the SDP  $P_d$  and FAP  $P_f$  are set to  $P_d = 0.99$   
568 and  $P_f = 0.01$ , unless otherwise stated. The primary signal-  
569 to-noise ratio (SNR) of  $\gamma_p = 10$  dB and the data rate of  
570  $R = 1$  bit/s/Hz are used in our numerical evaluations.

571 The artificial noise based method [35], [36] is also consid-  
572 ered for the purpose of numerical comparison with the relay  
573 selection schemes. To be specific, in the artificial noise based  
574 scheme, ST directly transmits its signal  $x_s$  to SD, while  $N$  SRs  
575 attempt to confuse the eavesdropper by sending an interfering  
576 signal (referred to as artificial noise) that is approximately  
577 designed to lie in the null-space of the legitimate main channel.  
578 In this way, the artificial noise will impose interference on the  
579 eavesdropper without affecting the SD. For a fair comparison,  
580 the total transmit power of the desired signal  $x_s$  and the artificial  
581 noise are constrained to  $P_s$ . Moreover, the equal power alloca-  
582 tion method [35] is used in the numerical evaluation.

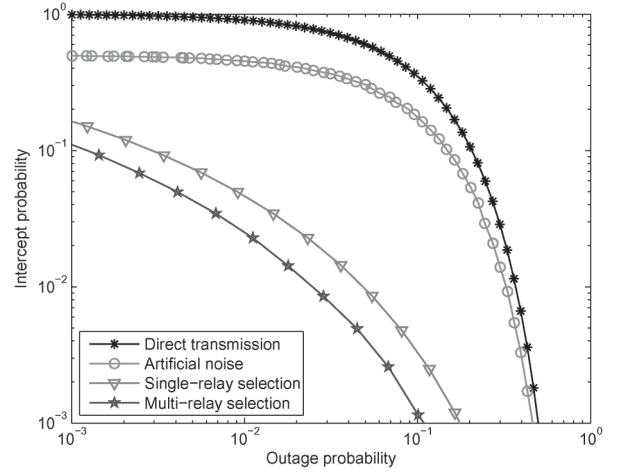


Fig. 3. IP versus OP of the direct transmission, the SRS and the MRS schemes for different  $P_0$  with  $P_0 = 0.8$ ,  $\gamma_s \in [0, 35]$  dB,  $N = 6$ ,  $\sigma_{sd}^2 = \sigma_{si}^2 = \sigma_{id}^2 = 1$ ,  $\sigma_{se}^2 = \sigma_{ie}^2 = 0.1$ , and  $\sigma_{pd}^2 = \sigma_{pe}^2 = \sigma_{pi}^2 = 0.2$ .

Fig. 3 shows the IP versus OP of the direct transmission, 583  
as well as the SRS and MRS schemes for  $P_0 = 0.8$ , where 584  
the solid lines and discrete marker symbols represent the an- 585  
alytic and simulated results, respectively. It can be seen from 586  
Fig. 3 that the IP of the direct transmission, the artificial noise 587  
based as well as of the proposed SRS and MRS schemes all 588  
improve upon tolerating a higher OP, implying that a trade-off 589  
exists between the IP (security) and the OP (reliability) of CR 590  
transmissions. Fig. 3 also shows that both the proposed SRS 591  
and MRS schemes outperform the direct transmission and the 592  
artificial noise based approaches in terms of their SRT, showing 593  
the advantage of exploiting relay selection against the eaves- 594  
dropping attack. Moreover, the SRT performance of the MRS is 595  
better than that of the SRS. Although the MRS achieves a better 596  
SRT performance than its SRS-aided counterpart, this result 597  
is obtained at the cost of a higher implementation complexity, 598  
since multiple SRs require high-complexity symbol-level syn- 599  
chronization for simultaneously transmitting to the SD, whereas 600  
the SRS does not require such elaborate synchronization. 601

Fig. 4 illustrates our numerical SRT comparison between the 602  
SRS and MRS schemes for  $P_0 = 0.2$  and  $P_0 = 0.8$ . Observe 603  
from Fig. 4 that the MRS scheme performs better than the SRS 604  
in terms of its SRT performance for both  $P_0 = 0.2$  and  $P_0 = 0.8$ . 605  
It is also seen from Fig. 4 that as  $P_0$  increases from 0.2 to 606  
0.8, the SRT of both the SRS and MRS schemes improves. 607  
This is because upon increasing  $P_0$ , the licensed band becomes 608  
unoccupied by the PUs with a higher probability and hence the 609  
secondary users (SUs) have more opportunities for accessing 610  
the licensed band for their data transmissions, which leads 611  
to a reduction of the OP for CR transmissions. Meanwhile, 612  
increasing  $P_0$  may simultaneously result in an increase of the IP, 613  
since the eavesdropper also has more opportunities for tapping 614  
the cognitive transmissions. However, in both the SRS and 615  
MRS schemes, the relay selection is performed for the sake 616  
of maximizing the legitimate transmission capacity without 617  
affecting the eavesdropper's channel capacity. Hence, upon 618  
increasing  $P_0$ , it becomes more likely that the reduction of OP 619  
is more significant than the increase of IP, hence leading to an 620  
overall SRT improvement for the SRS and MRS schemes. 621

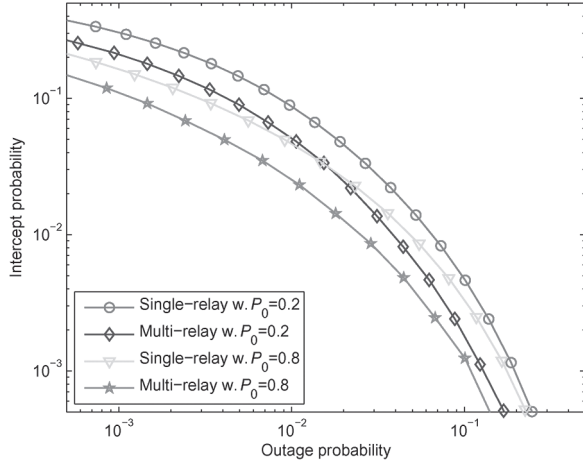


Fig. 4. IP versus OP of the SRS and MRS schemes for different  $P_0$  with  $\gamma_s \in [0, 30 \text{ dB}]$ ,  $N = 6$ ,  $\sigma_{sd}^2 = \sigma_{si}^2 = \sigma_{id}^2 = 1$ ,  $\sigma_{se}^2 = \sigma_{ie}^2 = 0.1$ , and  $\sigma_{pd}^2 = \sigma_{pe}^2 = \sigma_{pi}^2 = 0.2$ .

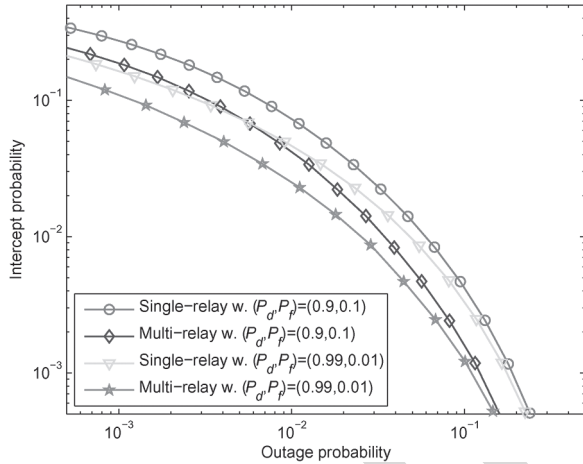


Fig. 5. IP versus OP of the SRS and the MRS schemes for different  $(P_d, P_f)$  with  $P_0 = 0.8$ ,  $\gamma_s \in [0, 30 \text{ dB}]$ ,  $N = 6$ ,  $\sigma_{sd}^2 = \sigma_{si}^2 = \sigma_{id}^2 = 1$ ,  $\sigma_{se}^2 = \sigma_{ie}^2 = 0.1$ , and  $\sigma_{pd}^2 = \sigma_{pe}^2 = \sigma_{pi}^2 = 0.2$ .

In Fig. 5, we depict the IP versus OP of the SRS and MRS schemes for different spectrum sensing reliabilities, where  $(P_d, P_f) = (0.9, 0.1)$  and  $(P_d, P_f) = (0.99, 0.01)$  are considered. It is observed that as the spectrum sensing reliability is improved from  $(P_d, P_f) = (0.9, 0.1)$  to  $(P_d, P_f) = (0.99, 0.01)$ , the SRTs of the SRS and MRS schemes improve accordingly. This is due to the fact that for an improved sensing reliability, an unoccupied licensed band would be detected more accurately and hence less mutual interference occurs between the PUs and SUs, which results in a better SRT for the secondary transmissions. Fig. 5 also shows that for  $(P_d, P_f) = (0.9, 0.1)$  and  $(P_d, P_f) = (0.99, 0.01)$ , the MRS approach outperforms the SRS scheme in terms of the SRT, which further confirms the advantage of the MRS for protecting the secondary transmissions against eavesdropping attacks.

Fig. 6 shows the IP versus OP of the conventional direct transmission as well as of the proposed SRS and MRS schemes for  $N = 2, N = 4$ , and  $N = 8$ . It is seen from Fig. 6 that the SRTs

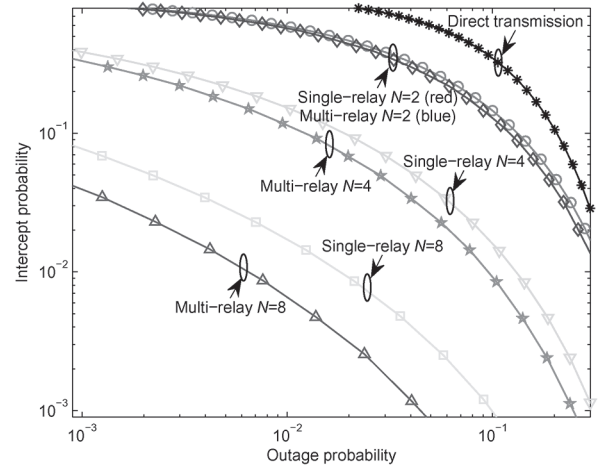


Fig. 6. IP versus OP of the direct transmission, the SRS and the MRS schemes for different  $N$  with  $P_0 = 0.8$ ,  $\gamma_s \in [0, 30 \text{ dB}]$ ,  $\sigma_{sd}^2 = \sigma_{si}^2 = \sigma_{id}^2 = 1$ ,  $\sigma_{se}^2 = \sigma_{ie}^2 = 0.1$ , and  $\sigma_{pd}^2 = \sigma_{pe}^2 = \sigma_{pi}^2 = 0.2$ .

of the proposed SRS and MRS schemes are generally better than that of the conventional direct transmission for  $N = 2, N = 4$  and  $N = 8$ . Moreover, as the number of SRs increases from  $N = 2$  to  $N = 8$ , the SRT of the SRS and MRS schemes significantly improves, explicitly demonstrating the security and reliability benefits of exploiting multiple SRs for assisting the secondary transmissions. In other words, the security and reliability of the secondary transmissions can be concurrently improved by increasing the number of SRs. Additionally, as shown in Fig. 6, upon increasing the number of SRs from  $N = 2$  to  $N = 8$ , the SRT improvement of MRS over SRS becomes more notable. Again, the SRT advantage of the MRS over the SRS comes at the expense of requiring elaborate symbol-level synchronization among the multiple SRs for simultaneously transmitting to the SD.

## V. CONCLUSION

In this paper, we proposed relay selection schemes for a CR network consisting of a ST, a SD and multiple SRs communicating in the presence of an eavesdropper. We examined the SRT performance of the SRS and MRS assisted secondary transmissions in the presence of realistic spectrum sensing, where both the security and reliability of secondary transmissions are characterized in terms of their IP and OP respectively. We also analyzed the SRT of the conventional direct transmission as a benchmark. It was illustrated that as the spectrum sensing reliability increases, the SRTs of both the SRS and MRS schemes improve. We also showed that the proposed SRS and MRS schemes generally outperform the conventional direct transmission and artificial noise based approaches in terms of their SRT. Moreover, the SRT performance of MRS is better than that of SRS. Additionally, as the number of SRs increases, the SRTs of both the SRS and of the MRS schemes improve significantly, demonstrating their benefits in terms of enhancing both the security and reliability of secondary transmissions.

675 APPENDIX A  
676 DERIVATION OF (45) AND (46)

677 Letting  $|h_{id}|^2 = x_i$  and  $|h_{pd}|^2 = y$ , the left hand side of (45)  
678 and (46) can be rewritten as  $\Pr(\max_{i \in \mathcal{D}_n} x_i < \Lambda)$  and  $\Pr(\max_{i \in \mathcal{D}_n} x_i <$   
679  $\Lambda \gamma_p y + \Lambda)$ , respectively. Noting that random variables  $|h_{id}|^2$  and  
680  $|h_{pd}|^2$  are exponentially distributed with respective means  $\sigma_{id}^2$   
681 and  $\sigma_{pd}^2$ , and independent of each other, we obtain

$$\begin{aligned} \Pr\left(\max_{i \in \mathcal{D}_n} x_i < \Lambda\right) &= \prod_{i \in \mathcal{D}_n} \Pr(|h_{id}|^2 < \Lambda) \\ &= \prod_{i \in \mathcal{D}_n} \left[1 - \exp\left(-\frac{\Lambda}{\sigma_{id}^2}\right)\right], \end{aligned} \quad (\text{A.1})$$

682 which is (45). Similarly, the term  $\Pr(\max_{i \in \mathcal{D}_n} x_i < \Lambda \gamma_p y + \Lambda)$  can be  
683 computed as

$$\begin{aligned} \Pr\left(\max_{i \in \mathcal{D}_n} x_i < \Lambda \gamma_p y + \Lambda\right) \\ &= \int_0^\infty \frac{1}{\sigma_{pd}^2} \exp\left(-\frac{y}{\sigma_{pd}^2}\right) \prod_{i \in \mathcal{D}_n} \left(1 - \exp\left(-\frac{\Lambda \gamma_p y + \Lambda}{\sigma_{id}^2}\right)\right) dy, \end{aligned} \quad (\text{A.2})$$

684 wherein  $\prod_{i \in \mathcal{D}_n} \left(1 - \exp\left(-\frac{\Lambda \gamma_p y + \Lambda}{\sigma_{id}^2}\right)\right)$  can be further expanded  
685 as

$$\begin{aligned} \prod_{i \in \mathcal{D}_n} \left(1 - \exp\left(-\frac{\Lambda \gamma_p y + \Lambda}{\sigma_{id}^2}\right)\right) &= 1 \\ &+ \sum_{m=1}^{2^{|\mathcal{D}_n|-1}} (-1)^{|\tilde{\mathcal{D}}_n(m)|} \exp\left(-\sum_{i \in \tilde{\mathcal{D}}_n(m)} \frac{\Lambda \gamma_p y + \Lambda}{\sigma_{id}^2}\right), \end{aligned} \quad (\text{A.3})$$

686 where  $|\mathcal{D}_n|$  is the cardinality of set  $\mathcal{D}_n$ ,  $\tilde{\mathcal{D}}_n(m)$  represents the  
687  $m$ -th non-empty subset of  $\mathcal{D}_n$ , and  $|\tilde{\mathcal{D}}_n(m)|$  is the cardinality  
688 of set  $\tilde{\mathcal{D}}_n(m)$ . Substituting  $\prod_{i \in \mathcal{D}_n} \left(1 - \exp\left(-\frac{\Lambda \gamma_p y + \Lambda}{\sigma_{id}^2}\right)\right)$  from  
689 (A.3) into (A.2) yields

$$\begin{aligned} \Pr\left(\max_{i \in \mathcal{D}_n} x_i < \Lambda \gamma_p y + \Lambda\right) &= \int_0^\infty \frac{1}{\sigma_{pd}^2} \exp\left(-\frac{y}{\sigma_{pd}^2}\right) dy \\ &+ \sum_{m=1}^{2^{|\mathcal{D}_n|-1}} (-1)^{|\tilde{\mathcal{D}}_n(m)|} \frac{1}{\sigma_{pd}^2} \\ &\times \int_0^\infty \exp\left(-\frac{y}{\sigma_{pd}^2} - \sum_{i \in \tilde{\mathcal{D}}_n(m)} \frac{\Lambda \gamma_p y + \Lambda}{\sigma_{id}^2}\right) dy. \end{aligned} \quad (\text{A.4})$$

Finally, performing the integration of (A.4) yields

$$\begin{aligned} \Pr\left(\max_{i \in \mathcal{D}_n} x_i < \Lambda \gamma_p y + \Lambda\right) &= 1 \\ &+ \sum_{m=1}^{2^{|\mathcal{D}_n|-1}} (-1)^{|\tilde{\mathcal{D}}_n(m)|} \exp\left(-\sum_{i \in \tilde{\mathcal{D}}_n(m)} \frac{\Lambda}{\sigma_{id}^2}\right) \\ &\times \left(1 + \sum_{i \in \tilde{\mathcal{D}}_n(m)} \frac{\Lambda \gamma_p \sigma_{pd}^2}{\sigma_{id}^2}\right)^{-1}. \end{aligned} \quad (\text{A.5})$$

This completes the proof of (45) and (46).

692 APPENDIX B  
693 PROOF OF (49) AND (50)

Given  $\mathcal{D} = \mathcal{D}_n$ , any SR within  $\mathcal{D}_n$  can be selected as the  
“best” relay for forwarding the source signal. Thus, using the  
law of total probability, we have

$$\begin{aligned} \Pr(|h_{be}|^2 > \Lambda) &= \sum_{i \in \mathcal{D}_n} \Pr(|h_{ie}|^2 > \Lambda, b = i) \\ &= \sum_{i \in \mathcal{D}_n} \Pr\left(|h_{ie}|^2 > \Lambda, |h_{id}|^2 > \max_{j \in \mathcal{D}_n - \{i\}} |h_{jd}|^2\right) \\ &= \sum_{i \in \mathcal{D}_n} \Pr(|h_{ie}|^2 > \Lambda) \Pr\left(\max_{j \in \mathcal{D}_n - \{i\}} |h_{jd}|^2 < |h_{id}|^2\right), \end{aligned} \quad (\text{B.1})$$

where in the first line, variable ‘ $b$ ’ stands for the best SR and  
the second equality is obtained from (13) and ‘ $-$ ’ represents the  
set difference. Noting that  $|h_{ie}|^2$  is an exponentially distributed  
random variable with a mean of  $\sigma_{ie}^2$ , we obtain

$$\Pr(|h_{ie}|^2 > \Lambda) = \exp\left(-\frac{\Lambda}{\sigma_{ie}^2}\right). \quad (\text{B.2})$$

Letting  $|h_{jd}|^2 = x_j$  and  $|h_{id}|^2 = y$ , we have

$$\begin{aligned} \Pr\left(\max_{j \in \mathcal{D}_n - \{i\}} |h_{jd}|^2 < |h_{id}|^2\right) \\ &= \int_0^\infty \frac{1}{\sigma_{id}^2} \exp\left(-\frac{y}{\sigma_{id}^2}\right) \prod_{j \in \mathcal{D}_n - \{i\}} \left(1 - \exp\left(-\frac{y}{\sigma_{jd}^2}\right)\right) dy, \end{aligned} \quad (\text{B.3})$$

wherein  $\prod_{j \in \mathcal{D}_n - \{i\}} \left(1 - \exp\left(-\frac{y}{\sigma_{jd}^2}\right)\right)$  is expanded by

$$\begin{aligned} \prod_{j \in \mathcal{D}_n - \{i\}} \left(1 - \exp\left(-\frac{y}{\sigma_{jd}^2}\right)\right) &= 1 \\ &+ \sum_{m=1}^{2^{|\mathcal{D}_n|-1}-1} (-1)^{|C_n(m)|} \exp\left(-\sum_{j \in C_n(m)} \frac{y}{\sigma_{jd}^2}\right), \end{aligned} \quad (\text{B.4})$$

where  $|\mathcal{D}_n|$  denotes the cardinality of the set  $\mathcal{D}_n$  and  $C_n(m)$   
represents the  $m$ -th non-empty subset of “ $\mathcal{D}_n - \{i\}$ ”. Combining  
(B.3) and (B.4), we obtain

$$\begin{aligned} \Pr\left(\max_{j \in \mathcal{D}_n - \{i\}} |h_{jd}|^2 < |h_{id}|^2\right) &= 1 \\ &+ \sum_{m=1}^{2^{|\mathcal{D}_n|-1}-1} (-1)^{|C_n(m)|} \left(1 + \sum_{j \in C_n(m)} \frac{\sigma_{id}^2}{\sigma_{jd}^2}\right)^{-1}. \end{aligned} \quad (\text{B.5})$$

706 Substituting (B.2) and (B.5) into (B.1) gives (B.6), shown at  
707 the bottom of the page, which is (49). Similarly to (B.1), we  
708 can rewrite  $\Pr(|h_{be}|^2 > \Lambda|h_{pe}|^2\gamma_p + \Lambda)$  as

$$\begin{aligned} & \Pr(|h_{be}|^2 > \Lambda|h_{pe}|^2\gamma_p + \Lambda) \\ &= \sum_{i \in \mathcal{D}_n} \Pr(|h_{ie}|^2 > \Lambda|h_{pe}|^2\gamma_p + \Lambda) \\ & \quad \times \Pr\left(\max_{j \in \{\mathcal{D}_n - i\}} |h_{jd}|^2 < |h_{id}|^2\right). \end{aligned} \quad (\text{B.7})$$

709 Since the random variables  $|h_{ie}|^2$  and  $|h_{pe}|^2$  are independently  
710 and exponentially distributed with respective means of  $\sigma_{ie}^2$  and  
711  $\sigma_{pe}^2$ , we readily arrive at

$$\Pr(|h_{ie}|^2 > \Lambda|h_{pe}|^2\gamma_p + \Lambda) = \frac{\sigma_{ie}^2}{\sigma_{pe}^2\gamma_p\Lambda + \sigma_{ie}^2} \exp\left(-\frac{\Lambda}{\sigma_{ie}^2}\right). \quad (\text{B.8})$$

712 Substituting (B.5) and (B.8) into (B.7) gives (B.9), shown at the  
713 bottom of the page, which is (50).

#### APPENDIX C

##### PROOF OF (53) AND (54)

714 Upon introducing the notation of  $X = \sum_{i \in \mathcal{D}_n} |h_{id}|^2$  and  $Y =$   
715  $|h_{pd}|^2$ , we can rewrite the terms  $\Pr(\sum_{i \in \mathcal{D}_n} |h_{id}|^2 < \Lambda)$  and  
716  $\Pr(\sum_{i \in \mathcal{D}_n} |h_{id}|^2 < \gamma_p\Lambda|h_{pd}|^2 + \Lambda)$  as  $\Pr(X < \Lambda)$  and  $\Pr(X <$   
717  $\gamma_p\Lambda Y + \Lambda)$ , respectively. Noting that the fading coefficients of  
718 all SR-SD channels, i.e.  $|h_{id}|^2$  for  $i \in \{1, 2, \dots, N\}$ , are assumed  
719 to be i.i.d., we obtain the probability density function (PDF) of  
720  $X = \sum_{i \in \mathcal{D}_n} |h_{id}|^2$  as

$$f_X(x) = \frac{1}{\Gamma(|\mathcal{D}_n|)\sigma_d^{2|\mathcal{D}_n|}} x^{|\mathcal{D}_n|-1} \exp\left(-\frac{x}{\sigma_d^2}\right), \quad (\text{C.1})$$

723 where  $\sigma_d^2 = E(|h_{id}|^2)$ . Meanwhile, the random variable  $Y =$   
724  $|h_{pd}|^2$  is exponentially distributed and its PDF is given by

$$f_Y(y) = \frac{1}{\sigma_{pd}^2} \exp\left(-\frac{y}{\sigma_{pd}^2}\right), \quad (\text{C.2})$$

where  $\sigma_{pd}^2 = E(|h_{pd}|^2)$ . Using (C.1), we arrive at

$$\begin{aligned} \Pr(X < \Lambda) &= \int_0^\Lambda \frac{1}{\Gamma(|\mathcal{D}_n|)\sigma_d^{2|\mathcal{D}_n|}} x^{|\mathcal{D}_n|-1} \exp\left(-\frac{x}{\sigma_d^2}\right) dx \\ &= \int_0^{\frac{\Lambda}{\sigma_d^2}} \frac{t^{|\mathcal{D}_n|-1}}{\Gamma(|\mathcal{D}_n|)} \exp(-t) dt \\ &= \Gamma\left(\frac{\Lambda}{\sigma_d^2}, |\mathcal{D}_n|\right), \end{aligned} \quad (\text{C.3})$$

725 where the second equality is obtained by substituting  $\frac{x}{\sigma_d^2} = t$  and

726  $\Gamma(a, k) = \int_0^k \frac{t^{a-1}}{\Gamma(a)} \exp(-t) dt$  is known as the incomplete Gamma  
727 function. Additionally, considering that the random variables  $X$   
728 and  $Y$  are independent of each other, we obtain  $\Pr(X < \gamma_p\Lambda Y +$   
729  $\Lambda)$  as

$$\begin{aligned} \Pr(X < \gamma_p\Lambda Y + \Lambda) &= \int_0^\Lambda f_X(x) dx \\ & \quad + \int_\Lambda^\infty \int_{-\frac{x}{\gamma_p\Lambda} - \frac{1}{\gamma_p}}^\infty f_X(x) f_Y(y) dx dy. \end{aligned} \quad (\text{C.4})$$

730 Substituting  $f_X(x)$  and  $f_Y(y)$  from (C.1) and (C.2) into (C.4)  
731 yields

$$\begin{aligned} & \Pr(X < \gamma_p\Lambda Y + \Lambda) \\ &= \Gamma\left(\frac{\Lambda}{\sigma_d^2}, |\mathcal{D}_n|\right) \\ & \quad + \int_\Lambda^\infty \frac{e^{1/(\sigma_{pd}^2\gamma_p)} x^{|\mathcal{D}_n|-1}}{\Gamma(|\mathcal{D}_n|)\sigma_d^{2|\mathcal{D}_n|}} \exp\left(-\frac{x}{\sigma_d^2} - \frac{x}{\sigma_{pd}^2\gamma_p\Lambda}\right) dx \\ &= \Gamma\left(\frac{\Lambda}{\sigma_d^2}, |\mathcal{D}_n|\right) + \frac{\left[1 - \Gamma\left(\Lambda\sigma_d^{-2} + \sigma_{pd}^{-2}\gamma_p^{-1}, |\mathcal{D}_n|\right)\right]}{\left(1 + \sigma_d^2\sigma_{pd}^{-2}\gamma_p^{-1}\Lambda^{-1}\right)^{|\mathcal{D}_n|}} e^{1/(\sigma_{pd}^2\gamma_p)}, \end{aligned} \quad (\text{C.5})$$

732 where the second equality is obtained by using  $\frac{x}{\sigma_d^2} + \frac{x}{\sigma_{pd}^2\gamma_p\Lambda} = t$ .  
733 Hence, we have completed the proof of (53) and (54) as (C.3)  
734 and (C.5), respectively. 735

---


$$\Pr(|h_{be}|^2 > \Lambda) = \sum_{i \in \mathcal{D}_n} \exp\left(-\frac{\Lambda}{\sigma_{ie}^2}\right) \left[1 + \sum_{m=1}^{2^{|\mathcal{D}_n|-1}-1} (-1)^{|C_n(m)|} \left(1 + \sum_{j \in C_n(m)} \frac{\sigma_{id}^2}{\sigma_{jd}^2}\right)^{-1}\right] \quad (\text{B.6})$$


---

$$\Pr(|h_{be}|^2 > \Lambda|h_{pe}|^2\gamma_p + \Lambda) = \sum_{i \in \mathcal{D}_n} \frac{\sigma_{ie}^2}{\sigma_{pe}^2\gamma_p\Lambda + \sigma_{ie}^2} \exp\left(-\frac{\Lambda}{\sigma_{ie}^2}\right) \left[1 + \sum_{m=1}^{2^{|\mathcal{D}_n|-1}-1} (-1)^{|C_n(m)|} \left(1 + \sum_{j \in C_n(m)} \frac{\sigma_{id}^2}{\sigma_{jd}^2}\right)^{-1}\right] \quad (\text{B.9})$$

## REFERENCES

- 736
- 737 [1] J. Mitola and G. Q. Maguire, "Cognitive radio: Making software radios  
738 more personal," *IEEE Pers. Commun.*, vol. 6, no. 4, pp. 13–18, Aug. 1999.
- 739 [2] IEEE 802.22 Working Group, IEEE P802.22/D1.0 draft standard for  
740 wireless regional area networks part 22: Cognitive wireless RAN medium  
741 access control (MAC) and physical layer (PHY) specifications: Policies  
742 and procedures for operation in the TV bands, Apr. 2008.
- 743 [3] G. Baldini, T. Sturman, A. R. Biswas, and R. Leschhorn, "Security aspects  
744 in software defined radio and cognitive radio networks: A survey and a  
745 way ahead," *IEEE Commun. Surveys Tuts.*, vol. 14, no. 2, pp. 355–379,  
746 May 2012.
- 747 [4] D. Cabric, S. M. Mishra, and R. W. Brodersen, "Implementation issues in  
748 spectrum sensing for cognitive radios," in *Proc. 38th Asil. Conf. Signal,  
749 Syst. Comput.*, Pacific Grove, CA, USA, Nov. 2004, pp. 772–776.
- 750 [5] H. Li, "Cooperative spectrum sensing via belief propagation in spectrum-  
751 heterogeneous cognitive radio systems," in *Proc. IEEE WCNC*, Sydney,  
752 N.S.W., Australia, Apr. 2010, pp. 1–6.
- 753 [6] J. Ma, G. Zhao, and Y. Li, "Soft combination and detection for cooperative  
754 spectrum sensing in cognitive radio networks," *IEEE Trans. Wireless  
755 Commun.*, vol. 7, no. 11, pp. 4502–4507, Nov. 2008.
- 756 [7] A. Ghasemi and E. S. Sousa, "Fundamental limits of spectrum-sharing  
757 in fading environments," *IEEE Trans. Wireless Commun.*, vol. 6, no. 2,  
758 pp. 649–658, Feb. 2007.
- 759 [8] R. Southwell, J. Huang, and X. Liu, "Spectrum mobility games," in *Proc.  
760 31st INFOCOM*, Orlando, FL, USA, Mar. 2012, pp. 37–45.
- 761 [9] I. F. Akyildiz, W.-Y. Lee, M. C. Vuran, and S. Mohanty, "A survey on  
762 spectrum management in cognitive radio networks," *IEEE Commun.  
763 Mag.*, vol. 46, no. 4, pp. 40–48, Apr. 2008.
- 764 [10] H. Li and Z. Han, "Dogfight in spectrum: Combating primary user em-  
765 ulation attacks in cognitive radio systems part I: Known channel statis-  
766 tics," *IEEE Trans. Wireless Commun.*, vol. 9, no. 11, pp. 3566–3577,  
767 Nov. 2010.
- 768 [11] T. Brown and A. Sethi, "Potential cognitive radio denial-of-service vulner-  
769 abilities and protection countermeasures: A multi-dimensional analysis  
770 and assessment," in *Proc. 2nd Int. Conf. CROWCOM*, Orlando, FL,  
771 USA, Aug. 2007, pp. 456–464.
- 772 [12] S. Lakshmanan, C. Tsao, R. Sivakumar, and K. Sundaresan, "Securing  
773 wireless data networks against eavesdropping using smart antennas," in  
774 *Proc. 28th ICDCS*, Beijing, China, Jun. 2008, pp. 19–27.
- 775 [13] A. Olteanu and Y. Xiao, "Security overhead and performance for aggrega-  
776 tion with fragment retransmission (AFR) in very high-speed wireless  
777 802.11 LANs," *IEEE Trans. Wireless Commun.*, vol. 9, no. 1, pp. 218–  
778 226, Jan. 2010.
- 779 [14] Y. Xiao, V. K. Rayi, X. Du, F. Hu, and M. Galloway, "A survey of key  
780 management schemes in wireless sensor networks," *Comput. Commun.*,  
781 vol. 30, no. 11–12, pp. 2314–2341, Sep. 2007.
- 782 [15] A. Mukherjee, S. A. Fakoorian, J. Huang, and A. L. Swindlehurst,  
783 "Principles of physical layer security in multiuser wireless networks: A  
784 survey," *IEEE Commun. Surveys Tuts.*, vol. 16, no. 3, pp. 1550–1573,  
785 Aug. 2014.
- 786 [16] A. D. Wyner, "The wire-tap channel," *Bell Syst. Tech. J.*, vol. 54, no. 8,  
787 pp. 1355–1387, 1975.
- 788 [17] S. K. Leung-Yan-Cheong and M. E. Hellman, "The Gaussian wire-  
789 tap channel," *IEEE Trans. Inf. Theory*, vol. 24, no. 4, pp. 451–456,  
790 Jul. 1978.
- 791 [18] P. Parada and R. Blahut, "Secrecy capacity of SIMO and slow fading  
792 channels," in *Proc. IEEE ISIT*, Adelaide, SA, Australia, Sep. 2005,  
793 pp. 2152–2155.
- 794 [19] M. Bloch, J. O. Barros, M. R. D. Rodrigues, and S. W. McLaughlin,  
795 "Wireless information-theoretic security," *IEEE Trans. Inf. Theory*, vol. 54,  
796 no. 6, pp. 2515–2534, Jun. 2008.
- 797 [20] P. K. Gopala, L. Lai, and H. Gamal, "On the secrecy capacity of fading  
798 channels," *IEEE Trans. Inf. Theory*, vol. 54, no. 10, pp. 4687–4698,  
799 Oct. 2008.
- 800 [21] Z. Li, W. Trappe, and R. Yates, "Secret communication via multi-antenna  
801 transmission," in *Proc. 41st Conf. Inf. Sci. Syst.*, Baltimore, MD, USA,  
802 Mar. 2007, pp. 905–910.
- 803 [22] F. Oggier and B. Hassibi, "The secrecy capacity of the MIMO wire-  
804 tap channel," *IEEE Trans. Inf. Theory*, vol. 57, no. 8, pp. 4961–4972,  
805 Aug. 2007.
- 806 [23] M. Yuksel and E. Erkip, "Secure communication with a relay helping the  
807 wiretapper," in *Proc. IEEE Inf. Theory Workshop*, Lake Tahoe, CA, USA,  
808 Sep. 2007, pp. 595–600.
- 809 [24] L. Dong, Z. Han, A. P. Petropulu, and H. V. Poor, "Improving wire-  
810 less physical layer security via cooperating relays," *IEEE Trans. Signal  
811 Process.*, vol. 58, no. 3, pp. 1875–1888, Mar. 2010.
- [25] Y. Zou, X. Wang, and W. Shen, "Optimal relay selection for physical-layer  
812 security in cooperative wireless networks," *IEEE J. Sel. Areas Commun.*, 813  
vol. 31, no. 10, pp. 2099–2111, Oct. 2013. 814
- [26] A. Mukherjee and A. Swindlehurst, "Robust beamforming for security  
815 in MIMO wiretap channels with imperfect CSI," *IEEE Trans. Signal  
816 Process.*, vol. 59, no. 1, pp. 351–361, Jan. 2011. 817
- [27] C. Jeong, I. Kim, and K. Dong, "Joint secure beamforming design at  
818 the source and the relay for an amplify-and-forward MIMO untrusted  
819 relay system," *IEEE Trans. Signal Process.*, vol. 60, no. 1, pp. 310–325, 820  
Jan. 2012. 821
- [28] Y. Pei, Y.-C. Liang, K. C. Teh, and K. Li, "Secure communication in  
822 multiantenna cognitive radio networks with imperfect channel state in-  
823 formation," *IEEE Trans. Signal Process.*, vol. 59, no. 4, pp. 1683–1693, 824  
Apr. 2011. 825
- [29] Y. Zou, X. Wang, and W. Shen, "Physical-layer security with multiuser  
826 scheduling in cognitive radio networks," *IEEE Trans. Commun.*, vol. 61,  
827 no. 12, pp. 5103–5113, Dec. 2013. 828
- [30] Z. Shu, Y. Qian, and S. Ci, "On physical layer security for cognitive radio  
829 networks," *IEEE Netw. Mag.*, vol. 27, no. 3, pp. 28–33, Jun. 2013. 830
- [31] Y. Zou, X. Wang, W. Shen, and L. Hanzo, "Security versus reliability  
831 analysis of opportunistic relaying," *IEEE Trans. Veh. Tech.*, vol. 63, no. 6,  
832 pp. 2653–2661, Jun. 2014. 833
- [32] L. Di Stefano and S. Mattoccia, "A sufficient condition based on the  
834 Cauchy-Schwarz inequality for efficient template matching," in *Proc. Int.  
835 Conf. Image Process.*, Catalonia, Spain, Sep. 2003, pp. 269–272. 836
- [33] M. Abramowitz and I. A. Stegun, *Handbook of Mathematical Functions  
837 with Formulas, Graphs, Mathematical Tables*, 9th ed. New York, NY, 838  
USA: Dover, 1970. 839
- [34] Y. Zou, Y.-D. Yao, and B. Zheng, "Diversity-multiplexing tradeoff in  
840 selective cooperation for cognitive radio," *IEEE Trans. Commun.*, vol. 60,  
841 no. 9, pp. 2467–2481, Sep. 2012. 842
- [35] S. Goel and R. Negi, "Guaranteeing secrecy using artificial noise," *IEEE  
843 Trans. Wireless Commun.*, vol. 7, no. 6, pp. 2180–2189, Jun. 2008. 844
- [36] W. Li, M. Ghogho, B. Chen, and C. Xiong, "Artificial noise by the  
845 receiver: Outage secrecy capacity/region analysis," *IEEE Commun. Lett.*, 846  
vol. 16, no. 10, pp. 1628–1631, Oct. 2012. 847



**Yulong Zou** (S'07–M'12–SM'13) received the 848  
B.Eng. degree in information engineering from 849  
NUPT, Nanjing, China, in July 2006, the first Ph.D. 850  
degree in electrical engineering from the Stevens In- 851  
stitute of Technology, New Jersey, the United States, 852  
in May 2012, and the second Ph.D. degree in signal 853  
and information processing from NUPT, Nanjing, 854  
China, in July 2012. He is a Full Professor at the 855  
Nanjing University of Posts and Telecommunica- 856  
tions (NUPT), Nanjing, China. His research interests 857  
span a wide range of topics in wireless commu- 858  
nications and signal processing, including the cooperative 859  
cognitive radio, wireless security, and energy-efficient communications. 860

He is currently serving as an editor for the IEEE Communications Surveys 861  
& Tutorials, IEEE COMMUNICATIONS LETTERS, EURASIP Journal on Ad- 862  
vances in Signal Processing, and KSII Transactions on Internet and Information 863  
Systems. He served as the lead guest editor for a special issue on "Security 864  
Challenges and Issues in Cognitive Radio Networks" in the EURASIP Journal 865  
on Advances in Signal Processing. He is also serving as the lead guest 866  
editor for a special issue on "Security and Reliability Challenges in Industrial 867  
Wireless Sensor Networks" in the IEEE TRANSACTIONS ON INDUSTRIAL 868  
INFORMATICS. In addition, he has acted as symposium chairs, session chairs, 869  
and TPC members for a number of IEEE sponsored conferences, including the 870  
IEEE WIRELESS COMMUNICATIONS and Networking Conference (WCNC), 871  
IEEE Global Communications Conference (GLOBECOM), IEEE International 872  
Conference on Communications (ICC), IEEE Vehicular Technology Confer- 873  
ence (VTC), International Conference on Communications in China (ICCC), 874  
and so on. 875



**Benoit Champagne** (S'87–M'89–SM'03) was born in Joliette (PQ), Canada, in 1961. He received the B.Eng. degree in engineering physics and the M.Sc. degree in physics from the University of Montreal in 1983 and 1985, respectively, and the Ph.D. degree in electrical engineering from the University of Toronto in 1990. From 1990 to 1999, he was with INRS, University of Quebec, where he held the positions of Assistant and then Associate Professor. In 1999, he joined McGill University, Montreal, as an Associate Professor with the Department of Electrical and

Computer Engineering. He served as Associate Chairman of Graduate Studies in the Department from 2004 to 2007 and is now a Full Professor. His research interests focus on the investigation of new computational algorithms for the digital processing of information bearing signals and overlap many sub-areas of statistical signal processing, including: detection and estimation, sensor array processing, adaptive filtering, multirate systems, and applications thereof to broadband voice and data communications. Over the years, he has supervised many graduate students in these areas and co-authored several papers, including key works on subspace tracking, speech enhancement, time delay estimation and spread sources localization.



**Wei-Ping Zhu** (SM'97) received the B.E. and M.E. degrees from Nanjing University of Posts and Telecommunications, and the Ph.D. degree from Southeast University, Nanjing, China, in 1982, 1985, and 1991, respectively, all in electrical engineering. He was a Postdoctoral Fellow from 1991 to 1992 and a Research Associate from 1996 to 1998 with the Department of Electrical and Computer Engineering, Concordia University, Montreal, Canada. During 1993–1996, he was an Associate Professor with the Department of Information Engineering,

Nanjing University of Posts and Telecommunications. From 1998 to 2001, he worked with hi-tech companies in Ottawa, Canada, including Nortel Networks and SR Telecom Inc. Since July 2001, he has been with Concordia's Electrical and Computer Engineering Department as a full-time faculty member, where he is presently a Full Professor. His research interests include digital signal processing fundamentals, speech and audio processing, and signal processing for wireless communication with a particular focus on MIMO systems and cooperative relay networks.

Dr. Zhu was an Associate Editor of the IEEE TRANSACTIONS ON CIRCUITS AND SYSTEMS PART I: Fundamental Theory and Applications from 2001 to 2003, and an Associate Editor of Circuits, Systems and Signal Processing from 2006 to 2009. He was also a Guest Editor for the IEEE JOURNAL ON SELECTED AREAS IN COMMUNICATIONS for the special issues of: Broadband Wireless Communications for High Speed Vehicles, and Virtual MIMO during 2011–2013. Since 2011, he has served as an Associate Editor for the IEEE TRANSACTIONS ON CIRCUITS AND SYSTEMS PART II: Express Briefs. Dr. Zhu was the Secretary of Digital Signal Processing Technical Committee (DSPTC) of the IEEE Circuits and System Society during 2012–2014, where he is presently the Chair of the DSPTC.



**Lajos Hanzo** received the degree in electronics in 1976 and the doctorate in 1983. In 2009 he was awarded "Doctor Honoris Causa" by the Technical University of Budapest. During his 37-year career in telecommunications he has held various research and academic posts in Hungary, Germany, and the UK. Since 1986 he has been with the School of Electronics and Computer Science, University of Southampton, UK, where he holds the chair in telecommunications. He has successfully supervised 80+ Ph.D. students, co-authored 20 John Wiley/IEEE Press books

on mobile radio communications totalling in excess of 10 000 pages, published 1400+ research entries at IEEE Xplore, acted both as TPC and General Chair of IEEE conferences, presented keynote lectures and has been awarded a number of distinctions. Currently he is directing a 100-strong academic research team working on a range of research projects in the field of wireless multimedia communications sponsored by industry, the Engineering and Physical Sciences Research Council (EPSRC) UK, the European Research Council's Advanced Fellow Grant and the Royal Society's Wolfson Research Merit Award. He is an enthusiastic supporter of industrial and academic liaison and he offers a range of industrial courses. He is also a Governor of the IEEE VTS. During 2008–2012 he was the Editor-in-Chief of the IEEE Press and a Chaired Professor also at Tsinghua University, Beijing. His research is funded by the European Research Council's Senior Research Fellow Grant. For further information on research in progress and associated publications please refer to <http://www-mobile.ecs.soton.ac.uk> Lajos has 20 000+ citations.

952

AUTHOR QUERY

NO QUERY.

IEEE  
Proof